Drosophila Information Service

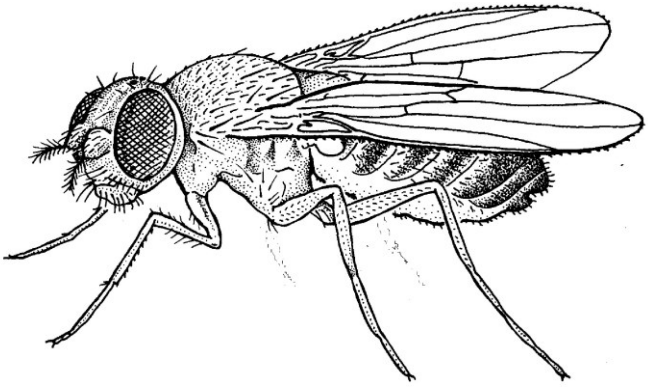

Number 103

December 2020

Prepared at the
Department of Biology
University of Oklahoma
Norman, OK 73019 U.S.A.

Preface

Drosophila Information Service (often called "DIS" by those in the field) was first printed in March, 1934. For those first issues, material contributed by *Drosophila* workers was arranged by C.B. Bridges and M. Demerec. As noted in its preface, which is reprinted in Dros. Inf. Serv. 75 (1994), Drosophila Information Service was undertaken because, "An appreciable share of credit for the fine accomplishments in *Drosophila* genetics is due to the broadmindedness of the original *Drosophila* workers who established the policy of a free exchange of material and information among all actively interested in *Drosophila* research. This policy has proved to be a great stimulus for the use of *Drosophila* material in genetic research and is directly responsible for many important contributions." Since that first issue, DIS has continued to promote open communication.

The production of this volume of DIS could not have been completed without the generous efforts of many people. Except for the special issues that contained mutant and stock information now provided in detail by FlyBase and similar material in the annual volumes, all issues are now freely-accessible from our web site: www.ou.edu/journals/dis. For early issues that only exist as aging typed or mimeographed copies, some notes and announcements have not yet been fully brought on line, but key information in those issues is available from FlyBase. We intend to fill in those gaps for historical purposes in the future.

We continue to encourage all researchers to consider submitting articles that use *Drosophila* for teaching as well as articles that report new techniques, research results, and interesting new mutations. In the interests of honoring the long-standing philosophy of open exchange of ideas, we sometimes accept articles that have unusual or limited perspectives. We thank the many contributors from around the world who sent material for this issue, and we invite your submissions for future annual issues as well as any suggestions you have for maintaining this as a useful *Drosophila* research community resource.

James N. Thompson, jr., Editor
David Ross Boyd Professor of Biology
Department of Biology
University of Oklahoma, Norman

Jenna J. Hellack, Associate Editor
Department of Biology, Emeritus
University of Central Oklahoma, Edmond
Department of Biology, Adjunct Professor
University of Oklahoma, Norman

Contributions and Inquiries should be sent to:

James N. Thompson, jr., Department of Biology, University of Oklahoma, Norman, OK 73019; Phone: (405) 325-2001, FAX (405) 325-6202, email: jthompson@ou.edu

Printed copies of the recent volumes can be ordered from lulu.com.

List of Contributions

General Announcements

Research Notes

Technique Notes

Teaching Notes

Other Reports

Research Notes

Determination of the protective effects of fungus species belonging to the genus *Pleurotus* against the longevity toxicity of guaiazulene in *Drosophila melanogaster* (Oregon R).

Uysal, Handan[1*], Hatice Çelik[1], Halit Kizilet[2], Bilal Yilmaz[3], Murat Özdal[1,] and Özlem Gülmez[1]. [1]Department of Biology, Faculty of Science, Atatürk University, 25240, Erzurum, Turkey; [2]Department of Cardiology, Erzurum Training and Research Hospital, 25100, Erzurum, Turkey; [3]Department of Analytical Chemistry, Faculty of Pharmacy, Ataturk University, 25240, Erzurum, Turkey; *Corresponding author: hauysal@atauni.edu.tr

Abstract

Lactarius indigo is an edible fungus and contains various secondary metabolites. One of these metabolites, Guaiazulene (GUA), is a kind of terpene. In this study, it was observed that *Drosophila melanogaster* shortened the life span of both male and female populations based on Guaiazulene's dose-time interaction (25, 50, 100, 200 ppm GUA and chronic application every three days). The average life span in the control group was 48.83 ± 1.95 days in the ♀ population and 48.30 ± 2.22 days in the ♂ population. These values in the ♀♀ were found to be 44.91 ± 1.45 to 12.11 ± 0.26 in the lowest and highest Gua application groups (25-200 ppm); in ♂♂, it decreased from 44.70 ± 1.22 to 11.44 ± 0.21 ($P < 0.05$).

In the second part of the study, water extracts of two edible fungi, *Pleurotus sajor-caju* (PSC_{wt}) and *Pleurotus osteratus* (PO_{wt}), were used together with GUA (200 ppm GUA+PSC_{wt} and GUA+PO_{wt}, 1:1 v/v ratio). Both extracts showed a healing effect and increased longevity compared to 200 ppm GUA application. Namely, in GUA+PSC_{wt} application, the longevity was extended to 21.93 ± 0.62 days for females and 19.05 ± 0.46 days for males. These values were found as 21.83 ± 0.66 and 18.75 ± 0.39 days in GUA+PO_{wt} application, respectively ($P < 0.05$). In this study, both fungal extracts were also analyzed by gas chromatography-mass spectrometry (GS-MS). A total of 13 and 10 components were identified in PO_{wt} and PSC_{wt}, respectively. In addition, total phenol and flavanoid contents of two extracts were determined. Key words: *Drosophila melanogaster, Lactarius indigo*, *Pleurotus*, longevity

Introduction

Every living thing has a certain life span. In this process, living things are born, grow, age, and die. In accordance with the programmed genetic information, these development parameters are completed in certain processes. Adults begin to age after giving new fertilization. As a result of aging, death occurs. Here we can ask a question like this: Do we want to grow old. The answer is, of course, no. Well, can this process be stopped? This is not possible. However, what can be done to delay aging? For example, organic nutrition should be preferred. Flour, salt and sugar should be reduced in the daily diet or vegetables and fruits should be emphasized in nutrition.

Mushrooms all over the world have been used as food and medicine for thousands of years. Because different types of fungi carry different proteins, generally, 100 g of fungi contain 3-8 g of protein. Proteins of fungi are not stored in the body and are spent daily. In addition, the proteins in the fungi contain all the amino acids necessary for human nutrition. Although the amount of protein in mushrooms is slightly less than the amount of protein in animal foods, it should be preferred because there is no risk of accumulation in the body. One of the most important features of fungi is that they contain very little sugar and fat. Therefore, the place of fungi in nutrition is important today. When different fungal species were examined, vitamins B1 and B2

were found mostly in *Pleurotus* species. This type of fungus contains 10 times more vitamin B3 than other vegetables. Fungi are also called a "miniature pharmaceutical factory" because of the beneficial ingredients in its content.

Mushrooms produce different secondary bioactive molecules (phenols, polysaccharides, pigments, tocopherols, terpenes, and steroids) with high therapeutic importance. These molecules have pharmacological activities such as antimicrobial, antiviral, antioxidant, antiinflammatory, antitumor, antiallergic, antiaging, antidiabetic, anti-Alzheimer, and hypocholesterolemic (Özdal, 2018). Among the metabolites, phenolic and flavonoid compounds show excellent antioxidant capacity (Yildiz *et al*., 2015). These metabolites can be obtainable (with water or different organic solvents) from both fruit body of mushrooms and mycelia biomass (Lee *et al*., 2007; Özdal *et al*., 2019), and, they are used as a capsule or tablet to prevention diseases and improve the quality of health (De Silva *et al*., 2013).

Pleurotus species are found throughout world and are among the most widely-cultivated. It well known that *Pleurotus* species produce bioactive molecules such as phenolic, pigment, polysaccharide, and terpenoid (Özdal *et al*., 2019). These molecules, obtained from *Pleurotus*, show antioxidant and antimicrobial activities (Younis *et al*., 2015). Outside these activities, recent studies have shown that bioactive molecules found in these species stop the development of tumors called "Sarcoma-180 by 80% (Patel and Goyal, 2012) However, several researchers have also shown that terpenes from secondary metabolites found in fungi may be toxic (Azirak and Rencüzoğulları, 2008; Büyükleyla and Rencüzoğulları, 2009). Guaiazulene is also a kind of terpenes and this terpene is found in *Lactarius indigo*, an edible fungus. Does continuous intake through nutrients and overdose of guaiazulene reduce the life span of organisms? In other words, does this terpene cause aging? In the presented study, answers to these questions were sought. If guaiazulene is toxic, can these toxic effects be prevented by nutrition? Hot water extracts obtained from mycelia of two *Pleurotus* species, *Pleurotus sajor-caju* (PSCwt) and *Pleurotus ostreatus* (POwt), were also used for this purpose, because these two types of mushrooms are widely used as nutrients. In our experiments, male and female populations of wild species of *Drosophila melanogaster* (Oregon R) as model organisms were used. This species has a short life cycle and rapid reproduction. Therefore, it gives a new generation in 9-10 days. In addition to these features, they are very easy to feed. For these reasons, *D. melanogaster* is preferred in toxicological and genoprotectivity studies.

Materials and Methods

Chemicals

Guaiazulene (CAS no:489-84-9, Figure 1), dimethylsulfoxide (CAS no:67-68-5),N-methyl-N-trimethylsilyl-trifluoroacetamide (MSTFA), ethyl acetate, diethylether, and acetonitrile were purchased from Sigma–Aldrich (St. Louis, MO, USA).

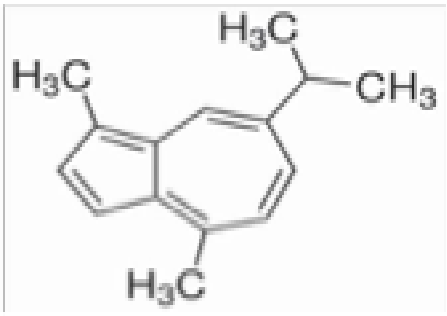

Figure 1. Chemical structure of guaiazulene.

Fungal Cultures and Storage Conditions

The *Pleurotus ostreatus* was obtained from the Erkel Gıda A.Ş., İzmir, Turkey, *P. sajor-caju* from Dr. Abdurrahman Dündar, Mardin Artuklu University. The mushrooms are stored on potato dextrose agar (PDA) at 4°C.

Media Preparation and Fermentation Conditions

The *Pleurotus* mushrooms were firstly grown on PDA petri plates at 25°C for 7 days. Submerged fermentation was carried out in 250 mL Erlenmeyer flasks containing 100 ml of liquid medium (Glucose 20 g/l, peptone 2 g/l, yeast extract 3 g/l, KH_2PO_4 1 g/l, $MgSO_4$ 0.5 g/l). Each flask was inoculated with five 5-mm agar plugs. Each flask was maintained at 25°C and 150 rpm for 15 days. After growth, the fungal

biomasses were obtained from the aqueous medium by filtration. The obtained biomasses were washed 4 times with sterilized distilled water, and then dried in the oven.

Preparation of Pleurotus Extracts

To obtain hot water extraction, 5 g dry and powdered mycelial biomass was boiled with 100 ml deionized water for 30 min. and then cooled. The cooled solution was filtered through Whatman filter paper (no. 4). To obtain dried extract, filtered solution evaporated in the oven (55°C). The dried extracts were dissolved in sterilized distilled water as 100 mg/ml and kept at 4°C for further studies.

Experimental Animals and Laboratory Condition

The flies used in the experiments were Oregon-R wild type strain of *D. melanogaster* Meigen (Diptera; Drosophilidae) with normal round-red eyed, normal length wings, normal thoracic bristles and hair and without any mutant characters. This stock had been maintained for many years in the laboratory at the Department of Biology, Ataturk University, Erzurum and was, therefore, highly inbred with little genetic variation. The flies were kept at a constant temperature of 25±1°C in a standard medium composed of maize flour, agar, sucrose, dried yeast and propionic acid (Standard Drosophila Medium = SDM). The flies were kept in darkness, except during the transfers onto a fresh medium (usually twice weekly). The humidity of the experimental chamber was 40–60% (Uysal *et al*., 2006). The females used in this experiment were virgins.

Longevity Experiments

Effects of GUA on life span were studied separately in male and female populations. For this purpose, a pre-stock of *D. melanogaster*'s Oregon R strain was created and the parents were removed when the pupae were seen after the date of crossing. Male and female individuals exiting the pupae were collected for three days every 4 hours before mating and taken into separate culture bottles (containing only SDB) for the experimental and control groups. Dimethyl sulfoxide (DMSO), a solvent of GUA, was used as a negative control group.

Our experiments were initiated simultaneously for the control, DMSO control, and experimental groups. Experimental groups were prepared in two different ways. One of them is the experimental group which contains only different doses of GUA (SDB+25, 50, 100, 200 ppm GUA). The other is the experimental group in which PSC_{wt} and PO_{wt} extracts are added to the highest GUA application group (SDB+200 ppm GUA+PSC_{wt}; SDB+200 ppm GUA+PO_{wt}, 1:1 v/v). For this purpose, all of the adult flies in the experimental and control groups fasted for 2 hours in the culture flasks. Then the individuals of the DMSO control group were placed in a culture in a flask which contained a 1% DMSO impregnated disk used as a solvent for GUA and were kept in this medium for 2 hours. The individuals of the application groups which previously fasted were exposed separately to different concentrations of GUA, GUA+PSC_{wt} and GUA+PO_{wt} in culture flasks. In each of the control ve applications groups ♀♀ and ♂♂ individuals were separated into four groups to simplify censuses and 25 individuals were placed into each culture flask. GUA and GUA+ extract applications were performed chronically in the experimental groups. All culture flasks of the experimental and control groups were kept under the same conditions in a suitable temperature cabin. Nutrients were refreshed twice a week during the experiment. The number of individuals were checked and recorded at the end of each application day and the dead individuals were removed. The experiment continued until the last individual of the control and experimental groups died. The experiments were repeated three times.

The Statistical Analysis of Longevity

The obtained data were analyzed with the SPSS version 13.0. The mean longevity values of the control and application groups were subjected to Duncan's one-way range test.

Determination of Volatile Organic Compounds

Chromatographic analyses were carried out on an Agilent 7820A gas chromatography system equipped with 5977 series mass selective detector, 7673 series autosampler and chemstation (Agilent Technologies, Palo Alto, CA). HP-5 MS column with 0.25 μm film thickness (30 m × 0.25 mm I.D., USA)

was used for separation. The temperatures of the inlet, transfer line, and detector were 250, 250, and 300°C, respectively. The GC temperature gradient program was as follows: initial temperature was 50°C, held for 1 min, increased to 100°C at a rate of 20°C /min held for 1 min, increased to 180°C at a rate of 10°C /min held for 1 min, increased to 220°C at a rate of 5°C /min held for 5 min, and finally to 300°C at a rate of 10°C /min and held for 5.5 min. The injector volume was 1 µl in splitless mode and the carrier gas was helium at a flow rate of 1 ml/min.

Identification of Components

Identification was based on the molecular structure, molecular mass, and calculated fragments. Interpretation on mass spectrum GC-MS was conducted using the database on National Institute Standard and Technology having more than 62,000 patterns. The name, molecular weight, and structure of the components of the test materials were ascertained. The relative percentage amount of each component was calculated by comparing its average peak area to the total areas. The spectrum of the unknown component was compared with the spectrum of the component stored in the National Institute of Standards and Technology Library Version (2005), Software, Turbomass 5.2.

Determination of Total Phenolic and Flavonoid Content

Total flavonoid and phenolic contents of hot water extracts were calculated with using quercetin (QE) (Turkoglu *et al*., 2007) and gallic acid (GAE) (Vamanu, 2012) as standards, respectively.

Results

The maximum life span in control (no. 1) and the DMSO control (no. 2) groups were observed as 78-74 days for ♀♀ and 76-74 days for ♂♂ (Table 1). The difference between those two groups was found statistically insignificant ($P > 0.05$). However, this time (in days) declined in both male and female populations due to increased GUA concentration. Namely; the maximum life span in the lowest (25 ppm, no. 3) and highest (200 ppm, no. 6) application groups in the female population from 63 to 21 days; in the male population, it decreased from 57 days to 14 days (Table 1). This regression in GUA experimental groups is

Table 1. The lifespan of male and female populations of *Drosophila melanogaster* and the probability levels between groups.

		GUAIAZULENE					
		Female Population			Male Population		
Experiment groups	N	Maximum lifespan	Mean lifespan ± SE	P	Maximum lifespan	Mean lifespan ± SE	P
Control (1)	100	78	49.15 ± 1.99		76	48.48 ± 2.24	
DMSO (2)	100	74	48.83 ± 1.95	-4,5,6	74	48.30 ± 2.22	-4,5,6*
25 ppm GUA (3)	100	63	44.91 ± 1.45	-4,5,6*	57	44.70 ± 1.22	-4,5,6*
50 ppm GUA (4)	100	57	41.01 ± 1.32	-5,6*	54	37.38 ± 1.45	-4,5,6*
100 ppm GUA (5)	100	28	21.47 ± 0.40	-5,6*	25	15.42 ± 0.34	-5,6*
200 ppm GUA (6	100	21	12.11 ± 0.26	-6*	14	11.44 ± 0.21	
200 ppm GUA + PSC_{wt} (7)	100	42	21.93 ± 0.62	-6*	28	19.05 ± 0.46	-6*
200 ppm GUA +PO_{wt} (8)	100	45	21.83 ± 0.66	-6*	28	18.75 ± 0.39	-6*
Regression Value			R = -699			R = -722	

N: Total number of individuals, SE: Standard error, *: The mean difference is not significant at 0.05

important compared to DMSO control group ($P < 0.05$). Besides, these values indicate a negative correlation between the maximum life span of the application groups and changing GUA concentrations ($R = -699$ for ♀♀ and $R = -722$ for ♂♂).

The regression in maximum lifespan was observed in the highest application group of GUA (200 ppm) for both populations (Table 1). Therefore, the therapeutic effects of *Pleurotus* extracts were studied in this application group of GUA [application groups: 200 ppm GUA+PSC$_{wt}$ (no. 7); 200 ppm GUA+PO$_{wt}$ (no. 8)]. In PSC$_{wt}$ and PO$_{wt}$ applications (1:1 v/v), the maximum life spans were found to be 42-45 days for ♀♀; 28-28 days for ♂♂, respectively. The difference observed in maximum life span between the 200 ppm GUA application group (no. 6 used as control group) and experimental groups (no. 7-8) is statistically significant ($P < 0.05$). These values indicate that the maximum life span increases and *Pleurotus* extracts have healing properties. Survival lines for control and application groups are shown separately for male and female populations (Figure 2).

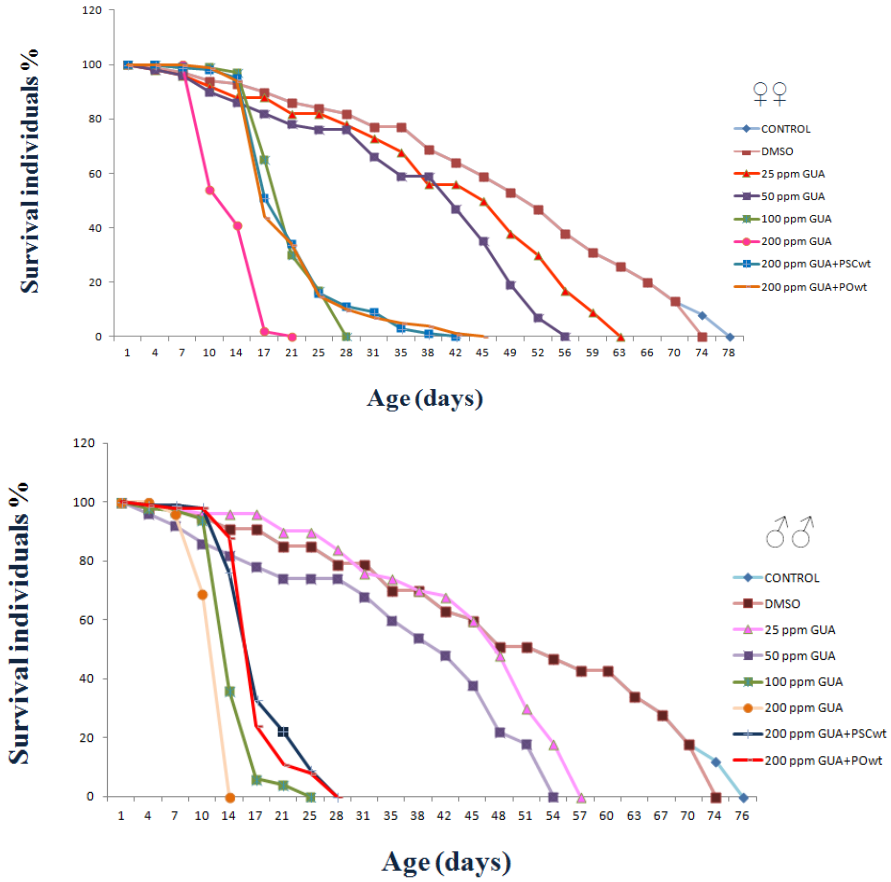

Figure 2. The survivorship lines of individuals of *Drosophila melanogaster* living medium applied with different concentrations of guaiazulene during adult stages.

In this study, the effects of GUA upon average life span of *D. melanogaster* have also been determined. The average life span in the control (no. 1) and DMSO control (no. 2) groups were found, respectively, as 49.15 ± 1.99 (no. 1), 48.83 ± 1.95 (no. 2) in the ♀♀ population and 48.48 ± 2.24 (no. 1), 48.30 ± 2.22 (no. 2) in the ♂♂ population. The difference between the control and DMSO control groups for both male and female populations are insignificant ($P > 0.05$).

However, in the ♀♀ application groups for GUA, the average life span regressed from 44.91 ± 1.45 days (25 ppm, no. 3) to 12.11 ± 0.26 days (200 ppm, no. 6) and from 44.70 ± 1.22 days (25 ppm, no. 3) to 11.44 ± 0.21 days (200 ppm, no. 6) in the ♂♂ application groups (Table 1). As shown in Table 1, the average life span in all the application groups decreased in accordance with the increase in the dosage. The differences

between the DMSO control and application groups are significant ($P < 0.05$). This decrease is also seen in the survivorship lines in Figure 2.

Pleurotus extracts [(application groups; (1:1 v/v) 200 ppm GUA+PSC_{wt} (no.7); 200 ppm GUA+ PO_{wt} (no. 8)] showed a curative effect on the average life span, just like the maximum longevity. Namely, the average life span in the 200 ppm GUA application group (no. 6) was 12.11 ± 0.26 days in the ♀♀ population. This value increased to 21.93 ± 0.62 days with PSC_{wt} application (no. 7) and up to 21.83 ± 0.66 days with GUA + PO_{wt} application (no. 8). A similar effect was also observed in the ♂♂ population. While the average life span of this population was 11 days, it extended to 19 days with PSC_{wt} and 18 days with PO_{wt}. When the results of *Pleurotus* extracts were compared with 200 ppm GUA application group, the increase in the average lifetime was statistically significant ($P < 0.05$).

Table 2. Chemical components and derivates of the *P. ostreatus* water extract.

Retention time(min)	Compound name	% ratio
8.44	1,2-Ethandimine, N,N-ditrifluroacetyl (İmine derivative)	4.07
9.66	Thiazolo[5,4,f] quindine (Guanidine derivative)	15.07
9.92	4-chloro-2-methylmercapto-5-t-butylpyrimidine (Pyrimidine derivative)	3.79
10.75	Nitrosodimethyletylurea (Nitroso derivative)	2.31
10.95	N,N-dimethyltrifluroacetamide (Acetamide derivative)	4.96
11.13	Benzoxazole-3-carboxiamide,2,3-dihydro-N-(2-chlrophenyl)-2-oxo(Carboxamide derivative)	0.89
11.20	Ethyl 3-mercaptopyruvate (Pyruvate derivative)	0.64
11.83	Ethane 1,2-bis (methylthio)-	3.21
16.28	Desulphosinigin	0.88
19.66	Deoxyspergualin	0.42
Total		36.24

Table 3. Chemical components and derivates of the *P. sajor-caju* water extract.

Retention time (min)	Compound name	% ratio
7.96	Mannosamine	0.2
8.02	5-methyl dimethyl thio carbamate (**Carbamate derivative)**	25
8.94	3-Thiophenecarboxylic acid, 4-hydroxy-2methyl-ethyl ester (**Carboxylic acidderivative**)	14.2
9.02	Ethylamine, N- (4-acetyloxyphenpropanyl)- N- (4-acetyloxybutyl) 1-aminocyclopentane carboxylic acid (**Carboxylic acidderivative**)	14.61
9.37	4H-thiazole [5,4,b] indole, 4-ethyl-2-methyl (**Indole derivative**)	6.52
9.78	4-chloro-2-methylmecapto-5-t-butylpyrimidine (**Pyrimidine derivative**)	7.03
10.34	Nitrosodimethyletylurea (**Nitroso derivative**)	3.18
10.64	N,n-dimethyltrifluroacetamide	4.15
10.80	Benzoxazole-3-carboxamide, 2,3-dihydro-N-(2chlorophenyl)- 2oxo (**Carboxamide derivative**)	1.03
11.11	1,1,2-tri(methylthio)ethane	0.2
11.64	Ethane, 1,2-bis(methylthio)	6.10
12.22	Dimethyl fluromethyl phenylsilane	1.94
16.49	Paromomycin	0.3
Total		84.46

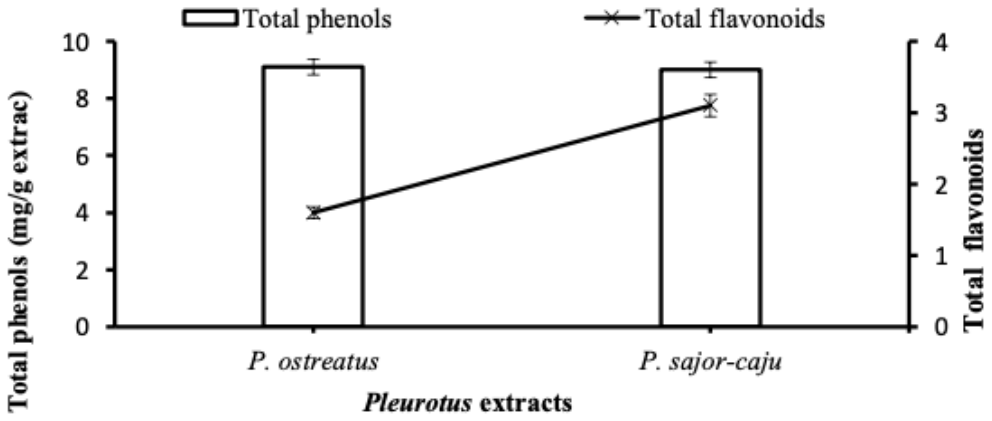

Figure 3. Total phenol and flavanoid amounts of *Pleurotus* extracts.

In this study, chemical components, derivates and ratios of the *P. ostreatus* and *P. sajor-caju* water extract were determined by GS-MS. *P. ostreatus* water extract compounds are given in Table 2. As shown in the Table 2, as a result of GS-MS, 10 different compounds were determined in the extract. Thiazolo [5,4,f] quindine (Guanidine derivative, 15.07%), N,N-dimethyltrifluroacetamide (Acetamide derivative, 4.96%), 1,2-Ethandimine, N,N-ditrifluroacetyl (İmine derivative), 4.07%), 4-chloro-2-methylmercapto-5-t-butylpyrimidine (Pyrimidine derivative, 3.79%) and Ethane 1,2-bis (methylthio) (3.21%) were found at high rates.

The contents of *P. sajor-caju* water extract are given in Table 3 and 13 different compounds were found. Ethylamine (Carboxylic acid derivative, 14.61%), 3-Thiophenecarboxylic acid, 4-hydroxy-2methyl-ethyl ester (Carboxylic acid derivative, 14.2%), 5-methyl dimethyl thio carbamate (Carbamate derivative, 25.0%), 4-chloro-2-methylmecapto-5-t-butylpyrimidine (Pyrimidine derivative, 7.03%), and 4H-thiazole [5,4,b] indole, 4-ethyl-2-methyl (Indole derivative, 6.52%) substances were determined at high rates.

Total phenol and flavanoid amounts of *Pleurotus* extracts were also calculated in this study (Figure 3). The total phenol content of *P. ostreatus* and *P. sajor caju* extracts were found to be 9.1 mg GAE/g extract and 9.0 mg GAE/g extract, respectively. The total flavonoids content of *P. sajor caju* (3.1 mgQE/g) was found to be higher than *P. ostreatus* (1.6 mg QE/g) (Figure 3).

Discussion

Terpenes are an important group of secondary metabolites. They are formed by the combination of five-carbon isoprene units and they are called hemiterpenes, monoterpenes, sesquiterpenes, diterpenes, sesterpenes, triterpenes, tetraterpenes, and polyterpenes, depending on the number of isoprene they carry. GUA, one of sesquiterpenes, consists of 3 isoprene units ($C_{15}H_{18}$). GUA is also found in *Guaiacum officinale*, *G. sanctum*, *G. coulteri*, and *Matricaria recutita* species besides *Lactarius indigo* fungus (Fiori *et al*., 2011). Terpenes are widely used in cosmetics, pharmaceuticals, food sectors due to their pharmacological properties and aromatherapy and phytotherapy due to their antioxidant and antimutagenic effects. These components are obtained from very different plants and their main active ingredients evaluated both economically and scientifically. Some of the previous studies are related to the antioxidant, antimutagen and antiaging properties of terpenes. In some studies, terpenes have been reported to be toxic, mutagenic and genotoxic. In our study, GUA also showed an *in vivo* effect of limiting the maximum and average longevity of *D. melanogaster* in female and male populations due to dose-time interaction. Thymol and carvacrol are terpenes derived from *Thymus* species. Antimicrobial and antioxidant properties of these terpenes are known (Shapiro *et al*., 1994). However, different doses of thymol and carvacrol stimulate chromosomal abnormalities in the bone marrow cells of rats and reduce mitotic index. These effects were evaluated by Azirak and

Rencüzoğulları (2008) as cytotoxic effects. According to Büyükleyla and Rencüzoğulları (2009), thymol is genotoxic, because it causes sister chromatid exchange and micronucleus formation. Several researchers have reported that terpenes can cause/have mutagenic, genotoxic and cytotoxic effects (İpek *et al*., 2005). Namely, *Salvia fruticosa* Mill. and *Mentha pulegium* have terpenes such as cineol, tujon, camphor, pulegon, and menton (Pavlidou *et al*., 2004). The toxic and genotoxic effects of these terpenes were determined by SMART in *Bactrocera oleae* and *D. melanogaster*. According to the obtained data, camphor, pulegon, and menton were mutagenic and cineol was toxic in *B. oleae* and *D. melanogaster*. Camfor was found to be weakly toxic in both organisms. In another study using different doses of GUA (0-400 $\mu g/mL^{-1}$), Togar *et al*. (2015) observed a cytotoxic effect on human peripheral lymphocytes. According to the same researchers, the total antioxidant level in neurons decreases with the use of GUA and the total oxidant level increases (Togar *et al*., 2015). Rotenone obtained from Papilionaceae, Mimosaceae, Cesalpiniaceae families caused oxidative stress, mitochondrial dysfunction, and neurotoxicity in *D. melanogaster* (Rao *et al*., 2016). Rotenone, a kind of terpene, caused oxidative stress in *D. melanogaster*.

As is known, oxidative stress plays an important role in the pathogenesis of cell and tissue damage. This is due to reactions of oxidant molecules on macromolecules such as protein, lipid, carbohydrate, nucleic acid, and enzymes which are the building blocks of the cell. In our opinion, cell cycle errors triggered by oxidative stress and deterioration of nuclear material "play a role in the etiopathology of shortening of life span in *D. melanogaster*."

Mushrooms are known to be an important source of biologically active compounds. Various secondary metabolites (such as phenolic, polypidides, terpenes, and steroids) generally accumulate in the mushrooms and have medicinal values. *P. ostreatus* and *P. sajor-caju* fungi also carry various flavanoid and phenolic substances. In this study, total flavanoid and phenolic contents of these species were also determined (Figure 3). Most of the flavonoids important biological feature is that they have antioxidative effect. Because of these unique properties, the use of phenolic substances in pharmacology, food, and pharmaceutical industries is quite wide. It is a natural source rich in phenolic substances in fruits, vegetables, and various types of mushrooms. Nowadays, the importance of natural phenolic substances has increased due to the escape from artificial substances.

Pleurotus fungi used in our study are also considered rich in these compounds. Total phenolic content of hot water extracts were in the range of 9.0 to 9.1 mg GAE/g. The flavanoid content of *P. sajor caju* (3.1 mgQE/g) was higher than *P. ostreatus* (1.6 mgQE/g) (Figure 2). González-Palma *et al*. (2016) reported in aqueous mycelium extracts (obtained by boiling) of *P. ostreatus* 4.09 mg GAE/g and 0.192 mgQE/g. Lee *et al*. (2007) showed the hot water extract from mycelia of *P. citrinopileatus* as 7.85 mgGAE/g. It should be noted that the amounts of these compounds may vary according to the fungus species, fermentation time, and fermentation medium.

Apart from these two compounds, derivatives of different substances were also found in *Pleurotus* extracts (Table 2 and Table 3). For example; Substances Thiazolo[5,4,f] quindine (Guanidine derivative (Anticancer), 15.07%), N,N-dimethyltrifluroacetamide (Acetamide derivative (Analgesic and antipyretic) 4.96%), 1,2-Ethandimine, N,N-ditrifluroacetyl (İmine derivative (Anticholinesterases),4.07%) and 4-chloro- 2-methylmercapto-5-t-butylpyrimidine (Pyrimidine derivative (Anticancer), 3.79%) were found to be high in *P. osteratus* water extract.

The Ethylamine (Carboxylic acid derivative (Analgesic and antiinflammatory) 14.61%), 3-Thiophenecarboxylic acid, 4-hydroxy-2methyl-ethyl ester (Carboxylic acid derivative) 14.2%), 5-methyl dimethyl thio carbamate (Carbamate derivative) 25.0%), 4-chloro-2-methylmecapto-5-t-butylpyrimidine (Pyrimidine derivative (Anticancer), 7.03%) and 4H-thiazole [5,4,b] indole, 4-ethyl-2-methyl (Indole derivative (Anticancer), 6.52%) substances were also determined at high rates in *P. sajor-caju* water extract.

According to Özgüneş and Atasayar (2009), guanidine derivates were shown to act as an antioxidant, preventing reactive oxygen species formation and lipid peroxidation in cells and tissues. The antiaging and the protective effects of guanidine derivates in conditions such as cardiovascular disease, diabetes, cataract, and atherosclerosis have been reported. Other derivatives have antipyretic, antimicrobial, analgesic, and anti-inflammatory properties. For example, imine compounds occupy an important place in the pharmaceutical and medical industries with their antibacterial, antifungal, and antitumor activities. Carbamate derivatives are used in cosmetics and pharmaceutical production.

Probably, the increase in total oxidant level caused by GUA at the cellular level was eliminated by PSC_{wt} and PO_{wt}. In other words, Pleurotus extracts increased total antioxidant capacity in the cell with their biologically active substances. According to the authors, we, in this case, " *D. melanogaster* has led to an increase in life span". However, it should be noted that new studies are needed to determine total oxidant level and total antioxidant capacity.

References: Azirak, S., and E. Rencuzogullari 2008, Environ. Toxicol. 23(6): 728-735; Büyükleyla, M., and E. Rencüzoğulları, 2009, Ecotoxicol. Environ. Saf. 72(3): 943-947; De Silva, D.D., S. Rapior, E. Sudarman, M. Stadler, J. Xu, S.A. Alias, and K.D. Hyde 2013, Fungal. Divers. 62: 1-40; Fiori, J., G. Teti, R. Gotti, G. Mazzotti, and M. Falcon 2011, Toxicol. In Vitro 25: 64-72; González-Palma, I., H.B. Escalona-Buendía, E. PonceAlquicira, M. Téllez-Téllez, V.K. Gupta, G. DíazGodínez, and J. Soriano-Santos 2016, Front. Microbiol. 7: 1-9; Lee, Y.L., G.W. Huang, Z.C. Liang, and J.L. Mau 2007, LWT-Food Sci. Technol. 40: 823-833; Özdal, M., 2018, J. Mol. Biol. Biotechnol. (Molbiotech). 2(2): 24-27; Özdal, M., Ö. Gülmez, Ö.G. Özdal, and Ö.F. Algur 2019, Food And Health. 5(1):12-18; Özgüneş, H., and T. Atasayar 2009, Turkiye Klinikleri J. Med. Sci. 29(4): 976-986; Patel, S., and A. Goyal 2012, 3 Biotech. https://doi.org/10.1007/s13205-011-0036-2; Pavlidou, V. , L. Karpouhtsis, G. Franzios, A. Zambetaki, Z. Scouras, and P. Mavragani-Tsipidou 2004, J. Agric. Urban. Entomol. 21:39-49; Rao, S.V., Muralidhara. S.C. Yenisetti, and P.S. Rajini. 2016, Neurotoxicology 52: 230-42; Shapiro, S., A. Meier, and B. Guggenheim 1994, Oral. Microbiol. Immunol. 9(4): 202-208; Togar, B., H. Turkez, A. Hacimuftuoglu, A. Tatar, and F. Geyikoglu 2015, J. Intercult Ethnopharmacol. 4(1): 29–33; Togar, B., K. Çelik, and H. Türkez 2015, Braz. Arch. Biol. Technol. 58(1):61-67; Turkoglu, A., M.E. Duru, N. Mercan, I. Kivrak, and K. Gezer 2007, Murrill. Food. Chem. 101: 267-273; Uysal, H., T. Şişman, and H. Aşkın 2006, *Drosophila* Biyolojisi ve Çaprazlama Yöntemleri. Erzurum, Türkiye ISBN:975-442-111-0; Vamanu, E., 2012, Molecules 17(4): 3653-3671; Yildiz, O., Z. Can, A.Q. Laghari, H. Şahin, and M. Malkoç 2015, J. Food. Biochem. 39:148-154; Younis, A.M., F.S. Wu, and H.H. El Shikh 2015, Int. J. Med. Mushrooms. 17: 579-590.

Variable fitness effects of *Drosophila* mutant markers across genetic backgrounds, temperatures, and containers.

Shoben, Chelsea R., and Mohamed A.F. Noor. Biology Department, Duke University, Durham, NC, USA.

Introduction

Morphological mutant markers have been a mainstay for *Drosophila* genetics research for over a century, and they were used to develop the first linkage maps (Morgan *et al.,* 1915). Even today, such mutations are still used to tag specific regions of the genome for study. One area of special interest in this regard is the study of recombination. While recombination rates can be assayed using molecular markers, larger numbers of flies can be assayed for recombination using pairs of morphological mutant markers at lower cost and effort.

However, such morphological mutant markers are well-known to affect fitness, and such fitness effects can bias estimates of recombination, because certain genotypes are less likely to make it to adulthood and be scored. One way of assessing this effect is to compare the recovery of genotypes within two classes: non-recombinant and recombinant (*e.g*., Hunter *et al.,* 2016). In a backcross between an F_1 heterozygous for two mutations in the same gametic phase, one expects recovery of similar numbers of wildtype and double-mutant backcross progeny (the non-recombinant class). Similarly, one expects similar numbers of each of the two single-mutant backcross progeny (the recombinant class).

We initially sought to build on the GWAS analysis of Hunter *et al.* (2016) by identifying variation associated with temperature-induced recombination rate plasticity. We employed an experimental design

similar to theirs (albeit using different morphological markers) and did a backcross between a subset of the DGRP (Drosophila Genetic Reference Panel; Mackay *et al.,* 2012) lines and a double-mutant stock. However, as described below, we found unexpected fitness effects of the mutations that varied by genetic background, by temperature, and even by the type of container which housed the flies.

Materials and Methods

Nine DGRP lines (41, 309, 360, 492, 555, 861, 879, 882, 897) were obtained from the Bloomington Stock Center in Bloomington, IN in August of 2019. The autosomal mutant line (*e/st*) used in the crossing scheme (st[1] cv-d[H209] e[1], RRID:BDSC_63067) was obtained from the Bloomington Stock Center in November 2019. Both the mutation in the *ebony* gene and the *scarlet* gene of the *e/st* line are recessive, with homozygous mutants having black bodies and bright red eyes, respectively. DGRP lines are wildtype for these two phenotypic traits. Stocks were kept at 24°C, and experimental crosses were conducted at their respective temperature (24°C control or 29°C experimental). All stocks and experiments were executed under a 12-hour light/ dark cycle, and efforts were made to keep relative humidity at 65% or higher. All maintenance and experimental crosses were conducted on media consisting of dextrose, sucrose, yeast, and agar in either plastic vials with 8 mL of media or plastic bottles with 30 mL of media.

A series of crosses were conducted at two temperatures (24°C control, and 29°C experimental) to resolve variation in crossover rate plasticity between the *ebony* and *scarlet* genes among the DGRP lines. First, virgin DGRP females (5-7 days old) were crossed to male *e/st* (5-7 days old) at either 24°C or 29°C in vials (1X cross) to create wildtype heterozygous progeny. An equal ratio of males to females were set up for each cross, ranging from a total of 10 to 30 flies. 48 hours after 1X cross set up, flies were moved from vials to bottles. Ten virgin heterozygous female offspring from the 1X cross were collected within the first four days of offspring eclosion, aged for 6-7 days, and then backcrossed to ten 7-day-old *e/st* males in vials to create the 2X cross for each experimental treatment (each line at each temperature). 48 hours after 2X set up, flies were moved from vials to bottles. Five days after flies were put into the bottle, the adults were removed. Resulting progeny from the 2X cross containers were scored for body and eye color, with double wildtype and double mutant (black body and bright red eyes) classified as non-recombinant, and only black body or only bright red eyes classified as recombinant. Due to variation in development timing between temperatures, only the first 8 days of enclosed progeny from each 2X cross container were used in the analysis for the 29°C 2X crosses. Progeny from the first 10 days of eclosion were used from the 24°C 2X crosses. Flies collected past the 8 or 10 day mark, respectively, risked being 3X progeny. 2X progeny were collected, frozen at -20°C for 45 minutes to 1 hour, and stored at 4°C to be scored within 72 hours from time of freeze. Chi-square analyses were done using the website http://www.quantpsy.org/chisq/chisq.htm (Preacher, 2001).

Results

Table 1 presents the phenotypic counts separated by temperature, line, and container type. If there are no fitness effects and no transmission ratio distortions, then we predict similar counts within the two non-recombinant and within the two recombinant classes. The most striking deviations from symmetry were observed in the 29°C treatment non-recombinant classes, in which *e/st* progeny counts never exceeded 3 even when more than 40 non-recombinant offspring were produced. Higher temperature and production in vials both independently contribute to this strong asymmetry: crosses conducted in vials magnified the asymmetry compared to bottles in both temperature conditions; however, higher temperature further increased the observed asymmetry. Effects of genotype (line) are less pronounced, with results from a chi-square analysis across the 9 lines of the non-recombinant class counts for 24°C only marginally statistically significant (chi-square = 14.661, 8 df, $p = 0.066$). However, doing the same analysis of the 9 lines on the non-recombinant class counts at 24°C in vials, the result is more striking than in bottles (chi-square = 20.336, 8 df, $p = 0.009$), suggesting that there is some variation in the degree of asymmetry by background genotype. All of these patterns are less striking when examining asymmetry in the recombinant classes, suggesting the fitness effects are especially pronounced in interactions between the *ebony* and *scarlet* mutations.

Table 1. Counts of phenotypes recovered from backcross to double mutant line, separated by temperature, by DGRP line, and by container (V=vial, B=bottle). Line 41 backcross progeny were not recovered at 29°C.

		24°C				29°C			
Stock #	Line	Nonrecombinants		Recombinants		Nonrecombinants		Recombinants	
N N		+/+	e/st	e/+	+/st	+/+	e/st	e/+	+/s
28166	309V	52	19	10	9	68	1	5	6
	309B	127	84	22	28	61	17	22	5
25186	360V	57	17	11	11	55	1	6	4
	360B	88	72	24	14	84	33	22	10
28203	492V	44	14	16	16	37	0	10	6
	492B	94	88	39	40	58	14	22	9
25198	861V	64	10	4	8	25	3	8	5
	861B	101	72	8	5	61	16	13	3
28254	879V	39	2	13	12	41	1	7	4
	879B	84	64	29	33	81	38	15	16
28255	882V	50	12	23	6	48	1	15	3
	882B	112	58	51	30	73	28	23	14
28260	897V	52	5	15	11	14	0	7	2
	897B	60	58	31	27	33	9	5	3
28126	41V	31	14	11	4	N/A			
	41B	37	35	11	10				

Discussion

The expectation from our backcross to an autosomal mutant line was similar recovery of the two non-recombinant phenotypes and similar recovery of the two recombinant phenotypes. We saw a striking deviation from this expectation particularly in the case of the non-recombinant phenotypes: wildtype progeny were more abundant than the double-mutant class. This bias toward wildtype progeny was more striking at 29°C than at 24°C, when flies were reared in vials rather than in bottles, and in some genotypic backgrounds (DGRP lines) over others.

We assayed offspring for a set number of days after eggs were laid to limit the possibility that we accidentally score offspring from a subsequent generation. As such, we cannot exclude the possibility that, rather than "fitness" per se, the less-abundant class simply had much slower development time. That said, slower development time would generally reduce fitness in an evolutionary sense, and would still bias estimates of recombination if offspring from multiple generations were intermingled. We did continue to score past the formal end of experiment dates reported in our table, and larger-still fractions of wildtype offspring emerged, demonstrating the practical issue with waiting longer for the missing phenotypic class.

While temperature- or genotype-specific effects of morphological mutations are perhaps expected, the container-specific effect was unusual. We hypothesize that the smaller volume of media in vials than bottles contributed to higher larval density and competition, wherein the wildtype progeny were at an advantage over the double-mutant ones.

Overall, our study provides a strong cautionary note to the use of morphological mutant markers. Simply checking for similar recovery of non-recombinant or of recombinant classes in one temperature, in one type of container, or in one genotypic background does not necessarily generalize. While morphological mutant markers may provide a means of rapid genotyping, their fitness (or perhaps more precisely, development time) effects can often result in mis-estimation of recombination rates in unmarked flies and in nature.

Acknowledgments: We thank Brenda Manzano-Winkler for assistance with this project and for comments on this manuscript. Stocks obtained from the Bloomington Drosophila Stock Center (NIH P40OD018537) were used in this study.

References: Hunter, C.M., W. Huang, T.F.C. Mackay, and N.D. Singh 2016, PLoS Genet. 12: e1005951; Mackay, T.F.C., *et al.,* 2012, Nature 482: 173-178; Morgan, T.H., A.H. Sturtevant, H.J. Muller, and C.B. Bridges 1915, *The Mechanism of Mendelian Heredity*. H Holt and Company, New York, NY; Preacher, K.J., 2001, Calculation for the chi-square test: An interactive calculation tool for chi-square tests of goodness of fit and independence. URL: http://quantpsy.org. Date of access: 22-August-2020.

The *Drosophila Antennapedia* mutation is associated with sex-specific effects on circadian activity rhythms.

He, W., T. Renoni, S. Brigida, and B. Possidente. Biology Department, Skidmore College, Saratoga Springs, NY 12866; email: bposside@skidmore.edu

Introduction

Drosophila locomotor activity has been widely used as a marker for circadian clock function, facilitating an in-depth understanding of the molecular, anatomical, and physiological properties of a central light-entrainable circadian clock composed of a network of neurons in the brain (Hardin, 2011). Circadian rhythms may, however, be driven by more than one endogenous biological clock as a function of a circadian system of coupled pacemakers and oscillators (Brown *et al.*, 2019). The third segment of the antennae in *Drosophila,* for example, which has a high density of odor receptors (de Bruyne *et al.*, 2001) has a peripheral circadian oscillator regulating olfaction (Tenoue *et al.*, 2004; Zhou *et al.*, 2005). Here we ask whether the peripheral circadian oscillator located in the third antennal segment plays a role in regulating the circadian activity rhythm by comparing locomotor activity in wild-type flies to homeotic *Antennapedia* mutants (*Antp*) whose antennae are transformed into ectopic legs. We used the dominant, temperature sensitive allele *Antp*$^{[73b]}$, originally isolated against an Oregon-R wild type background, which transforms the antennae into legs in a proximal to distal manner (Postlethwaite and Schneiderman, 1971), starting with the second antennal segment, although a microscopic patch of third antennal segment, approximately 1,000-2,000 square microns, remains untransformed in *Antp[73b]* (Stocker, 1976; Possidente *et al.*, 1990). Despite their ectopic location, the homeotic legs provide neural input to the brain (Stocker *et al.*, 1976). We outcrossed the *Antp* mutation to a wild-type Oregon-R strain, and selected flies with 100% expression from the F2 generation. We show that *Antp* flies display robust entrained and free-running circadian activity rhythms despite the replacement of their antennae by legs. Segregation of the *Antp* mutation in the F2, however, was associated with altered patterns of circadian activity in a sex-specific manner. These results suggest that the peripheral circadian oscillators in the antennae, while not necessary for expression of the circadian locomotor activity rhythm, may modulate the waveform of the locomotor activity rhythm in wild-type flies and may also play a role in sex-specific differences in entrained circadian locomotor activity rhythms typically observed in the lab (Helfrisch-Förster, 2000).

Methods

We conducted three replicate experiments, each starting with a cross between Oregon-R females (Skidmore College stock obtained in 1983 from Carolina Biological Supply, Wilmington, NC USA) and *Antp* males (Bloomington Stock Center #2259). The *Antp* mutation in this stock, a homozygous lethal, is balanced against a TM3 chromosome marked with the dominant Stubble mutation. F1 flies inherit either the *Antp* or the balancer chromosome in a 50/50 ratio. We selected only *Antennapedia* males and virgin females from the F1 progeny and crossed them to generate the F2. The expected 25% homozygous *Antp* flies are a lethal genotype. Among the viable F2 flies, two thirds are expected to be heterozygous for the dominant *Antp* mutation and one third should be wild type, both sharing a common Oregon-R genetic background derived from the original parent strains. Expression of *Antp* in the F2 flies was variable, and we selected only adults with fully transformed antennae as subjects, and phenotypically wild-type flies as controls. All three replicates were raised, bred and tested in a 12:12 LD photoperiod in Percival model 36VL incubators set at 25° C. Ten to 15 vials of four males and four virgin females were made for each cross. Parents were cleared on the seventh day post-mating and collected for activity monitoring on day fourteen so that subjects ranged in age from one to four days old. Flies were maintained on Carolina 4-54 Instant *Drosophila* Medium (Carolina Biological Supply, Wilmington, NC, USA) in polycarbonate shell vials 75mm tall and 23mm in diameter. Circadian activity rhythms were assayed in Trikinetics DAM2 *Drosophila* Activity Monitors (Waltham, MA USA) and data collected in ten-minute bins using Trikinetics DAMSystem3 software. Individual flies were placed in polycarbonate tubes 65mm long with a 5mm outer diameter. Each tube contained approximately one cm of agar food (2% agar and 5% sucrose) sealed with a plastic cap at one end, and a cotton plug at the other end. Thirty-two flies of each sex and genotype were assayed in each of two replicate experiments, and 16 of each in a third replicate. Flies were anesthetized with FlyNap (Carolina Biological Supply) and placed in the monitors at approximately 1600 hours. Data were downloaded starting at midnight for two days in a 12:12 LD cycle, followed by 10 days in constant dark. Activity counts were analyzed with RhythmWatch software (Minimitter Corporation, Bend, OR USA). Variables scored for each fly were mean activity counts per 10-mintues in 12:12 LD (XLD), only the 12 hours of light during entrainment (XL), only the 12 hours of dark during entrainment (XD), and activity in constant dark (XDD). The ratio of daytime activity to total activity (XL/XLD = LDratio) provides a measure of the distribution of activity between the light and dark phases of the 12:12 LD photoperiod. Free-running circadian period in constant dark (tauDD) was assayed using Actogram-J software (Schmid *et al.*, 2011). TauDD was only estimated for flies surviving for at least 10 days in order to minimize and standardize aging effects, and to maximize the number of circadian cycles in DD for estimation of the circadian period. Ten-day survival rate was significantly less for *Antp* flies than Oregon-R ($p < 0.05$, chi-square). TauDD was estimated using both the Bushell-Sokolove and Lombard Scargle Chi-Square periodogram. Flies showing a statistically significant circadian period ($p < 0.05$) within a 20-28-hour range for both measures were labelled “rhythmic” and their two period estimates were averaged to estimate tauDD. All other flies were labelled “arrhythmic” and their data were not included in tauDD estimates. There were no significant differences in the proportion of rhythmic flies among the male and female wild-type and *Antp* treatment groups. Actogram-J was also used to construct composite actograms (from all subjects regardless of rhythmicity scores).

Results

F2 *Antp* flies displayed sex-specific differences in circadian activity rhythms with females showing more effects than males (Tables 1, 2; Figure 1). Males expressing *Antp* displayed significantly less night-time activity than wild-type males (XD) and, as a result, the overall proportion of male activity in the daytime in the 12:12 LD photoperiod was significantly greater than wild-type males when measured as LDratio. *Antp* females were significantly less active than wild type females for all measures of activity (mean activity in the 12:12 LD photoperiod (XLD), daytime activity (XL), nighttime activity (XD), and activity in constant darkness (XDD)). These differences were observed in all three replicates, with no genotype by replicate interactions except for XD in females where nighttime activity decreases were significantly greater in some replicates than others. Since activity decreases in females were proportional between daytime and nighttime

the overall LDratio was not significantly altered in female *Antp* flies. XLD and XD showed significant three-way interactions among genotype, sex and replicate, and LDratio sex differences also showed a replicate effect, so interactions between sex and genotype were not as consistent across replicates as main effects of genotype. *Antp* F2 females displayed a longer free-running circadian period than wild-type F2 flies in all three replicate experiments suggesting that the *Antp* mutation alters circadian clock function in females in addition to decreasing activity levels.

Table 1. ANOVA p-values for circadian locomotor activity measures for Oregon-R wild type and mutant *Antp*$^{[73b]}$ F2 flies.

ANOVA	XLD	XL	XD	XDD	TAUDD	LDRATIO
Genotype	*	ns	***	**	**	**
Sex	ns	ns	***	ns	***	***
Replicate	**	**	***	***	ns	***
Gen*Sex	**	***	ns	***	ns	ns
Gen*Rep	ns	ns	ns	ns	ns	ns
Sex*Rep	ns	ns	ns	ns	ns	**
Gen*Sex*Rep*	*	ns	*	ns	ns	Ns

* ($p < 0.05$), ** ($p < 0.01$), *** ($p < 0.001$), ns (non-significant: $p > 0.05$)

Table 2. Mean (± SEM) and sample size for circadian locomotor activity measures for Oregon-R wild type and mutant *Antp*$^{[73b]}$ F2 flies.

VARIABLE	*Antp* FEMALES	*Antp* MALES	OR-R FEMALES	OR-R MALES
XLD	5.7 ± 0.3 (69)	7.1 ± 0.6 (46)	8.0 ± 0.4 (76)	7.5 ± 0.4 (72)
XL	7.7 ± 0.5 (69)	8.2 ± 0.8 (46)	10.3 ± 0.5 (76)	7.4 ± 0.5 (72)
XD	3.4 ± 0.2 (69)	6.0 ± 0.6 (46)	5.8 ± 0.4 (76)	7.7 ± 0.5 (72)
XDD	5.4 ± 0.4 (63)	7.3 ± 0.8 (39)	9.4 ± 0.4 (73)	6.8 ± 0.4 (70)
tauDD	24.9 ± 0.05 (57)	24.4 ± 0.1 (35)	24.66 ± 0.06 (64)	24.24 ± 0.06 (64)
Ldratio	1.35 ± 0.03 (69)	1.14 ± 0.04 (46)	1.29 ± 0.03 (76)	0.99 ± 0.03 (72)

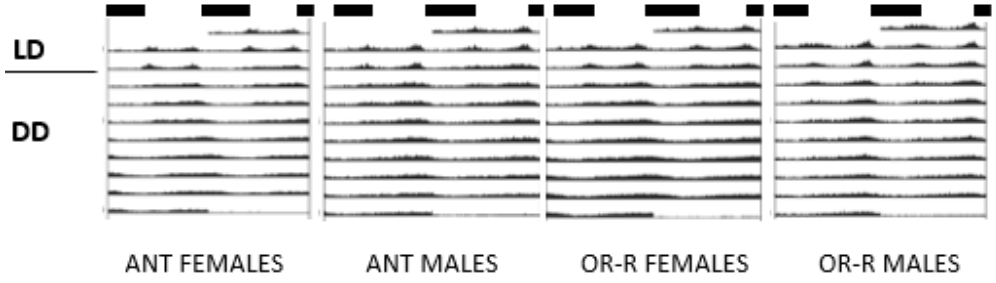

Figure 1. Composite actograms for each treatment group combined across three replicates. The X-axis is 48 hours. The Y-axis shows ten successive days of locomotor activity with the first two days in the 12:12 LD cycle followed by eight days in constant darkness. Twenty-four-hour periods of activity are double plotted so that the first row represents day one (hours 25-48), and the second row repeats day one from hours zero to 24 followed by day two. Each day is repeated in this fashion through day 10. Light-dark bars show the photoperiod for the first two days.

Discussion

Here we show that the *Antp* mutation, segregating in an F2 generation against an Oregon-R background, is associated with a significant decrease in activity in female flies, an increase in diurnal activity in males, and an approximate 15-minute lengthening of the free-running circadian period. We suggest that these results are consistent with a modulatory input from the circadian antennal oscillator to the circadian locomotor activity rhythm driven by the light-sensitive central circadian pacemaker. Such an influence could be direct or mediated through altered brain development in *Antp* flies resulting from abnormal innervation from the ectopic legs replacing antennae. A simpler interpretation is that the physical anomaly of legs replacing antennae may alter activity levels, but this seems unlikely since *Antp* males displayed activity levels comparable to wild-type flies. It's also possible that the *Antp* mutation influences circadian locomotor activity patterns through pleiotropic effects, for example on nervous system development, since *Antp* protein is expressed in neuromere progenitors of the brain in 10-hour *Drosophila* embryos (Wirz *et al.*, 1986) in addition to its main expression in the embryonic thorax. Since we only outcrossed *Antp* for two generations, differences in circadian activity rhythms may also be caused by allelic differences between the two different Oregon-R sub-strain backgrounds that remained linked to the *Antp* locus. Our results also suggest that input from the Antennae contribute to the typical pattern of sex-differences in circadian locomotor activity observed in *Drosophila melanogaster* in the lab (Helfrich-Förster, 2000), since the decrease in overall activity we observed in *Antp* females, and the shift in *Antp* males toward more diurnal behavior are both contrary to typical sex-differences in activity patterns in wild-type flies. This observation is consistent with Kent *et al.*'s (2008) findings that show pheromonal regulation of circadian locomotor activity rhythms in *Drosophila*. Overall, our results are consistent with a role for a peripheral circadian oscillator in the antennae in modulating circadian activity rhythms driven by a central clock in the brain. Effects on mean activity levels likely occur downstream from a central circadian clock, but our observation of a small increase in free-running circadian period suggests some input to central circadian clock mechanisms. Further studies are needed to confirm an association between the $Antp^{[73b]}$ mutation and changes in circadian locomotor rhythms and to clarify potential mechanisms involved.

References: Brown, A.J., J.S. Pendergast, and S. Yamazaki 2019, Yale J. Bio. Med. 92: 327-335; de Bruyne, M., K. Foster, and J.R. Carlson 2001, Neuron 30(2): 537-552; Hardin, P.E., 2011, Adv. Genet. 74: 141-173; Helfrich-Förster, C., 2000, J. Biol. Rhythms 15: 135-154; Kent, C., R. Azanchi, B. Smigh, A. Formosa, and J.D. Levine 2008, Current Biology 18: 1384-1389; Possidente, D.R., J. Greaux, and B. Possidente 1990, Heredity 65: 321-327; Postlethwaite, J.A. and H.A. Schneiderman 1971, Dev. Biol. 25: 606-640; Schmid, B., C. Helfrisch-Förster, and T. Yoshii 2011, J. Biol. Rhythms 26: 464-467; Stocker, R.F., J.S. Edwards, J. Palka, and G. Schubiger 1976, Dev. Biol. 52: 210-220; Tanoue, S., P. Krishnan, B. Krishnan, S.E. Dryer, and P.E. Hardin 2004, Curr. Biol. 14: 638–649; Wirz, J., I. Liselotte, and W. Gehring 1986, EMBO 5: 3327-3334; Zhou, X., C. Yuan, and A. Guo 2005, J. Biol. Rhythms 20: 237-244.

List of species of Family Drosophilidae described and recorded from North Chotanagpur Division of Jharkhand, India.

Mahato, Shakti Pada, and Kishore Kumar Gupta. University Department of Zoology, Vinoba Bhave University, Hazaribag; Author for correspondence - Email: shakti.eco@gmail.com

Family – Drosophilidae

Subfamily – Steganinae
Genus - *Amiota* Loew

Subgenus – *Phortica* Schiner

1. *Amiota (Phortica) shillongensis* Singh & Gupta, 1979

Subfamily – Drosophilinae
Genus – *Drosophila* Fallen

Subgenus – *Dorsilopha* Sturtevant

2. *Drosophila (Dorsilopha) busckii* Coquillet, 1901

Subgenus – Sophophora Sturtevant

3. *Drosophila (Sophophora) melanogaster* Meigen, 1830
4. *Drosophila (Sophophora) kikkawai* Burla, 1954
5. *Drosophila (Sophophora) jambulina* Parshad & Paika, 1979
6. *Drosophila (Sophophora) ananassae* Doleschall, 1858
7. *Drosophila (Sophophora) bipectinata* Duda, 1923
8. *Drosophila (Sophophora) malerkotliana* Parshad & Paika, 1964
9. *Drosophila (Sophophora) eugracilis* Bock & Wheeler, 1972
10. *Drosophila (Sophophora) biarmipes* Malloch, 1924
11. *Drosophila (Sophophora) takahashii* Sturtevant, 1927
12. *Drosophila (Sophophora) trilutea* Bock & Wheeler, 1972

Subgenus – *Drosophila* Fallen

13. *Drosophila (Drosophila) immigrans* Sturtevant, 1921
14. *Drosophila (Drosophila) nasuta* Lamb, 1914
15. *Drosophila (Drosophila) albomicans* Duda, 1923
16. *Drosophila (Drosophila) annulipes* Duda, 1924
17. *Drosophila (Drosophila) penispina* Singh & Gupta, 1979

Genus – *Scaptodrosophila*

18. *Scaptodrosophila bryani* Malloch, 1934

Genus – *Zaprionus* Coquillett

Subgenus – *Aprionus* Okada

19. *Zaprionus (Aprionus) pyinoolwinensis* Wynn & Toda, 1988

Subgenus – *Zaprionus* Coquillett

20. *Zaprionus (Zaprionus) indianus* Gupta, 1991

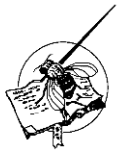

A survey of drosophilid fauna of the Guilan province in north Iran.

Khadem, M. Faculdade de Ciências da Vida, Universidade da Madeira, Portugal; khadem@staff.uma.pt

Drosophila genus has been used as a model organism in different areas of biology for more than a century. So far about 3500 species of drosophilidis have been identified worldwide; 370 of them are recorded in the Palearctic region (Bachli, 2008). In Iran, traditionally, the drosophilids fauna have not received much attention since in general they are considered not to be harmful. In recent years, due to invasions of the two harmful drosophilidade species (*Zaprianus indianus* and *Drosophila suzukii*), the researchers have paid more

attention to this rich and interesting fauna and some surveys have been done (Parchami-Araghi and Mohammadi-Khorramabadi, 2009; Parchami-Araghi *et al*., 2015, 2016).

This report describes a survey of drosophilids from two adjacent areas in north Iran, near the city of Rasht. The survey was conducted firstly, at the campus of the University of Guilan (coordinates 37º 16´50 N, 49º 34´ 59 E) and secondly, samples were taken from the edge of Saravan forest (37º 19´ 80 N, 49º 66´77 E) ~10 Km from the campus. The samplings were carried out during October and November 2019. Flies were collected in the early morning and the late afternoon by the netting of open banana baits. The captured flies were transferred to the laboratory for separation and kept in capped bottles containing alcohol (70%) for further identification.

A total of 1132 (386 females and 746 males) samples were collected from the University of Guilan campus (1st site) and 148 (95 females and 53 males) near Saravan forest (2nd site). The significant difference in the number of the samples in the two sites is related to the difference in duration and number of collections between them, being more frequent at the University location. Altogether 9 Drosophilidae species were present in the collections (Table 1).

Table 1. The number and frequency of the drosophilids samples in two localities near city of Rasht in North of Iran.

	University of Guilan Campus (site 1)			Saravan forest (site 2)		
Species	nº	female%	male%	nº	female%	male%
Zaprionus indianus	210	36.7	63.3	72	57	43
Drosophila busckii	18	44.4	55.6	0	0	0
Drosophila immgrans	16	50	50	4	0	100
Drosophila melanogaster	322*	36.7	10.2	57*	73.7	1.7
Drosophila simulans			53.1			24.6
Drosophila repleta	11	36.4	63.6	0	0	0
Drosophila hydei	0	0	0	1	100	0
Drosophila subobscura	371	38	62	14	78.6	21.4
Drosophila suzukii	183	16.4	83.6	0	0	0
Total sample	1132			148		

* indicates the combined number of females of the two sibling species (D. melanogaster & D. simulans) due to difficulties in their identification.

At the 1st site *D. subobscura* was the most abundant species (371/1132 = 32.8%), followed by melanogaster (322/1132 = 28.4%) sibling species (*D. melanogaster* and *D. simulans*), *Zaprionus indianus* (201/1132 = 18.5%), and *D. suzukii* (183/1132 = 16.2%). In all of these cases males were more numerous compared to females (Table 1). Three more species were also present but with a very low frequency (0.9-1.6%).

At the 2nd site *Zaprionus indianus* was the most common species (72/148 = 48.9%) followed by *melanogaster* sibling species (57/148 = 38.5%) and *D. subobscura* (14/148 = 9.4%). Unlike the 1st site females were more numerous than males at the 2nd site. *Drosophila suzukii* was not captured at the 2nd site (Table 1). This pest species was first discovered in Japan (Kanazawa 1934), and it has invaded Asian, European, and American continents (for review Calabria *et al.*, 2012). In Iran, *D. suzukii* was first reported in 2015 (Parchami-Araghi *et al*., 2015). The authors suggested that this species entered Iran through the Pakistan border. Therefore, the absence of *D. suzukii* at the 2 nd site only indicates its temporary absence at the time of

the collection since this site is on the route to the 1st site. *D. subobscura* was also significantly more frequent at the 1st than the 2nd site (Table 1). The greater number of specimens at the 1st site cannot solely account for the higher frequencies of *D. suzukii* and *D. subobscura,* so other causes such as anthropogenic factors, microclimate differences, local vegetations and so forth could have played an important role in their prevalence. These factors could also be related to the differences in numbers of females/males at the two sites. Long term and seasonal sampling are necessary to give a clear picture to the species abundances at different sites. A similar work surveying the Drosophildae in north Croatia from two vineyards separated by 15 km and sharing the same microclimate (Zivkovic *et al*., 2016) showed that in one vineyard *D. suzukii* was the most abundant species at 90%, compared with 7% at the other. In the same study, Zivkovic *et al*. (2016) reported a low number of *D. subobscura* in their samples that can be related to the sampling vegetations. This species has been reported to be quite abundant in Europe (Calabria *et al*., 2012; Zengin, 2020).

The other invasive species in our samples, *Zaprionus indianus*, first reported in south Iran (Parchami-Araghi and Mohammadi-Khorramabadi, 2009) have since spread throughout the country (Parchami-Araghi *et al*., 2015). In the present work *Z. indianus* specimens were found in both sampling sites although more frequently at the 2nd site (18.5% and 48.6%, respectively).

Acknowledgment: I am grateful to Dr. A. Sahragard (Faculty of Agriculture, University of Guilan, Guilan, Iran) for making this research possible.

References: Bachli, G., 2008, TaxoDros, http://taxodros.uzh.ch; Calabria, G., J. Máca, G. Bachli, L. Serra, and M. Pascual 2012, J. applied Entomology 136: 139-147; Kanazawa, T., 1934, Studies on a fruit fly, *Drosophila* sp. Kontyua 8: 302-303; Krimbas, C., 1993, *Drosophila subobscura* Biology, Genetics and Inversion Polymorphism. Verlag Dr. Kovac, Humburg; Parchami-Araghi. M., and A. Mohammadi-Khorramabadi 2009, Short note No. 9/2009. Studia Dipterological 16(1/2): 243-244; Parchami-Araghi, M., E. Gilasian, and A.A. Keyhanian 2015, Dros. Inf. Serv. 98: 59-60; Parchami-Araghi, M., E. Gilasian, R Vahabzadeh, and G. Bachli 2016, Dros. Inf. Serv. 99: 63-69; Zivkovic, I., B. Baric, D. Lemic, I Blazevic, M. Subic, G. Seljak, and A. Mesic 2016, Agric. Conspec. Sci. 81 (4): 231-234.

Influence of urea on the morphology of *D. melanogaster.*

Shivanna*, N., B.S. Srinath, and A.S. Tarafdar. Department of Zoology, Karnatak University Dharwad – 580 003; *Corresponding author email: drnshivanna@rediffmail.com

Abstract

The influence of urea on the morphological characters of *D. melanogaster* was studied. The concentration of 10%, 20%, 30%, and 40% of urea was treated along with control on the first instar larvae. The larval mortality was observed and it showed 50% mortality for 40% urea concentration. Then the length and breadth of pupae was measured. It revealed a significant difference ($P < 0.01\%$) between different concentrations of urea treatment. Later the different morphological characters of metamorphosed adult flies of both males and females such as Face Width (FW), Head Width (HW), Thorax Length (TL), Wing Length and Wing Width (WW) were quantified separately. It revealed a significant difference ($P < 0.001\%$) between the different characters and also it showed that as the concentration of urea increased the size of the morphological characters increased. The *t* test was conducted to check the difference between male and female morphological characters. It revealed a significant difference between male and female flies. The study mainly highlights that maximum urea concentration can cause 50% mortality in larvae, and the ones that survived have shown to have developed larger morphological characters.

Introduction

In nature many a time an organism or a population is tested for its survival and reproduction by various factors such as a novel chemical. The organism has to use its physiological mechanism to overcome

the novel chemical (if toxin) when the animal is not able to avoid it behaviourally (Etienne *et al.,* 2001). In such a situation significant changes might occur in the life history traits of the animal such as life span, productivity, size variations, maturation, and so forth (Saaristo *et al.,* 2018).

Drosophila melanogaster is a popular model organism used in biological research. Its cosmopolitan nature, robustness in survival and development in minimum laboratory conditions makes this organism suitable for versatile experiments. *Drosophila* has been used in many toxicological experiments where it has been treated with several toxic chemicals (Herskowitz, 1951; Vogel and Nivard, 1993; Affleck *et al.,* 2006; Eom *et al.,* 2017).

Urea is a common toxin found in the natural environment. It is one of the major excretory products and occurs in high levels in many organisms such as sharks, mammals and associated microorganisms (Yancey *et al.,* 1982). It interferes with basic cell processes (Etienne *et al.,* 2001 c.f.). Effect of urea has been studied in *Drosophila melanogaster* with respect to its viability, mean development time, short and long term exposure, mechanisms to larval adaptation, tolerance, osmoregulation and Pupation Site Preference (PSP) (Botella *et al.,* 1983, 1985; Joshi *et al.,* 1996, 1998; Pierce *et al.,* 1999; Etienne *et al.,* 2001; Borash *et al.,* 2000; Shivanna *et al.,* 2012; Belloni *et al.,* 2018).

Natural populations of *D. melanogaster* show adaptive geographic variation in adult body size. Conditions during larval development also affect adult size with larger flies emerging at lower temperatures (Zoltan *et al.,* 2003). Adult body size in insects is determined by the duration of growth period and the amount of mass gained during that period. The differential sensitivity of the physiological processes that regulate the body size may enable insects to adjust body size in response to simultaneous variation to multiple types of environmental stimuli (Davidowitz *et al.,* 2004).

Many workers used thorax length as the index of body size in *Drosophila*. Wing length is another phenotypic trait that can be used as an index of body size. Wing was known to exhibit sexual dimorphism in overall size and the X-chromosome was shown to have a substantial effect on wing length (Sokoloff, 1966; Bird and Schaffer, 1972; Patridge *et al.,* 1987; Santos *et al.,* 1988, 1992). Mating success, larval gene expression, environmental variation and temperature with relation to body size, heritability, phenotypic and genetic correlations of size and shape of different species of *Drosophila* was studied (Singh and Singh, 1999; Blanche and Klaczho, 1999; Imasheva *et al.,* 2000; Zoltan *et al.,* 2003; Davidovitz *et al.,* 2003).

The effect of urea on size of the pupae and morphology of adult flies of *D. melanogaster* has not been analysed. In view of these lacunae the present study has been undertaken.

Materials and Method

Stock culture

D. melanogaster flies were obtained from *Drosophila* Stock Center, Department of Zoology, University of Mysore, Mysuru. The stocks were maintained at a constant temperature of 22 ± 1°C and RH 80% in the laboratory.

Synchronization of age

Uniformity was maintained with respect to larval age and density of larval population during development. The eggs were collected as per the Delcour method modified by Ramachandra and Ranganath (1988). About 200-250 well fed adults aged 5-7 days were released into a wide mouthed bottle and were starved for 6 hours. At the end of this starvation period, a small container filled with Delcour medium, supplemented with layer of yeast was introduced into the bottle containing starved flies. Abundant egg laying ensued when the flies were provided with food and at the same time stimulated by acetic acid. The first batch of eggs (laid overnight) was discarded and the subsequent batches of eggs were harvested at regular intervals of 3 hours. The eggs thus collected were placed in petri dish of 4 inch diameter or culture bottle containing standard wheat cream agar medium seeded with yeast and were stored at 22±1°C. First instar larvae about 50 from the culture were isolated and transferred into vials (10×3.8) containing equal quantity of wheat cream agar media. Wheat cream agar medium was prepared as per the procedure described by Shivanna *et al.* (1996).

Urea treatment

The eggs collected by Delcour method were allowed to hatch. After hatching equal numbers of first instar larvae (50) were isolated and transferred to vials containing an equal quantity of fresh wheat cream agar medium with different concentrations of urea (10%, 20%, 30%, and 40%) (Shivanna *et al.,* 2012) and one set of control was maintained. Yeast granules were dissolved in different concentrations of urea and added to vials every day. Control was maintained by dissolving yeast granules in distilled water and was fed to the larvae every day. Ten replicates were carried out for control and all treatment experiments.

Morphometric analysis

The size of the pupae and the morphometric traits [Face Width (FW), Head Width (HW), Thorax Length (TL), Wing Length, and Wing Width (WW)] of urea treated and control flies were measured using stereo microscope attached with image analyser ProgRes C3 (ProgRes Image Capture Software) (Figure 1A and B). The length (from anterior spiracle to posterior spiracle of the pupae) and breadth (from left to right in the middle region of pupae) of the pupae (Figure 1C) was measured in mm, and the mean values were based on the data collected from 25 replicates of each concentration. SPSS software 16.0 version was used for data analysis. The data were subjected to one way ANOVA to assess the level of significance between length and breadth of pupae at different concentrations.

The morphometric traits of adult male and female flies from treated and control experiments were measured separately. The mean values were calculated based on the data collected from 10 replicates for each concentration of urea and control. The data of morphometric traits (FW, HW, TL, WL and WW) at different concentrations of urea for male and female flies were analyzed by one way ANOVA to assess the level of significance. Student's *'t'* test was carried out to analyse the significance of difference between male and female morphometric traits.

Table 1. Larval mortality and Mean values (Mean ± S.D.) of length and breadth of the pupae treated with different concentrations of urea.

% of urea	% of larval mortality	Length (mm)	Breadth (mm)
control	6.4	2.724 ± 0.118	0.816 ± 0.082
10	23.6	2.880 ± 0.134	0.914 ± 0.094
20	25.8	2.960 ± 0.133	0.936 ± 0.083
30	35.4	3.006 ± 0.130	0.972 ± 0.067
40	49.8	3.078 ± 0.102	1.016 ± 0.057

$df_1 = 3$, $df_2 = 36$ *, significant at $p < 0.01\%$

Results

Table 1 shows larval mortality and mean values of length and breadth of the pupae treated with different concentrations of Urea (Mean ± S.D.). There was an increase in larval mortality as the concentration of urea was increased in the food medium. The Mean values revealed a significant increase in length 'F' = 10.904 and breadth 'F' = 8.392 size of the pupa as concentration increased (ANOVA, $P < 0.01\%$).

The measurements (mm) of morphometric traits (FW, HW, TL, WL and WW) of male flies treated with Urea showed that all the trait size increased with increase in urea concentration (Table 2). The difference between control and different concentrations of urea are found significant (ANOVA, $P < 0.001\%$). Similar observation was made on measurements (mm) of morphometric traits (FW, HW, TL, WL and WW) of female flies treated with Urea (Table 3). It revealed a significant difference (ANOVA, $P < 0.001\%$) between control and different concentrations of urea treated flies. As the concentration of urea was increased in the media, the size of all the traits also increased simultaneously in an ascending manner.

Table 4 shows Student's *t* test values between male and female flies between different concentrations of urea and different morphometric parameters. It revealed a significant difference between different trait sizes of males and females (*t* test, $P < 0.001\%$).

Table 2. Measurements (mm) of morphometric traits (FW, HW, TL, WL and WW) of male flies treated with Urea. (Mean ± S.D.).

parameters	% of urea					'F' value
	control	10	20	30	40	
Face Width (FW)	0.202 ± 0.018	0.240 ± 0.012	0.257 ± 0.002	0.265 ± 0.012	0.270 ± 0.01	40.198*
Head Width (HW)	0.605 ± 0.036	0.730 ± 0.025	0.735 ± 0.024	0.830 ± 0.021	0.840 ± 0.021	123.683*
Thorax Length (TL)	0.760 ± 0.039	0.825 ± 0.026	0.885 ± 0.024	0.915 ± 0.024	0.985 ± 0.024	68.471*
Wing Length (WL)	1.320 ± 0.025	1.415 ± 0.041	1.490 ± 0.021	1.530 ± 0.025	1.540 ± 0.021	18.801*
Wing Width (WW)	0.800 ± 0.033	0.860 ± 0.039	0.990 ± 0.021	1.030 ± 0.025	1.040 ± 0.021	137.724*

$df_1 = 3$, $df_2 = 36$, *significant at $p < 0.01\%$

Table 3. Measurements (mm) of morphometric traits (FW, HW, TL, WL and WW) of female flies treated with Urea. (Mean ± S.D.).

parameters	% of urea					'F' value
	control	10	20	30	40	
Face Width (FW)	0.270 ± 0.022	0.287 ± 0.013	0.292 ± 0.012	0.295 ± 0.01	0.297 ± 0.079	5.908*
Head Width (HW)	0.820 ± 0.007	0.880 ± 0.025	0.920 ± 0.025	0.925 ± 0.026	0.935 ± 0.024	15.645*
Thorax Length (TL)	0.920 ± 0.025	0.925 ± 0.026	0.990 ± 0.021	1.005 ± 0.036	1.035 ± 0.024	34.167*
Wing Length (WL)	1.535 ± 0.004	1.575 ± 0.026	1.625 ± 0.026	1.665 ± 0.024	1.685 ± 0.024	61.646*
Wing Width (WW)	1.025 ± 0.026	1.085 ± 0.024	1.115 ± 0.024	1.125 ± 0.026	1.135 ± 0.026	31.381*

$df_1 = 3$, $df_2 = 36$, *significant at $p < 0.001\%$

Table 4. Student's *t* test values between male and female flies between different concentration of urea and different morphometric parameters.

	% of urea				
	control	10	20	30	40
Face Width (FW)	7.245*	8.143*	6.481*	5.692*	6.600*
Head Width (HW)	8.839*	12.990*	12.075*	8.143*	9.371*
Thorax Length (TL)	10.733*	8.485*	10.357*	6.454*	9.371*
Wing Length (WL)	19.230*	10.352*	12.650*	12.075*	5.605*
Wing Width (WW)	16.745*	15.385*	12.330*	8.143*	9.371*

df = 18, *significant at $p < 0.001\%$

Discussion:

In the present study, the effect of urea on larval mortality, pupae size and adult (male and female) morphological traits was analyzed. It revealed that the larval mortality was higher as the concentration of the urea was increased (Table 1). Earlier studies of urea effect on fecundity of *D. melanogaster* and *D. suzukii* revealed 50% and 70% reduction at higher concentration (Belloni *et al.,* 2018). Present results also show nearly 50% of larval mortality at higher concentration. This is mainly because urea is not a part of regular diet for *Drosophila* (Etienne *et al.,* 2001). Certain larval strains exposed for a longer duration of urea have shown adaptation and the rate of survival increased (Joshi *et al.,* 1996). But at the same time the larvae that have survived have shown significant changes in their development with respect to size. The pupae which forms after the metamorphosis of third instar larvae have increased sizes (length and breadth) which is significant at $P < 0.001\%$ (Table 1).

Pupal size increase can further lead to increased trait sizes of adult flies. The larvae exposed to 40% (highest) concentration have shown significant variations from control for both males and females (Table 2

and 3). This result is very important in understanding the fact that higher concentration of urea can affect the trait size. Trait sizes such as thorax length and wing length are used as index of body sizes (Santos *et al.,* 1988, 1992). Nutrition acts as one of the major environmental factors during juvenile growth and has major effects on adult morphology and life-history traits (Bergland *et al.,* 2008). The *t* test also showed significant variation between male and female morphometric traits (Table 4). The females were comparatively larger than the males. Hence the present study provides evidence for increased trait size because of urea treatment. The biochemical mechanism for metabolism of urea in *Drosophila* is not completely known, because urea is not a common diet for *Drosophila*. Etienne *et al.* (2001) had predicted three mechanisms of urea regulation in *Drosophila*, *i.e*., urea metabolism, increased excretion, and decreased uptake. For urea metabolism three enzymes are involved: arginase in the ornithine–urea cycle, and allantoicase and urease in the uricolytic pathway. Their study revealed no evidence for any of the urea-metabolizing enzyme activity in their larval samples. The second mechanism was tested for urea excretion. It revealed selected larvae did not alter their ability to excrete urea and the third mechanism was urea uptake. Urea concentration was more in the hemolymph of the control larvae than in the selected larvae. Thus the selected larvae have adapted to reduce the rate at which urea enters their body. This study in no way answers our question on the reasons for increase in size of the adult flies treated with urea. This requires further biochemical studies from a different perspective which will certainly help in detecting the precise pathway for urea metabolism in *Drosophila*.

Acknowledgment: Authors also thank Chairman, Dept. of Zoology, Karnatak University, Dharwad for providing necessary facilities and to UGC-SAP DSA III for financial assistance.

References: Affleck, J.G., K. Neuman, L. Wong, and V.K. Walker 2006, Toxicol. Sci. 89(2): 495 – 503; Belloni, V., A. Galeazzia, G. Berninia, M. Mandriolib, E. Versacec, and A. Haasea 2018, Physiol. Behav. 191:146 – 154; Bergland, A.O., A. Genissel, S.V. Nuzhdin, and M. Tatar 2008, Genetics 180: 567 – 582; Bird, M.A., and H.E. Shaffer 1972, Genetics 72: 475 – 487; Blanche, C.B., and L.B. Klaczko 1999, Heredity 83: 688 – 696; Borash, D.J., V.A. Pierce, A.G. Gibbs, and L.D. Mueller 2000, J. Insect Physiol. 46: 763 – 769; Botella, L.M., A. Moya, and J.L. Mensua 1983, Dros. Inf. Serv. 59: 23 – 24; Botella, L.M., A. Moya, M.C. Gonzalez, and J.L. Mensua 1985, J. Insect Physiol. 31: 179 – 185; Davidowitz, G., L.J. D'Amico, and H.F. Nijhout 2003, Evol. Dev. 5: 188 – 197; Davidowitz, G., L.J. D' Amico, and H.F. Nijihout 2004, Evol. Ecol. Res. 6: 49 – 62; Eom, H.J., Y. Liu, G.S. Kwak, M. Heo, K.S. Song, Y.D. Chung, T.S. Chon, and J. Choi 2017, Sci. Rep. 7: 46473 DOI: 10.1038/srep46473; Etienne, R., K. Fortunat, and V. Pierce 2001, J. Exp. Biol. 204: 2699 –2707; Herskowitz, I.H., 1951, Am. Nat. 822: 181 – 199; Imasheva, A.G., B. Moreteau, and J.R. David 2000, Genet. Res. 76: 237 – 247; Joshi, A., C.D. Knight, and L.D. Mueller 1996, Heredity 77: 33 – 39; Joshi, A., W.A. Oshiro, J. Shiotsugu, and L.D. Mueller 1998, J. Biosci. 23 (3): 279 – 283; Patridge, L., A. Hoffman, and J.S. Jones 1987, Anim. Behav. 35: 468 – 476; Pierce, V., L.D. Mueller, and A.G. Gibbs 1999, J. Exp. Biol. 202: 2349–2358; Ramachandra, N.B., and H.A. Ranganath 1988, Genome 30: 58 – 62; Saaristo, M., T. Brodin, S. Balshine, M.G. Bertram, B.W. Brooks, S.M. Ehlman, E.S. McCallum, A. Sih, J. Sundin, Bob B.M. Wong, and K.E. Arnold 2018, Proc. R. Soc. B 285: 1297. http://dx.doi.org/10.1098/rspb.2018.1297; Santos, M., A. Ruiz, A. Barbadilla, J.E. Quezada-Diaz, and A. Fontdevila 1988, Heredity 61: 255 – 262; Santos, M., A. Ruiz, A. Barbadilla, J.E. Quezada-Diaz, and A. Fontdevila 1992, J. Exp. Biol. 5: 403 – 422; Singh, S.R., and B.N. Singh 1999, Indian J. Exp. Biol. 37: 605 – 608; Shivanna, N., G.S. Siddalinga Murthy, and S.R. Ramesh 1996, Genome 39: 105 – 111; Shivanna, N., N.B. Vandal, S.L. Kudupali, and S.B. Shetty 2012, Mun. Ent. Zool. 7(2): 1116 – 1124; Sokoloff, A., 1966, Evolution 20: 49 – 71; Vogel, E.W., and M.J. Nivard 1993, Mutagenesis 8(1): 57 – 81; Yancey, P.H., M.E. Clark, S.C. Hand, R.D. Bowlus, and G.N. Somero 1982, Science 217: 1214 – 1222; Zoltan, B., K. Hreman van der, and G. de Jong 2003, Mol. Biol. Evol. 20 (11): 1760 – 1766.

Thermal stress induces catalase in apterous^{56f} *Drosophila melanogaster.*

Knox, M.T[1]., G.L. Harmon[1], and R.H. Blackmon[1,2]. [1]H.G. Cooke Department of Natural Sciences, [2]Cell Biology Lab, Elizabeth City State University, Elizabeth City, NC, 27909 USA, email: rhblackmon@ecsu.edu

In aerobic organisms, reactive oxygen species (ROS) are produced from the metabolism of oxygen. ROS molecules, such as oxygen free radicals, cause oxidative stress within aerobic organisms. This increased expression of free radicals can cause damage to biomolecules such as lipids, proteins, and DNA (Lobo, 2010). Antioxidant enzymes such as superoxide dismutase and catalase can protect against the effects of the overproduction of free radicals during periods of oxidative stress (Chelikani *et al*., 2004). Thermal stress is caused by heat generation that exceeds an organism's ability to distribute heat to its surroundings (Abdelnour *et al.*, 2018). Chronic heat stress can increase the metabolic rate within the organism. An increase in metabolic rate can enhance the production of oxygen free radicals leading to detrimental effects in an organism. Antioxidant defense mechanisms would therefore be important for continued viability. In this study, the activity of an antioxidant enzyme was determined during a period of early development in a mutant *Drosophila melanogaster* strain.

Drosophila melanogaster strain ap^{56f} flies were obtained from Carolina Biological Supply Company in Burlington, North Carolina. Flies were grown in vials containing 15 ml of Formula 4-24® Instant *Drosophila* medium (Carolina Biological Supply Company, Burlington, NC) mixed with 15 ml deionized water supplemented with yeast. *D. melanogaster^{ap56f}* were transferred to vials and maintained at room temperature (25±1°C). Every three weeks, the *D. melanogaster^{ap56f}* were transferred to fresh vials. Two-day old *D. melanogaster^{ap56f}* were separated into two groups with 25 males in each vial. Both groups were dehydrated for two hours, then transferred to vials containing 5 ml of 2% sucrose on a saturated Kimwipe. Group one (control) adults were incubated at 25°C for 18 hours and group two (treated) adults were incubated at 37°C for 18 hours. The flies were collected and stored in microcentrifuge tubes at -80°C until used for experimentation. A homogenizing solution was prepared by combining 1.5 ml of 50 mM potassium phosphate buffer (pH 7) and 1.5 µl of protease inhibitor cocktail (Sigma cat. no. P8340). Twenty-five *D. melanogaster^{ap56f}* were homogenized in 0.5 ml of homogenizing buffer (4°C), using chilled pestles and mortars. The homogenized solution was centrifuged at 16,000 × g (4°C) for 30 minutes. Supernatants were concentrated using Amicon® 30K Ultra 0.5 ml Centrifugal Filters and were centrifuged at 5,000 × g (4°C), until the retentate was reduced to a final volume of 50 µl for each sample. The supernatants were used for protein concentration determinations, enzyme assays and non-denaturing polyacrylamide gel electrophoresis. The Pierce 660 nm Protein Assay Kit (ThermoFisher Scientific Inc., Rockford, IL) was used to ascertain protein concentrations. A modified version of the Beers and Sizer catalase assay was performed to determine the enzymatic activity of the protein samples (Beers and Sizer, 1952). Each reaction mixture had a total volume of 3 ml. The assay was prepared by mixing 1.9 ml of deionized water, 1 ml of 0.059 M hydrogen peroxide (diluted in 0.05M potassium phosphate, pH 7) and 100 µl of diluted protein sample. Assays were performed at 25°C. The absorbance for the reaction mixture was read at a wavelength of 240 nm on a Genesys 5 UV-visible spectrophotometer and the readings were recorded every ten seconds for one minute. Five assay repetitions were performed for each sample. The enzyme unit was defined as µmol/min/mg. Novex™ WedgeWell™ 4-12% tris-glycine gradient gels were all run in a polyacrylamide gel electrophoresis unit from Invitrogen (Carlsbad, CA). Tris-glycine native running buffer was used for runs at 100 volts for 30 minutes and at 200 volts (4°C) for an additional 30 minutes with 30 micrograms of protein per sample mixed with 2X Novex™ tris-glycine native sample buffer. Gels were soaked in 100 ml of 0.03% hydrogen peroxide for 15 minutes with gentle agitation. The staining solution of 50 ml of two percent iron chloride ($FeCl_3$) and 50 ml of two percent potassium ferricyanide ($K_3Fe(CN)_6$) was poured on the gel to create a blue pigment in areas lacking catalase activity. The yellowish catalase bands were viewed and photographed using Bio-Rad ChemiDoc™ Imaging system.

Figure 1 is the image of a native 4-12% polyacrylamide gel with 30 µg of protein sample in each lane. A single major isoform was detected in samples from flies exposed to 25°C and those exposed to 37°C. There appears to be an up-regulation of catalase in *D. melanogaster*^{ap56f} incubated at 37°C for 18 hours where a larger and more intense band of catalase activity (lane 2) is discernible when compared to that of the control.

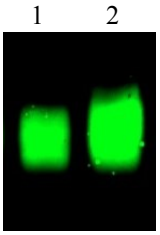

Figure 1. Catalase from 2-day old *D. melanogaster*^{ap56f} incubated at 37°C for 18 hours. A native 4-12% polyacrylamide gel loaded with 30 µg of protein: lane 1, 25°C (control); lane 2, 37°C.

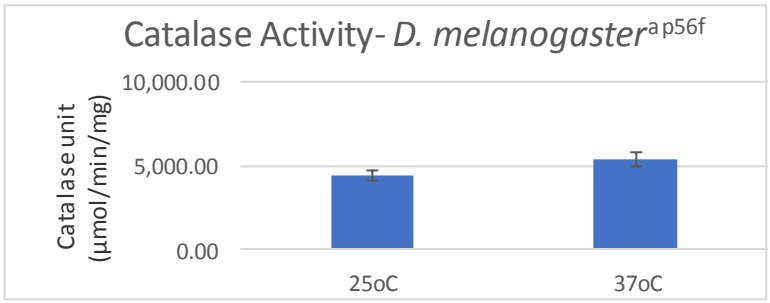

Figure 2. Mean catalase activity (µmol/min/mg ptn) for protein from 2-day old *D. melanogaster*^{ap56f} incubated at 25°C and 37°C for 18 hours.

The graph in Figure 2 represents the quantitative results from the enzyme assays of three independent experiments. Each experiment consisted of ten total vials: five vials each of which contained 25 flies for the control group and five vials each of which contained 25 flies per heat-stressed group. The data indicate significantly higher enzyme activities (mean µmol/min/mg ± std. dev.) in the samples from the heat-stressed flies (5,410.60 ± 412.35) [*$p < 0.05$] than in the samples from flies maintained at 25°C (4,416 ± 343.63). Catalase is an antioxidant enzyme that plays an important role in the defense of cells and organisms against the toxic effects of oxygen free radicals. For aerobic organisms, this is an essential function since damage to biological macromolecules can lead to aberrant biochemical and physiological functions and may ultimately result in death of the affected cells and organisms. Thermal stress can affect biological systems by escalating free radical production. This study suggests that apterous^{56f} mutants of *Drosophila melanogaster* may moderate the deleterious effects of a thermal stress induced oxygen free radical surge by increasing catalase activity.

References: Abdelnour, S.A., M.E.A. El-Hack, A.F. Khafaga, M. Arif, A.E. Taha, and A.E. Noreldin 2019, Journal of Thermal Biology 79: 120-134; Beers and Sizer 1952, Journal of Biological Chemistry 195(1): 133-140; Chelikani, P., I. Fita, and P.C. Loewen 2004, Cellular and Molecular Life Sciences CMLS 61(2): 192-208; Lobo, V., A. Patil, A. Phatak, and N. Chandra 2010, Pharmacognosy Reviews 4(8): 118-126.

Trichostatin A enhances catalase activity in *Drosophila melanogaster*^{ap56f}.

Blackmon, R.H.[1,2], and G.L. Harmon[2]. [1]Cell Biology Lab, [2]H.G. Cooke Department of Natural Sciences, Elizabeth City State University, Elizabeth City, NC 27909, USA, email: rhblackmon@ecsu.edu

In an aerobic environment, catalase plays an important role in the defense of cells and organisms against the toxic effects of oxygen. Possible consequences of the production of reactive oxygen species (ROS) from the metabolism of oxygen include damage to biological macromolecules such as lipids, proteins, and

nucleic acids. The detrimental effects on cellular metabolism can result in the loss of viability. Catalase, an antioxidant enzyme, prevents the accumulation of hydrogen peroxide, a reactive oxygen species, by catalyzing conversion of the substrate to water and molecular oxygen. In this inquiry, the role of an epigenetic agent on catalase levels was investigated to ascertain the potential of this approach for bolstering antioxidant defense systems in aerobic organisms. Trichostatin A (TSA) is a histone deacetylase inhibitor that targets the class I and class II histone deacetylases (HDAC) and histones H3 and H4 (Huidobro *et al*., 2013). Eukaryotic DNA is arranged into chromatin in which histone components of nucleosomes can be regulated by reversible acetylation. Histone acetylation is regulated by histone acetyltransferases and histone deacetylases (HDACs), which play important roles in transcription, DNA replication, and cell cycle progression (Benayoun *et al*., 2015). Trichostatin A, which inhibits HDAC, has been shown to stop cell cycling, induce differentiation, and reverse morphological changes seen in the cell cycle arrest (Santos *et al*., 2018). In this study, the activity of catalase in response to TSA was determined in four-day old adult flies of a mutant *Drosophila melanogaster* strain.

Drosophila melanogaster strain ap^{56f} flies used in this study were obtained from Carolina Biological Supply Company in Burlington, North Carolina. Flies were grown in vials containing 15 ml of Formula 4-24® Instant *Drosophila* medium (Carolina Biological Supply Company, Burlington, NC) mixed with 15 ml deionized water supplemented with yeast. *D. melanogaster^{ap56f}* were transferred to vials and maintained at room temperature (25±1°C). Every three weeks, the *D. melanogaster^{ap56f}* were transferred to fresh vials. Four-day old *D. melanogaster^{ap56f}* were separated into two groups with 25 males in each vial. Both groups were dehydrated for two hours, then transferred to vials containing 5 ml of 2% sucrose on a saturated Kimwipe. Group one (control) adults were incubated at 25°C for 24 hours in the absence of TSA and group two (treated) adults were incubated at 25°C for 24 hours in the presence of 50 µM TSA. The flies were collected and stored in microcentrifuge tubes at -80°C until used for further experimentation. A homogenizing solution was prepared by combining 1.5 ml of 50 mM potassium phosphate buffer (pH 7) and 1.5 µl of protease inhibitor cocktail (Sigma cat. no. P8340). Twenty-five *D. melanogaster^{ap56f}* were homogenized in 0.5 ml of homogenizing buffer (4°C), using chilled pestles and mortars. The homogenized solution was centrifuged at 16,000 × g (4°C) for 30 minutes. Supernatants were concentrated using Amicon® 30K Ultra 0.5 ml Centrifugal Filters and were centrifuged at 5,000 × g (4°C) until the retentate was reduced to a final volume of 50 µl for each sample**.** The concentrated samples were used for protein concentration determinations, enzyme assays and non-denaturing polyacrylamide gel electrophoresis. The Pierce 660 nm Protein Assay Kit (ThermoFisher Scientific Inc., Rockford, IL) was used to ascertain protein concentrations. A modified version of the Beers and Sizer catalase assay was performed to determine the enzymatic activity of the protein samples (Beers and Sizer, 1952). Each reaction mixture had a total volume of 3 ml. The assay was prepared by mixing 1.9 ml of deionized water, 1 ml of 0.059 M hydrogen peroxide (diluted in 0.05M potassium phosphate, pH 7) and 100 µl of diluted protein sample. Assays were performed at 25°C. The absorbance for the reaction mixture was read at a wavelength of 240 nm on a Genesys 5 UV-visible spectrophotometer and the readings were recorded every ten seconds for one minute. Five assay repetitions were performed for each sample. The enzyme unit was defined as µmol/min/mg. Novex™ WedgeWell™ 4-12% tris-glycine gradient gels were used (Invitrogen, Carlsbad, CA) for gel electrophoresis. Tris-glycine native running buffer was used for runs at 100 volts for 30 minutes and at 200 volts (4°C) for an additional 30 minutes with 25 micrograms of protein per sample mixed with 2X Novex™ tris-glycine native sample buffer. Gels were soaked in 100 ml of 0.03% hydrogen peroxide for 15 minutes with gentle agitation. The staining solution of 50 ml of two percent iron chloride ($FeCl_3$) and 50 ml of two percent potassium ferricyanide ($K_3Fe(CN)_6$) was poured on each gel to create a blue pigment in areas lacking catalase activity. The yellowish catalase bands were viewed and photographed using Bio-Rad ChemiDoc™ Imaging system.

Figure 1 is the image of a typical native 4-12% polyacrylamide gel with 25 µg of protein sample in each lane. A single major isoform was detected in samples from flies exposed to zero TSA and those exposed to 50 µM TSA. The gel results suggest an up-regulation of catalase in *D. melanogaster*^{ap56f} incubated for 24 hours in TSA where a larger and more intense band of catalase activity (lane 2) is discernible when compared to that of the [no TSA] controls.

Figure 2 represents the quantitative results from the enzyme assays of three independent experiments. Each experiment consisted of ten total vials: five vials each contained 25 flies for the control group and five

vials each of which contained 25 flies per TSA-treated group. The data indicate significantly higher enzyme activities (mean µmol/min/mg ± std. dev.) in the samples from the TSA-treated flies (3624.33±146.58) [*p < 0.05] than in the samples from control flies (no TSA) (2749.00±274.61). Catalase is an antioxidant enzyme that plays an important role in the defense of cells and organisms against the toxic effects of oxygen free radicals. For aerobic organisms, this is an essential function since damage to biological macromolecules can lead to aberrant biochemical and physiological functions and may ultimately result in death of the affected cells and organisms. This study suggests that apterous^{56f} mutants of *Drosophila melanogaster* may moderate the deleterious effects of a stress induced oxygen free radical surge by a process which exposes them to a histone deacetylase inhibitor agent like TSA to upregulate catalase levels. Future studies will be conducted to clarify the relationship between TSA concentration and catalase activity increases.

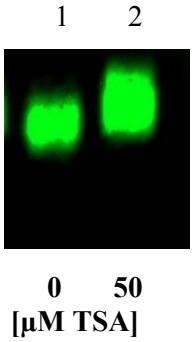

Figure 1. Catalase from four-day-old *D. melanogaster*^{ap56f} treated with 50 µM TSA. Samples were resolved on a native 4-12% polyacrylamide gel. lane 1, -- TSA; lane 2, 50 µM TSA.

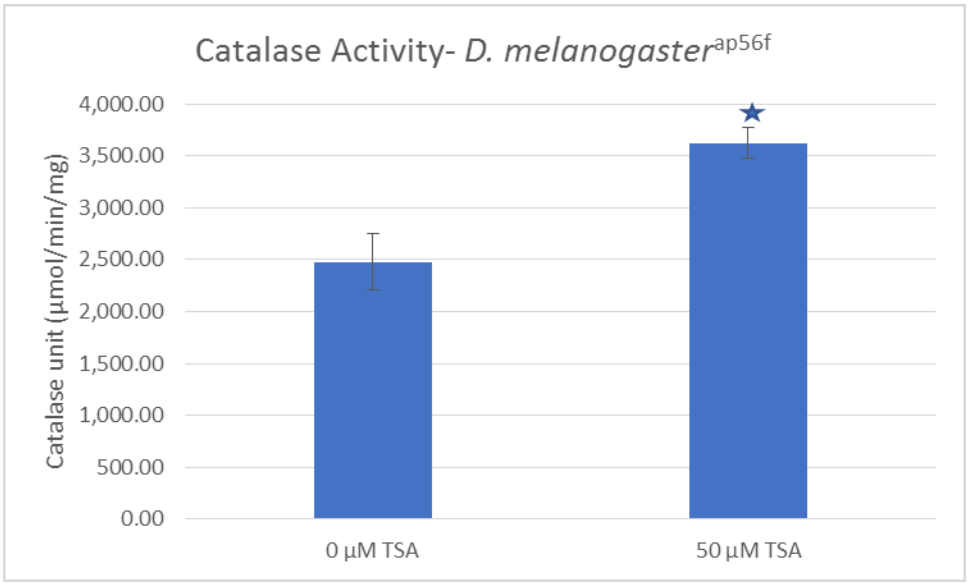

Figure 2. Mean catalase units (µmol/min/mg ptn). Four day old *D. melanogaster*^{ap56f} treated with 50 µM TSA. [★p < 0.05].

References: Huidobro, C., A.F. Fernandez, and M.F. Fraga 2013, Molecular Aspects of Medicine 34(4): 765-781; Benayoun, B., E.A. Pollina, and A. Brunet 2015, Nature Reviews Molecular Cell Biology 16: 593-610; Santos, J., A.A. Zuma, F.N. de Luna Vitorino, J.P.C. da Cunha, W. deSouza, and M.C.M. Motta 2018, Parasitology 146(4): 543-552; Beers, R.F., and I.W. Sizer 1952, J. Biol. Chem. 195(1): 133-140; Woodbury, W., A.K. Spencer, and M.A. Stahmann 1971, Analytical Biochemistry 44(1): 301-305.

A preliminary survey of *Drosophila* species in the fruit market, Mysuru, Karnataka, India.

Guruprasad, B.R. Department of Zoology, Yuvaraja's College, University of Mysore, Mysore.

Abstract

Drosophila flies were analyzed taxonomically by collecting in the four sites of the fruit market, Mysore, Karnataka, India. The present report is on collection. Identification of *Drosophila* species in the local fruit market was done to know the number of species. About 2,811 flies of different species of *Drosophila* were encountered in the collection with two genera, *Sophophora* and *Drosophila*. *D. nasuta* is a species which is common in collection and found in the highest number in the present preliminary study.

Introduction

Drosophila, the common fruit fly, is also known as vinegar fly. It is cosmopolitan in distribution. It is considered to be an excellent material for developmental biology, population genetics, genetics, evolutionary, biodiversity studies, because it is a small minute, tiny eukaryotic organism which can grow on simple medium in the laboratory. Thus a large number of flies occupy relatively lesser space with shorter life cycle extending over 15 days and high fecundity.

Drosophila has been extensively investigated by several workers for over 100 years and this fly has been the material for the discovery of a vast amount of genetic information with regards to patterns of inheritance. It is therefore referred as "Cinderella of Genetics". *Drosophila* has the potential to become the best model organism for investigating the influence of habit change on the biological community, as most species have rather limited realized niches and are dependent on a particular group of host organisms for feeding and reproduction (Parsons, 1991; Popps, Valante and Schmitz, 2013). In addition, *Drosophila* were used to study the influence of anthropologic disturbance, particular urbanization, on species diversity and abundance (Avondet, Blair Berg, and Ebert 2003; Dobzhansky and Pavan, 1950). The abundance of *Drosophila* species is influenced primarily by precipitation in tropical regions and influence of the flowers and fruiting bodies (Guruprasad *et al*., 2010). To the best of our knowledge, there is very little accessible information on the influence of fruit market on the *Drosophila* abundance and diversity. This is just a preliminary survey to know the composition of the flies found in the fruit market of Mysuru, Karnataka.

Materials and Methods

We collected samples from corner of four sites inside the fruit market in Mysore, Karnataka. The collection of the *Drosophila* was done using the sweeping method (Guruprasad *et al*., 2006a, 2006b, 2010) and also using an alcohol aspirator (Markow and O'Grady, 2005), where there is anthropological activity was also seen in the market during early morning around 8 am to 9 am in the month of August 2018. The collected flies were brought to the laboratory and were isolated and separated according to their respective sexes. The males were directly used for identified according to the (Markow and Grady 2006) whereas females were reared in separate vials having wheat soji cream agar medium. Later the males were used for identification of species (Markow and Grady, 2006).

Results

The results of survey of *Drosophila* species collected in the fruit market were predicted in the form of Table 1 and Figure 2, where we observed about 2,811 flies of different species of *Drosophila.* The subgenus

Sophophora which comprises *D. bipectinata, D. jambulina, D. malerkotliana, D. rajasekari, D. melanogaster, D. ananassae* were encountered with large number of flies, around 2,205. The subgenus Sophophora is predominant with *D. melanogaster* with highest number compared to the other subgenus *Drosophila,* where there is only one species such as *D. nasuta* which comprises 606 flies.

Table 1. The composition of the *Drosophila* species present in the fruit market of Mysuru, Karnataka, India.

Genus	Subgenus	Species	Fruit market				
			Site 1	Site 2	Site 3	Site 4	Total
Drosophila	*Sophophora*	*D. bipectinata*	95	105	99	87	386
		D. jambulina	*45*	*31*	*36*	88	200
		D. malerkotliana	104	108	98	95	405
		D. rajasekari	52	46	76	*65*	339
		D. melanogaster	127	136	147	165	575
		D. ananassae	*81*	83	80	*56*	300
		Total	504	509	536	556	2,205
	Drosophila	*D. nasuta*	165	132	149	160	606
		Total	669	641	685	716	2,811

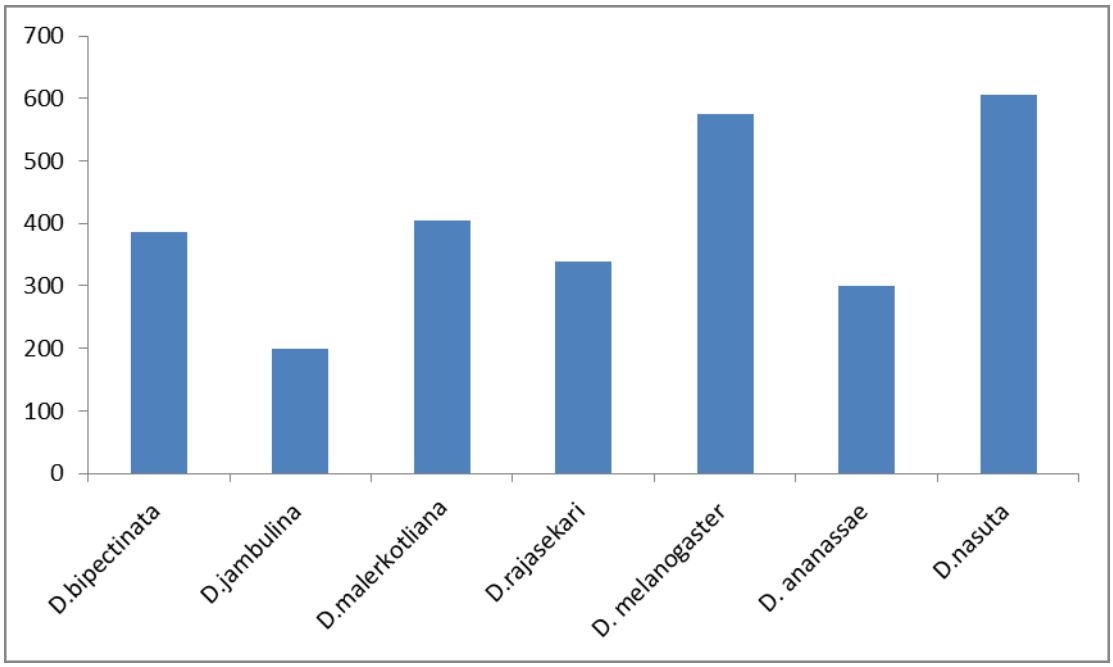

Figure 1. Showing the different species of *Drosophila* found in the fruit market of Mysuru, Karnataka, India.

Discussion

Drosophila is used as a best model organism in many fields of life science. The abundance of the *Drosophila* play very important role in the study of their habitat. At present there are 4217 species of *Drosophila* described, which consist of 77 genera. In genus *Drosophila* there are 1178 species among which 751 species belong to subgenus *Drosophila,* where 335 species belong to subgenus Sophophora (Bachli,

2014). In this preliminary study of *Drosophila* survey in the market, there are some interesting things analyzed during and after collection of flies: 1) There are mixed fruits available in the market shop, such as apple, orange, grapes, citrus fruits, guava, papaya, and many more. This suggests only genus Sophophora is commonly seen in the market, and also there is the dominance of *D. melanogaster* (Table 1 and Figure 1), which is a domestic fly which is seen along with anthropological activity in the market. 2) There is presence of *D. nasuta* in large number considering this species is most dominant species and companion species found in the fruit market. From our study, the author suggested *D. nasuta* is a common and cosmopolitan species found in this area; along with this it agrees with the work of Guruprasad *et al.* (2010).

References: Avondet, J.L., R.B. Blair, D.J. Berg, and M.A. Ebert 2003, Environmental Entomology 32: 347-358; Bachli, G., 2014, Taxodros: The database on taxonomy of Drosophilidae. URL: http:// www.taxodros.unizh.cw [Date of access: 10- August- 2014]; Dobzhansky, Th., and C. Pavan 1950, J. Anim. Ecol. 19(1): 1–14; Guruprasad, B.R., and S.N. Hegde 2006a, Dros. Inf. Serv. 89: 10–11; Guruprasad, B.R., and S.N. Hegde 2006b, Dros. Inf. Serv. 89: 23-31; Guruprasad, B.R., S.N. Hegde., and M.S. Krishna 2010, J. Ins. Sci. 10: 123; Markow, T.A., and P.M. O' Grady 2006, Drosophila, *A Guide to Species Identification and Use*. Academic Press, London. 247 pp.; Parsons, P.A., 1991, Global Ecology and Biogeography letters 1(3): 77; Popps, J.L., V. Valante, and L.S. Schmitz 2013, Neotropical Entomology 42: 269-277.

Initial population size fluctuation of introduced species *Zaprionus indianus* in drosophilids surveys in Brazil: data from periodic collections at early invasion.

Mateus, Rogério P.[1], Evandro M. Moraes[2], and Luciana P.B. Machado[1]. [1]Laboratório de Genética e Evolução, Departamento de Ciências Biológicas, UNICENTRO – Universidade Estadual do Centro-Oeste, Guarapuava-PR, Brazil. [2]Laboratório de Diversidade Genética e Evolução, Departamento de Biologia, Universidade Federal de São Carlos – UFSCar, Sorocaba-SP, Brazil, Corresponding author: rogeriopmateus@gmail.com

Introduction

Zaprionus indianus Gupta, 1970, (Diptera, Drosophilidae) is a generalist species of Afrotropical origin. It constitutes one of the most successful colonizing drosophilid species (Shakoori and Butt, 1979; Parkash and Yadav, 1993; Amoudi *et al*., 1995). Vilela (1999) was the first to publish its occurrence in Brazil, collecting this species on March 1999 in Santa Isabel, São Paulo State. In 2006, it was already detected in northeastern Argentina (Lavagnino *et al*., 2008) and in 2013 had reached Canada (Renkema *et al*., 2013).

In the year of 1999 we sent some unknown drosophilid specimens, collected in January of that year, to Dr. Carlos R. Vilela for identification, which he kindly identified for us as *Zaprionus indianus*. Therefore, *Z. indianus* was already introduced in Brazil prior to the first register published by Vilela (1999). Here, we show data from periodic collections that reveal *Z. indianus* initial population size fluctuation for seven months in two localities of natural areas with xerophytic vegetation of São Paulo state.

Material and Methods

The collections were performed in forest fragments, associated with xerophytic vegetation, situated in the southeast region of Brazil (Table 1). In ITA, ITI, SMS and SRT, only one collection was made. In ALT and SER, the collections were performed bimonthly for seven months, from January to July 1999. The flies were captured in open traps using orange and banana baits, fermented with yeast (*Saccharomyces cerevisiae*). The traps were set for three days at 1.5 meter above ground (Sene *et al*., 1981). After collection, initially unknown representative specimens of *Z. indianus* were sent to the drosophilid specialist Dr. Carlos R. Vilela for identification. The short-term fluctuation in population size was studied through the relative frequency of *Z. indianus* to the rest of the drosophilid collected.

Table 1. Localities, coordinates and dates of collection in the state of São Paulo. Localities in bold were periodic (bimonthly) sampled.

Localities	Coordinates	Collection dates
Altinópolis (ALT)	21°02' S, 47°19' W	Feb to Jul/1999
Itatiba (ITA)	22°56' S, 46°55' W	Apr/1999
Itirapina (ITI)	22°16' S, 47°48' W	Feb/2000
Santa Maria da Serra (SMS)	22°40' S, 48°12' W	Feb/2000
Serrana (SER)	21°15' S, 47°34' W	Jan to May/1999
Sertãozinho (SRT)	21°02' S, 47°19' W	Oct/1999

Results

Table 2 presents the relative frequencies of *Z. indianus* and total number of drosophilids in the localities where only one collection was performed. The invasive species was the most frequent among the species in ITI. In ITA and SMS, it was the second most frequent, and in SRT, it was among the five most frequent species.

Table 2. Relative frequency (*r*) of *Zaprionus indianus* and total number of flies collected (N) in the localities where only one survey was performed.

Localities	*r*	N
Itatiba (ITA)	0.34	936
Itirapina (ITI)	0.22	1,368
Santa Maria da Serra (SMS)	0.17	2,387
Sertãozinho (SRT)	0.06	2,565

In SER and ALT, where three collections were performed each, *Z. indianus* also reached the highest frequency among species. Figure 1 shows the relative frequency (*r*) fluctuation in both localities (A = SER; B = ALT). In January/1999 and February/1999, *Z. indianus* was collected in very low frequency in SER and ALT, respectively. In the next survey, it showed much higher relative population size in both areas, declining in the subsequent collections.

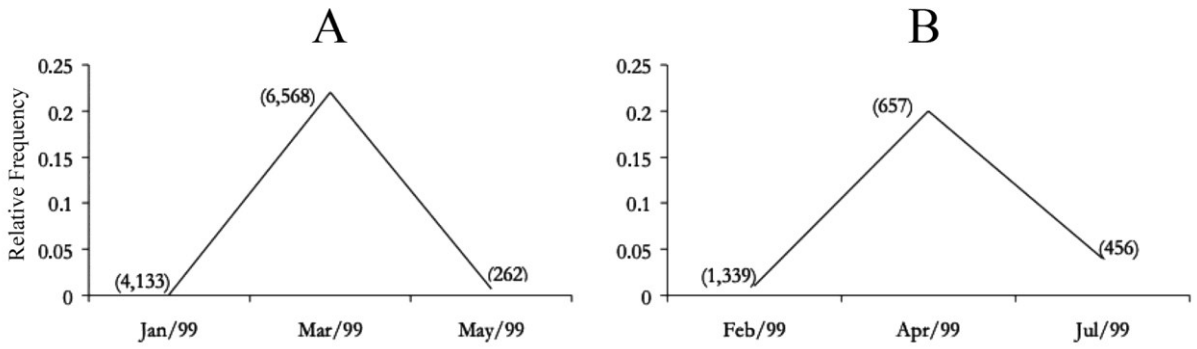

Figure 1. Variation in relative frequency of *Z. indianus* in A - Serrana (SER) and B - Altinópolis (ALT). The total number of flies in each survey is represented between parentheses.

Discussion

The introduction of an exotic species is not an uncommon event in Brazil. In 1976, Val and Sene (1980) collected for the first time, in northeastern Brazil, a large number of *Drosophila malerkotliana*, a species not recorded in the extensive earlier collections. Currently, *D. malerkotliana* is collected almost

throughout Brazil, always in low relative frequency. An invasion can threaten the stability of established *Drosophila* communities, especially in Brazil, where they are very rich and have delicate interactions between the different members. Therefore, it is important to understand the history of an invasion, trying to identify where and when the exotic species was introduced, and what was its behavior within the new community to which it now belongs.

In the case of *Zaprionus indianus*, we collected the first specimens in January and February of 1999, in natural areas associated with xerophytic vegetation. We were collecting in this area since July 1998, and every other month. We had performed a survey in November, and this species was not captured. Thus, we could state that it arrived in SER after November 1998.

The events surrounding biological invasions are divided into three categories: arrival, establishment, and integration (Vermeij, 1996). The factors influencing establishment are initially demographic. *Zaprionus indianus* showed a fast population expansion after arrival (Mar/1999 in SER, and Apr/1999 in ALT). However, the observed fall in relative frequency after two months indicated that it competed unfavorably with other similar species in xerophytic native areas. Now, this species is widely distributed, and it is showing lower relative frequency in localities with natural vegetation of Brazil (Silva *et al*., 2005; Lima, 2020, as an example), including in regions that show lower temperature, as highland Araucaria Forest (Cavasini *et al*., 2014).

References: Amoudi, M.A., F.M. Diab, and S.S.M. Abou-Fannah 1995, J. King Saud Univ. 5, Agri. Sci. 2: 263-273; Cavasini, R., M.L.T. Buschini, L.P.B. Machado, and R.P. Mateus 2014, Braz. J. Biol. 74: 761-768; Lavagnino, N.J., V.P. Carreira, J. Mensch, E. Hasson, and J.J. Fanara 2008, Rev. Soc. Entomol. Argent. 67: 189-192; Lima, W.C., 2020, TCC Universidade Federal de Santa Catarina; Parkash, R., and J.P. Yadav 1993, Hereditas 119: 161-170; Renkema, J.M., M. Miller, H. Fraser, J-PH. Légaré, and R.H. Hallett 2013, Scientific Note J. Ent. Soc. Ont. 144: 125–130; Sene, F.M., M.A.Q.R. Pereira, C.R. Vilela, and N.M.V. Bizzo 1981, Dros. Inf. Serv. 56: 118-121; Shakoori, A.R., and U. Butt 1979, Pak. J. Zool. 11: 315-328; Silva, N.M., C.C. Fantinel, V.L.S. Valente, and V.H. Valiati 2005, Iheringia, Sér. Zool. 95: 233-240; Val, F.C., and F.M. Sene 1980, Papéis Avulsos Zool. 33: 293-298; Vermeij, G.J., 1996, Biol. Conserv. 78: 3-9; Vilela, C.R., 1999, Dros. Inf. Serv. 82: 37-39.

Position effect variegation of the *dumpy* gene in *Drosophila melanogaster.*

MacIntyre, Ross. Department of Molecular Biology and Genetics, Cornell University.

The dumpy gene, originally discovered in the Morgan laboratory *ca*. 1910, is large, and encodes an important component of the extracellular matrix of epithelial cells where it plays a role in maintaining cell shape and tissue rigidity (Wilkin *et al*., 2000). A class of mutants, called *oblique* mutants, exhibit shorter wings, as exemplified by the canonical dp^{ov1} mutation from the Morgan lab. Oblique mutants result from a failure of cell-cuticle adhesion in the developing wing (Ray *et al*., 2015). We have obtained several chromosomal aberrations that exhibit asymmetric patterns of oblique mutant expression when heterozygous with dp^{ov1}. These aberrations are shown in Table 1.

Table 1. Several chromosomal aberrations that exhibit asymmetric patterns of oblique mutant expression when heterozygous with dp^{ov1}.

Aberration	Description	Discoverer
dp-23	T(2;3) -break in 2L proximal to dumpy, and in 3L heterochromatin	MacIntyre, 1994
dp-w1	T(2;3) – same as dp-23	E. Carlson, ca.1975
dp-w18	T(2;3) – same as dp-23	E. Carlson, ca.1975
H116	(Y;2) – break proximal to dumpy in 2L and in short arm of the Y	Lindsley and Sandler (1972)

All four aberrations are recessive lethals, but they complement for viability in *inter se* crosses. Therefore, the breakpoints are at different places in the genome (data not shown).

Suspecting that the asymmetric patterns of dumpy mutant expression might be due to the heterochromatic breakpoints near the dumpy gene in these aberrations, we made the following crosses listed in Table 2.

Table 2. Variegation crosses involving T(2;3) translocations (dp-var).

For	Female Parents	Male Parents
X/Y Males	C(1)DX; dp^{ov1}	X/Y; In(2LR) Gla/dp-var
X/0 Males	C(1)RM; dp^{ov1}	X/Y; In(2LR) Gla/dp-var
C(1)RM/Y Females	C(1)RM/0;dp^{ov1}	X/Y; In(2LR) Gla/dp-var
C(1)(DX/Y Females	C(1)DX/Y; dp^{ov1}	X/Y; In(2LR) Gla/dp-var

The effects of extra heterochromatin on gene expression in chromosomal aberrations are, of course, well known (Ashburner *et al*., 2005, see page 100). Hence we would expect to see more dumpy mutant gene expression in X/O *versus* X/Y male and C(1)DX *versus* C(1)RM female progeny from the above crosses if position effect variegation is operating.

To measure the extent of position effect on dumpy gene expression in the progenies from the crosses, we used the scoring system outlined in Carmon *et al*. (2010). In this system, individual wings are scored from zero (wild type) to five, with five being the most severe mutant oblique expression. A single fly can exhibit an asymmetric pattern where the two wings can have different scores, *e.g*., a fly with one wild type wing and one mutant wing might be scored as 0,3.

A typical pattern of *dumpy* mutant gene expression is shown in the following table, in this case in X/0; dp-23/ dp^{ov1} males.

Table 3. X/0: dp-23/dp^{ov1} males.

Score	No. of Flies	Score	No. of Flies	Score	No. of flies	Score	No. of flies
0,0	26	2,2	1	3,3	7	3,5	0
0,1	9	1,3	0	2,4	0	4,5	0
1,1	3	0,4	1	1,5	0	5,5	0
0,2	5	2,3	3	3,4	0		
1,2	6	1,4	0	2,5	0		
0,3	10	0,5	0	4,4	0		

The extent of variegation was measured in two ways. First was the percent of asymmetry or simply the number of flies scored minus the number of 0,0 and 1,1 and 2,2 and 3,3 and 4,4 and 5,5 flies / number of flies scored. In the dp-23 data set in Table 3, there is 48 per cent asymmetry. The second way to assess variegation is to measure a mean wing score which is the sum the flies in each class times the sum of both wing scores/ total wings scored. The mean wing score turns out in the X/Y dp-23/ dp^{ov1} data to be 0.97 indicating a slight mutational effect of the aberration. The data from all the crosses in this report were analyzed in these two ways.

A: Results from crosses involving T(2;3) translocations

The results from dp-23, dp^{w1} and dp^{w18} are shown in Table 4 below.

Table 4. The results from crosses involving T(2,3) translocations with dp-23, dp^{w1} and dp^{w18}.

Genotype	Percent Asymmetric	Mean wing score
X/Y; dp^{23}/dp^{ov1}	48	0.97
X/0; dp^{23}/dp^{ov1}	60	1.13
X/0 - 700	33	4.61
X/Y; dp^{w1}/dp^{ov1}	53	1.19
X/0; dp^{w1}/dp^{ov1}	44	2.39
X/0 - 700	36	4.72
X/Y; dp^{w18}/dp^{ov1}	50	0.46
X/0; dp^{w18}/dp^{ov1}	44	1.15
X/0 - 700	99	3.84
C(1)RM; dp^{23}/dp^{ov1}	2	0.03
C(1)DX/Y; dp^{23}/dp^{ov1}	40	0.77
C(1)RM/Y; dp^{w1}/dp^{ov1}	3	0.02
C(1)DX/Y; dp^{w1}/dp^{ov1}	65	1.91
C(1)RM/Y; dp^{w18}/dp^{ov1}	0	0
C(1)DX/Y; dp^{w18}/dp^{ov1}	41	0.24

There is an increase in *dumpy* mutant expression in X/0 males over X/Y males in each of the three translocations, particularly when C(1)RM/0 females from Bloomington stock number 700 are used as parents in the cross. This indicates there is a parental source effect operating on dumpy variegation as noted by Spofford (1959). The effect of extra heterochromatin is also seen, although less dramatically, in the comparisons between C(1)RM and C(1)DX females in the progeny from all three crosses.

B: Results from crosses involving T(Y;2) H116

The possibility of additional genotypes resulting from adjacent-1 disjunction in parents carrying this translocation makes a separate analysis necessary. The crosses made are shown below.

Table 5. Dumpy variegation- crosses with T(Y;2) H116, y^{+}Bar.

For Genotypes	Female Parent	Male parents
C(1)RM/0; H116/dp^{ov1} and C(1)RM/0; $Y^{P}2^{LD}/dp^{ov1}/dp^{ov1}$	C(1)RM/0; dp^{ov1}	C(1;Y)/0;H116/dp^{ov1}
C(1;Y)/0; H116/dp^{ov1} and C(1;Y)/0;$Y^{P}2^{LD}/dp^{ov1}/dp^{ov1}$	C(1)RM/0;H116/dp^{ov1}	C(1;Y)/0;dp^{ov1}
X/0; H116/dp^{ov1} and X/0; $Y^{P}2^{LD}/dp^{ov1}/dp^{ov1}$	X/X; dp^{ov1}	C(1;Y)/0;H116/dp^{ov1}

Table 6. Position effect variegation of *dumpy* in T(Y;2)H116.

Genotype	Per Cent Asymmetric	Mean Wing Score
C(1)RM/0; T(Y;2)H116/dp^{ov1}	0	0
C(1)RM/0 ; $Y^{P}2L^{D}/dp^{ov1}/dp^{ov1}$	5	0.11
C(1;Y)/0 ;T(Y;2)H116/dp^{ov1}	0.46	0.002
X/0; T(Y;2)H116/ dp^{ov1}	19	0.15
C(1;Y)/0 ;$Y^{P}2L^{D}/dp^{ov1}$ /dp^{ov1}	1.3	0.016
X/0; $Y^{P}2L^{D}$/ dp^{ov1}/dp^{ov1}	54	1.03

The additional male progeny in these crosses come from adjacent-1 disjunctional gametes from one of the parents and can be recognized from the *y*+ and Bar eyed markers on the translocation (Lindsley *et al*., 1968). These males, since they carry only a part of the Y chromosome, are sterile. As shown below in Table 6, they also variegate for *dumpy* due to the breakpoint in the Y^{P} element.

These data show that the breakpoint in the Y chromosome influences the expression of an autosomal gene located near it, in this case, *dumpy*. Clearly, however, the presence or absence of a complete Y chromosome in the genotype affects the expression of dumpy more profoundly.

C: Effects of suppressors and enhancers of variegation on dumpy expression

The following crosses were made to determine the effects of two enhancers of position effect variegation, Trl^{R67} and E(z) and two suppressors, su(Var)205 and su(Var) 3-9 (see references below).

Table 7. Female and male parents used in crosses made to detect enhancement and suppression of *dumpy* expression.

Female Parents	Male Parents	Phenotypes Compared
E(z) w; dp^{ov1}; In(3LR)TM3, Sb/ E(z)	w; In(2LR)Gla/dp^{w1}	Sb and Sb+
	C(1;Y); In(2LR)Cy O)/H116	Sb and Sb+
	In(2LR)/ dp-23	Sb and Sb+
Trl^{R67} w; dp ^{ov1}; In(3LR)TM3,Sb/Trl^{R67}	w; In(2LR)Gla/dp^{w1}	Sb and Sb+
	C(1;Y); In(2LR)Cy O)/H116	Sb and Sb+
	In(2LR)/ dp-23	Sb and Sb+
Su-205 w^{m4};dp^{ov1}su(var)205/In(2LR)Gla	w; In(2LR)Gla/dp^{w1}	Gla and Gla+
	C(1;Y); In(2LR)Cy O)/H116	Cy+,Gla+
	In(2LR)Gla/ dp-23	Gla and Gla+
Su-3-9 w^{m4}: dp^{ov1} ; In(3LR)TM3,Sb/su(Var)3-9	In(2LR)Gla/dp^{w1}	Sb and Sb+
	C(1;Y); In(2LR)Cy O)/H116	Sb and Sb+
	In(2LR)/ dp-23	Sb and Sb+

In these results, the effects of an enhancer or a suppressor are best seen by comparing the mean wing scores of the Sb versus the Sb+ progenies. The scores of the Sb+ flies should be higher if there is enhancement and lower if there is suppression. There is little, if any, enhancement, although the presence of Trl^{R67} seems to make the dumpy mutant stronger, albeit slightly, in all three aberrations tested. On the other hand, the effects of both suppressors are dramatic. In these crosses, the mean wing scores of the Sb+ or the Gla+ flies are virtually zero (wild type). Indeed, in most of the crosses with the two suppressors, the majority of the progeny flies have two wild type wings with only a few, even just one, fly or flies showing a single wing with a minor *dumpy* oblique phenotype, the other being wild type. It is not clear why there is such a difference

Conclusions

It is obvious that *dumpy* is subject to position effect variegation (PEV). Both the amount of extra heterochromatin in a genotype and especially the presence of PEV suppressors affect *dumpy* expression significantly in expected ways. Indeed, *dumpy* could serve as an experimental system to explore this intriguing phenomenon, as asymmetry and mean wing scores can be easily observed and measured. Thus, what are the sequences at variegating breakpoints and, importantly, what are the chromatin structures at these breakpoints in genotypes that show differences in *dumpy* expression?

Table 8. Results from crosses to assess enhancement and suppression of dumpy variegation.

Enhancers		
Cross	Percent Asymmetry	Mean Wing score
dp^{w1} and E(z) Sb (151)	59	1.36
dp^{w1} and E(z) Sb+ (214)	70	1.26
H116 and E(z) Sb(165)	17	0.13
H116 and E(z) Sb+(238)	8	0.68
dp-23 and E(z) Sb(221)	63	0.99
dp-23 and E(z) Sb+(267)	52	0.68
dp^{w1} and Trl^{R67} Sb (330)	42	2.10
dp^{w1} and Trl^{R67} Sb+ (428)	36	2.42
H116 and Trl^{R67} Sb (42)	65	1.31
H116 and Trl^{R67} Sb +(87)	88	1.45
dp-23 and Trl^{R67} Sb (183)	58	2.64
dp-23 and Trl^{R67} Sb+ (110	48	2.93
Suppressors		
dp^{w1} and su(Var)205 Gla+(103	2	0.001
H116 and su(Var)205 Gla+(127)	8	0.08
dp-23 and su(Var)205 Gla+(255)	6	0.03
dp^{w1} and su(Var)3-9 Sb(217)	56	0.58
dp^{w1} and su(Var)3-9 Sb+(317)	0.005	0.005
H116 and su(Var)3-9 Sb(72)	72	0.32
H116 and su(Var)3-9 Sb+(91)	0.04	0.02
dp-23 and su(Var)3-9 Sb(118)	70	1.61
dp-23 and su(Var)3-9 Sb+(127)	0.02	0.008

Acknowledgments: I thank Lauren MacIntyre for making important editorial changes.

References: Ashburner *et al*. 2005, Drosophila: *A Laboratory Handbook*. Cold Spring Harbor Press; Carmon *et al*. 2010, Fly 4: 117-137; Rae *et al*. 2015, Dev. Cell 34: 310-322; Spofford 1959, Proc. Nat'l. Acad. Sci. 45: 1003-1007; Wilkin *et al*. 2000, Curr. Biol. 10: 559-567; E(z): CG63502, Flybase number FBgn0000629; Su(Var)205: CG8404, Flybase number FBgn0003607; Su(Var)3-9: CG43664, Flybase number FBgn0263755; Trl^{R67}: CG42507, Flybase number FBal0034116.

Wing heritability variation in *Drosophila willistoni* isofemale lines from three Brazilian Atlantic Forest fragments.

Fonseca, B.B.E., M.C. Ferreira, L.P.B. Machado, and R.P. Mateus*. Laboratório de Genética e Evolução, Departamento de Ciências Biológicas, UNICENTRO – Universidade Estadual do Centro-Oeste, Guarapuava-PR, Brazil. *Corresponding author: rogeriopmateus@gmail.com.

Introduction

Wings are considered key structures in the evolution and diversification of insects (Nicholson *et al*., 2014). This morphological structure has proved to be a great model for studies of complex traits, and several works have shown that it has phenotypic plasticity in association with different sources of environmental

variation (Weber, 1990; David *et al*., 1994; Morin *et al*., 1999; Debat *et al*., 2003; Carreira *et al*., 2006; Soto *et al*., 2008). In addition, evidence suggests that different aspects of wing morphology, such as size and shape, are targets of natural selection (Gilchrist *et al*., 2004).

The heritability of a morphological trait can be used to quantify the capacity of a certain population to respond to the action of natural selection on a given character. Thus, heritability estimates can collaborate to understand character evolution under selection. Heritability estimates made from laboratory procedures tend, by their nature, to generate overestimates, since the laboratory homogeneous and controlled environment reduces the environmental variance, increasing the proportion of genetic determination on the phenotype (Riska *et al*., 1989). Morphological variance and size heritability appear to be very sensitive to small environmental variations, becoming difficult to obtain consistent estimates. However, regarding form, the variance is less sensitive to environmental variations and its heritability is high, allowing to obtain similar estimates in different collections and locations (Birdsall *et al*., 2000).

Thus, the objective of this work was to quantify the morphological variation and to estimate the heritability of the wing morphology in laboratory conditions using *D. willistoni* isofemale lines from different fragments of the Atlantic Forest, in order to use these parameters to understand aspects related to the morphological evolution of this marker in this species.

Material and Methods

All isofemale lines were collected in 2018 from three fragments of the Brazilian Atlantic forest (Table 1). After initial identification (Freire-Maia and Pavan, 1949), candidate females were placed individually in vials, and, from those in which offspring were obtained, males were used to identify the *D. willistoni* species (Zanini *et al*., 2015). The obtained isofemale lines of each population were maintained in the laboratory at a constant temperature of 20°C.

Table 1. Localities, coordinates, type of phytophisiognomy of the Brazilian Atlantic Forest and date of collection of the isofemale lines of *Drosophila willistoni* used in this work. SSF = Semidecidual Seasonal Forest; MOF = Mixed Ombrophilous Forest (Araucaria Forest).

Locality	Coordinates	Phitophisiognomy	Collection
Fazenda Santa Cecília, Cajuru/SP	21°20'33.33"S, 47°16'0.83"O	SSF	February 2018
Parque Natural Municipal das Araucárias, Guarapuava/PR	25°23'36"S, 51°27'19"O	MOF	June 2018
Morro Santana, Porto Alegre/RS	30°04'12.8"S, 51°07"37.5"O	SSF	February 2018

The analyses of the wing morphological variance and heritability were performed using 22 pregnant females from the Cajuru-SP (CAJ) isofemale line, 14 from Guarapuava-PR (PMA), and 18 from Porto Alegre-RS (POA). These females were placed in vials containing standard *Drosophila* culture medium (banana-agar), and they were kept in these vials until the offspring were obtained. Each female and up to 13 female offspring (all together here called families) were separated and frozen in a 1.5 mL tube containing 0.5 ml of 70% alcohol. Overall, 648 individuals were obtained for morphometric analysis (270 from CAJ; 231 from POA; 147 from PMA).

The right wings of all individuals of each family were removed and were placed on slides, submerged in 70% alcohol and overlaid with coverslips, to be photographed. Eleven distance measurements (OA, OB, OE, AB, AE, BC, BD, BE, CD, CE and DE, according to Bitner-Mathé and Klaczko, 1999) from six anatomical landmarks (O, A, B, C, D and E) were obtained, based on the trellis method (Bookstein *et al*., 1985). All measurements were obtained using the IMAGEJ v. 1.52a software (Rasband, 2018). In this work, the landmarks used, located on the wing, were all type I (Bookstein, 1991).

For each distance, measurements were obtained for each family, parental female and the mean value among the descendants. All these values were logarithm transformed, and the Principal Components Analysis

(PCA) was performed in PAST v.3.26 software (Hammer *et al*., 2001). The first three Principal Components (PC) were used to perform linear regression (ordinary least square) between the pairwise values of parental females and the mean values of their respective offspring. The straight line resulting from the linear regression is explained by the equation y = a + bx, where "a" refers to the point where the line crosses the "y" axis, and "b" is the slope of the line.

As individuals maintained in the laboratory were used, the heritability estimate was performed on the intraclass correlation between siblings based on the partition of the variance of the laboratory females for the components between and within the isofemale lines. This was obtained multiplying the correlation coefficient by 2 (Falconer and Mackay, 1996). Cross-environment heritability represents the strict sense heritability (VA/VP), while heritability in the laboratory is increased due to variance, due to dominance, and the common environment (2 [1/2VA + 1/4VD + VEc]/VP).

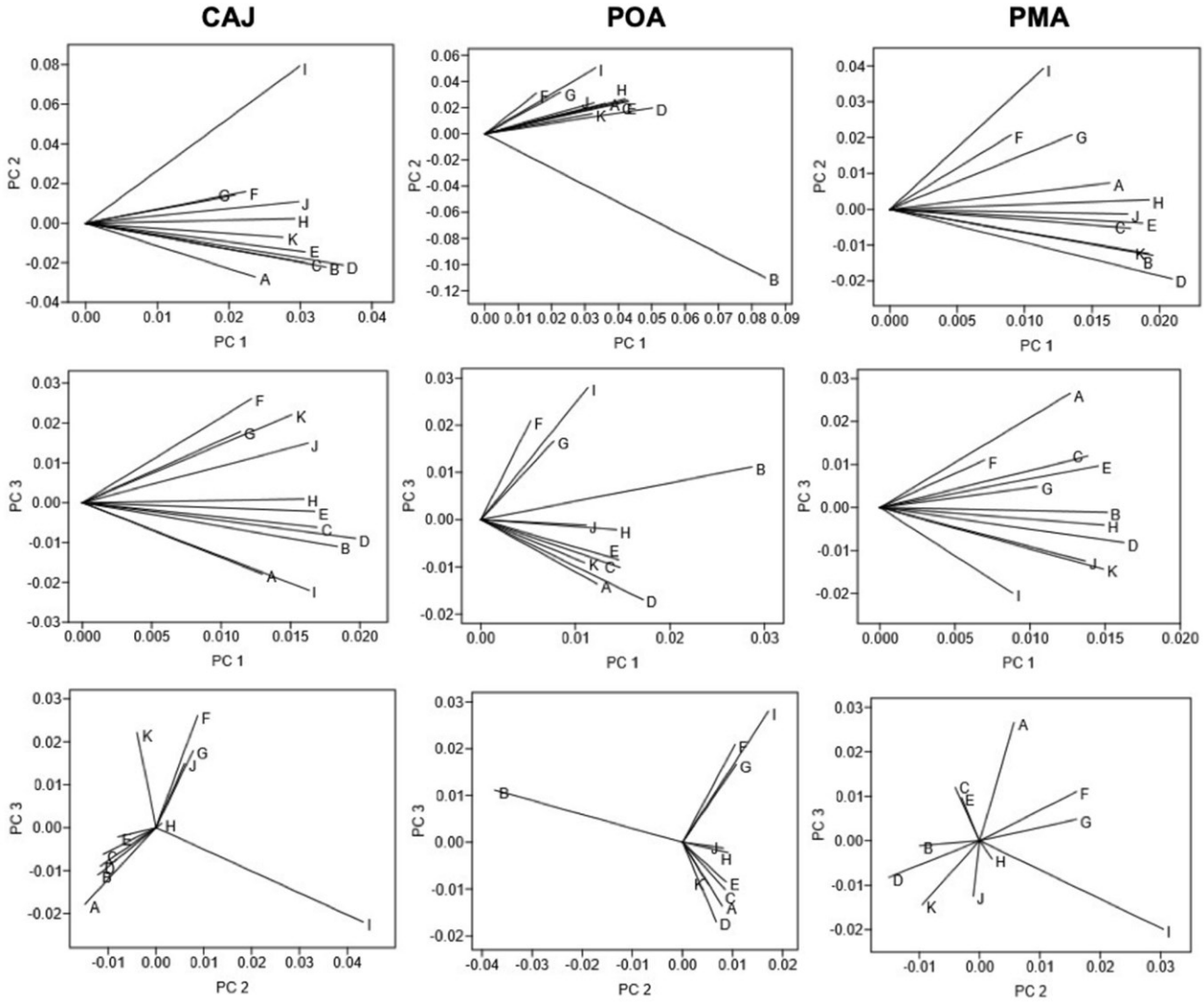

Figure 1. Correlations between each distance in the wing of *D. willistoni* and the three first Principal Components (PC1, PC2 and PC3) obtained from the covariance matrix. CAJ = Fazenda Santa Cecília – Cajuru/SP; POA = Morro Santana – Porto Alegre/RS; A = OA measurement; B = OB; C = OE; D = AB; E = AE; F = BC; G = BD; H = BE; I = CD; J = CE; K = DE; PMA = Parque Natural Municipal das Araucárias – Guarapuava/PR. Vectors indicate the direction of the maximum variation for each measure within the principal component plane.

Results and Discussion

The correlation analysis between the first three PC of *D. willistoni* (Figure 1) showed that all measurements had a positive correlation with PC1, which indicates that this is a component for wing size, while the other two, PC2 and PC3, are components related to the variation of wing shape. The wing shape variations in the three isofemale lines were highly correlated with the measurements OA, OB, and CD, which indicates that the region where most of the variation in shape occurs is in the anterior portion, both in the distal and in the proximal regions. Based on these results, PC1 was used as a measure of size variation, while PC2 and PC3 were used as measures of shape variation. From these data, the shape and size variances were calculated, and subsequently, linear regression graphs for size and shape values were obtained between each parental female and the mean value of its F1 females.

The PCA indicated that the variation components were responsible for more than 93% of the variance for CAJ, and for more than 88% and 92% in POA and PMA, respectively (Table 2). Regarding the total variances, comparing parental females with F1 females, it could be noted that the values are very close, with no significant difference. This may have occurred due to the fact that they were all created in the laboratory, and therefore, environmental interferences were minimized.

Table 2. Percentage that each PC explained of the total variance (% Var) and variance (Var) for size (PC1) and shape (PC2 and PC3) of *D. willistoni* parental females and the mean of their correspondent F1 female. CAJ = Fazenda Santa Cecília – Cajuru/SP; POA = Morro Santana – Porto Alegre/RS; PMA = Parque Natural Municipal das Araucárias – Guarapuava/PR.

	CAJ			POA			PMA		
		Variance (x 10^{-4})			Variance (x 10^{-4})			Variance (x 10^{-4})	
	% Var	Females	F1	% Var	Females	F1	% Var	Females	F1
Size	58.82	17.39	7.27	56.09	27.01	17.72	72.19	33.70	9.21
Shape PC2	27.09	10.97	6.87	23.08	3.96	1.23	11.90	6.57	2.26
Shape PC3	7.17	3.59	1.27	9.36	5.59	2.43	8.49	4.72	2.42
Total	93.08	31.95	15.41	88.53	36.56	21.38	92.58	44.99	13.89

Table 3. Correlation (r) and determination (r^2) coefficients, and heritability estimates (h^2) for wing size and shape of *D. willistoni*. CAJ = Fazenda Santa Cecília – Cajuru/SP; POA = Morro Santana – Porto Alegre/RS; PMA = Parque Natural Municipal das Araucárias – Guarapuava/PR. SE = standard error. ^{ns} p>0.05; *p<0.05; ** p<0.01.

	CAJ			POA			PMA		
	r	r^2	h^2 ± SE	r	r^2	h^2 ± SE	r	r^2	h^2 ± SE
Size	0.6788	0.4607	0.88±0.23^{ns}	0.6352	0.4035	0.74±0.27*	0.5779	0.3339	0.60±0.32^{ns}
Shape PC2	0.6053	0.3664	0.96±0.30^{ns}	0.2548	0.0649	0.28±0.30^{ns}	0.8612	0.7416	0.90±0.21**
Shape PC3	0.4562	0.2081	0.54±0.25^{ns}	0.5731	0.3284	0.76±0.29^{ns}	0.6685	0.4469	0.96±0.38^{ns}

Regressions showed positive correlations in all three isofemale lines; therefore, their slopes were positive (Figure 2). The slope values were multiplied by 2, which resulted in estimates of heritability for wing size and shape. For size, estimates ranged from 60% (PMA) to 88% (CAJ). Regarding form, they varied between 28% (POA) and 96% (CAJ) for PC2, and between 54% (CAJ) and 96% (PMA) for PC3 (Table 3).

It can be observed from the results that the wing morphology of *Drosophila willistoni* presented higher variation for size and smaller for shape. These results also showed that both individuals from nature and those created in the laboratory have the same pattern, as previous studies have found that the same type of variation occurred with individuals collected from nature (Ferreira, 2019). Of course, however, the laboratory

experiments produced less variation, as it is a controlled environment with fewer interventions and constant temperature.

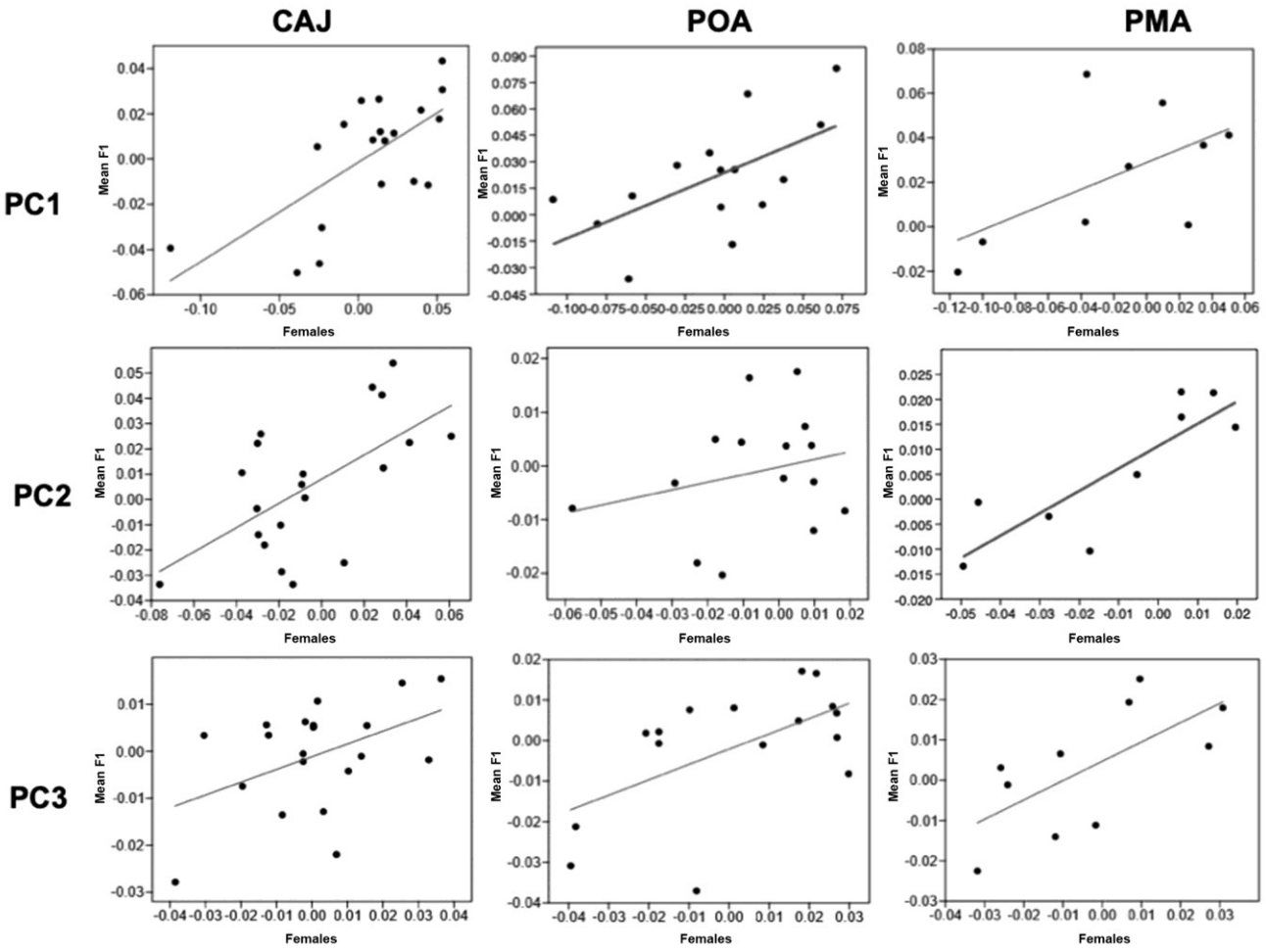

Figure 2. Size (PC1) and shape (PC2 and PC3) linear regression between *D. willistoni* parental female values and their respective F1 female mean values. CAJ = Fazenda Santa Cecília – Cajuru/SP; POA = Morro Santana – Porto Alegre/RS; PMA = Parque Natural Municipal das Araucárias – Guarapuava/PR.

Regarding heritability, our laboratory experiments did not show a clear pattern, as the estimate of size heritability was higher than those for shape in POA, and in CAJ and PMA, shape presented a higher heritability estimate than size (PC2 in CAJ; PC2 and PC3 in PMA). Higher shape heritability was also observed in individuals from nature, and in this case, as it is highly influenced by the environment, a certain genotype by environment interaction is expected. However, in laboratory, the influence of the environment is expected to be minimized; but nonetheless, no pattern emerged between the estimates of heritability. This observation could indicate that, in laboratory, the phenotype is influenced almost exclusively by genotype, of course to a lesser extent.

Even with this lack of pattern for heritability, it is clear that the estimates were higher in the laboratory than previously obtained for samples from nature. For example, Hoffmann and Schiffer (1998) found in *Drosophila melanogaster* that heritability is smaller in a stressful (nature) than in a controlled environment (laboratory). This was also observed in a previous study carried out by Ferreira (2019), where the same analyzes realized here were performed, however, with individuals collected from nature. Previous studies

have shown that the phenotypic correlation between parents and offspring for wing size, when in nature, is significantly lower when compared to laboratory strains (Gibert *et al*., 1998). However, Birdsall *et al*. (2000) point out that this does not happen in relation to the components of the wing shape. Therefore, our results are in agreement and corroborate that individuals maintained at constant temperature and with few environmental interventions will have higher heritability.

Keywords: morphometry, genotype by environment interaction, morphological variation.

Financial support: UNICENTRO, Fundação Araucaria de Apoio ao Desenvolvimento Científico e Tecnológico do Paraná - undergraduate research scholarship to B.B.E. Fonseca, and Coordenação de Aperfeiçoamento de Pessoal de Nível Superior (CAPES) Brasil - master degree scholarship for M.C. Ferreira.

References: Birdsall, K., E. Zimmerman, K. Teeter, and G. Gibson 2000, Blackwell Science 2: 16–24; Bitner-Mathé, B.C., and L.B. Klaczko 1999, Genetica 105: 35–42; Bookstein, F.L., 1991, Cambridge University Press; Bookstein, F.L., B. Chernoff, R.L. Elder, J.M. Humphries, G.R. Smith, and R.E. Strauss 1985, Academy of Natural Sciences 15: 1-277; Carreira, V., I.M. Soto, J.J. Fanara, and E. Hasson 2006, J. Evol. Biol. 9: 1275–1282; David, J.R., B. Moreteau, J.P. Gauthier, G. Pétavy, A. Stockel, and A.G. Imasheva 1994, Genet. Sel. Evol. 26: 229–251; Debat, V., M. Bégin, H. Legout, and J.R. David 2003, Evolution 57: 2773–2784; Falconer, D.S., and T.F.C. Mackay 1996, Essex; Ferreira, M.C., 2019, Dissertação de Mestrado do Programa de Pós-Graduação em Biologia Evolutiva da Universidade Estadual do Centro-Oeste; Freire, M.N., and C. Pavan 1949, Cultus 1: 3-66; Gibert, P., B. Moreteau, J.C. Moreteau, and J.R. David 1998, Heredity 80: 326–33; Gilchrist, G.W., R.B. Huey, J. Balanya, M. Pascual, and L. Serra 2004, Evolution 58: 768-780; Hammer, O., D.A.T. Harper, and P.D. Ryan 2001, Palaeontol. Electron 4: 9; Hoffmann, A.A., and M. Schiffer 1998, Evolution 52: 1207-1212; Morin, J.P., B. Moreteau, G. Petavy, and J.R. David 1999, Evol. Biol. 12: 329-339; Nicholson, D.B., A.J. Ross, and P.J. Mayhew 2014, Proc. Royal Soc. B 281: 1–7; Rasband, W.S., 2018, U.S. National Institutes of Health https://imagej.nih.gov/ij/, 1997-2018; Riska, B., T. Prout, and M. Turelli 1989, Genetics 123: 865–871; Soto, I.M., E. Hasson, and M.H. Manfrin 2008, Biol. J. Linn. Soc. Lond. 95: 655-665; Weber, K.E., 1990, Genetics 126: 975-989; Zanini, R., M. Deprá, and V.L.S. Valente 2015, Rev. Bras. Entomol. 59: 323-331.

Transferability of species-specific microsatellite primers from *D. prosaltans* to *D. austrosaltans.*

Paixão, Jéssica Fernanda, and Lilian Madi-Ravazzi. Laboratório de Genética, Ecologia e Evolução de *Drosophila*, Departamento de Biologia, Universidade Estadual Paulista "Júlio de Mesquita Filho" – Instituto de Biociências, Letras e Ciências Exatas – UNESP/IBILCE, São José do Rio Preto-SP, Brasil; email:lilian.madi@unesp.br

Abstract

A heterologous amplification test of 12 *Drosophila prosaltans* species-specific microsatellite primers for the species *Drosophila austrosaltans* is reported here. Of all the microsatellite primers tested, 66.7% had good amplification, a result superior to that found in the literature for tests on other pairs of species of *Drosophila*, probably due to the close phylogenetic relationship between the two species evaluated. The results presented here corroborate the possibility of transferability of microsatellite primers between closely related species phylogenetically and the potential of these markers in the investigation of the populational studies in species of the genus *Drosophila*, as well as in other species.

Introduction

Microsatellites (STR, SSR, or SSLP) are tandem repeats abundant in the genomes of prokaryotes and eukaryotes. Their presence favors different kinds of analyses in several areas of study (Zanella *et al*., 2017).

In genetics, they have been used, among others, in genetic mapping, species delimitation, kinship analysis, molecular profile, hybridization patterns, and phylogenetic proximity.

The possibility of using previously isolated and well-characterized microsatellite primers for a species in the study of phylogenetically related species has been a desirable and well-documented shortcut by researchers, especially when the aim is to optimize the availability of resources. In addition, the use of heterologous microsatellites allows analyzes of the relationship between species to be made with regard to different biological aspects (Laborda *et al.*, 2009).

In the present work, we tested the transferability of specific microsatellite loci from *D. prosaltans* (Duda, 1927) to *D. austrosaltans* (Spassky, 1957) (*Drosophila saltans* group). These species present complete pre-zygotic reproductive isolation from each other (Bicudo, 1973, 1978) and are closely related phylogenetically, although they do not form sister clades within the *saltans* subgroup (Roman, 2018).

Table 1. Microsatellite primers developed for *D. prosaltans*.

Loci	Primer Sequence (5'-3')	Motif	Size (bp)
Dpro_A	Primer F: TTCTGTTGAACGTCACATGC Primer R: ACCACTTACCACCTATCCCT	$(TG)_{10}$	238
Dpro_B	Primer F: CAAACTGTAGCTTGTGTGGG Primer R: TACTCATTCGCTTCCTGTCC	$(TG)_{7}$	170
Dpro_C	Primer F: GCATCACTAACCGAATCACG Primer R: CTAATGCTTCCTGCCCTCTC	$(GT)_{10}$	201
Dpro_D	Primer F: GACGGGCAAGAGAGTAGAAA Primer R: CCGCAACCAGAAAGAGAAAG	$(GT)_{7}$	235
Dpro_F	Primer F: TACTCATTCGCTTCCTGTCC Primer R: CAAACTGTAGCTTGTGTGGG	$(CA)_{8}$	172
Dpro_G	Primer F: TCTCCTTGTCATGATGGTCG Primer R: CTTGCAAGCGGTTGAGTAAA	$(GT)_{7}$	223
Dpro_J	Primer F: TGCCTGGTTGACTGACTAAC Primer R: CCGTAATGATGCTGCACAAA	$(ACTG)_{5}$	215
Dpro_K	Primer F: GCTTGGCCCATTTATCTTGG Primer R: CCAGTATCTATACCGGGCAC	$(CGG)_{5}$	167
Dpro_L	Primer F: AGCATTTTAAGCAACGCCAA Primer R: ATCATTCATTACGCGTTCGC	$(TG)_{8}$	292
Dpro_M	Primer F: GCTTCTTAGTCCTGACTGGG Primer R: TTTGTGAGTTTGCAGCACTC	$(GT)_{6}$	124
Dpro_N	Primer F: ACAAGCTTATGGAATGGGAA Primer R: CTGACTTCTTGCTGTTGGTG	$(GT)_{9}$	269
Dpro_O	Primer F: CAGGCACGTTAGCAACATTT Primer R: TGTCACTTTTTGCAGGCAAA	$(CA)_{9}$	173

Table 2. Information on Atlantic Forest populations of *D. austrosaltans*.

Collection site	Collection date	Coordinates	Phytophysiognomies	Area Size (ha)	Nº males by population
Fazenda Cambuhy, Matão/SP **(MAT)**	01/2016	21°37'S, 48°32'O	Semidecidual Seasonal Forest	2.189	10
Fazenda São João, Nova Granada/SP **(NGR)**	02/2016	20°32'S, 49º14'O	Semidecidual Seasonal Forest	1.359	15

Table 3. Data on the transferability of species-specific microsatellites primers from *D. prosaltans* to *D. austrosaltans*.

Loci	T1	T2	T3	Ta	[ ] $MgCl_2$	[ ] dNTP e Primers
Dpro_A	+	---	---	---	1,8 µl	0,8 µl
Dpro_B	-	-	---	---	---	---
Dpro_C	+	+	+	62°C	1,2 µl	0,6 µl
Dpro_D	+	---	---	---	1,6 µl	0,6 µl
Dpro_F	-	-	---	---	---	---
Dpro_G	+	+	+	62°C	1,2 µl	0,5 µl
Dpro_J	+	+	+	64°C	1,5 µl	0,8 µl
Dpro_K	-	-	---	---	---	---
Dpro_L	-	+	+	62°C	2,0 µl	0,8 µl
Dpro_M	+	+	+	62°C	1,5 µl	0,8 µl
Dpro_N	-	-	---	---	---	---
Dpro_O	+	+	+	62°C	1,4 µl	0,8 µl

T1 = Test with PCR cycle at Touchdown and the same concentration of reagents used for *D. prosaltans*; T2 = test with five variations in annealing temperature and adjustments in reagents concentrations; T3 = test with a specific optimal annealing temperature after the result of the T2 test. + = positive amplification; - = no amplification; --- = not tested due to previous results.

Materials and Methods

Twelve species-specific microsatellite loci of *D. prosaltans* (Table 1) were tested in two Atlantic Forest populations of *D. austrosaltans* (Table 2).

The transferability tests performed were: PCR in Touchdown (Laborda *et al.*, 2009) for each primer using the same concentrations of reagents that had been used for populations of *D. prosaltans* from the same collection sites (Test 1); for primers that had good Touchdown amplification, adjustments in reagent concentrations and tests with a variation of five different annealing temperatures (Test 2); for primers that had good amplification in one of the temperatures of Test 2, final adjustments in the concentrations of reagents (Test 3). Table 3 shows the test results and the positive or absent amplification for each locus. The PCR amplification products were visualized by electrophoresis in a 6% polyacrylamide gel stained with 15% silver nitrate (Sanguinetti *et al.*, 1994, with modifications). The gels were photographed using the BioDoc-It® 210 Imaging System.

Results and Discussion

The heterologous amplification of microsatellite markers specific from *D. prosaltans* to *D. austrosaltans* resulted in a transferability rate of 66.7%, that is, 8 out of the 12 pairs of primers tested had good amplification and could be used in population analyzes of the species. The microsatellite transferability rate reported here was high when compared to data from the microsatellite transferability literature among species of the genus *Drosophila*. Laborda *et al.* (2009) described 134 polymorphic microsatellite loci for the species *D. mediopunctata* (*tripunctata* group) and tested their heterologous amplification for 30 species of the subgenus *Drosophila* and *Sophophora*, obtaining an overall transferability rate of 48%.

These specific *D. mediopunctata* microsatellite loci were later tested in other studies. Tractz *et al.* (2012) obtained a transferability rate of 28% and 50% for the species *D. ornatifrons* and *D. maculifrons*

(*guarani* group), respectively. Trava *et al.* (2016) obtained a transferability rate of only 10% for the species *D. sturtevanti* of the *saltans* group. Trava (2018) described 13 polymorphic microsatellite loci for the species *D. sturtevanti* and tested their transferability to 15 species in the *saltans* group, obtaining a total transferability rate of 54.87%, since the test was for species within the same group.

In general, low transferability rates of microsatellite loci are correlated to the phylogenetic distance between the species being evaluated, since through the evolutionary processes of both species, mutations could have been fixed in the flank region of the loci, resulting in null alleles, responsible for low transferability (Trava *et al.*, 2016). This premise would explain the success in heterologous amplification between *D. prosaltans* and *D. austrosaltans*, species of the same subgroup, related phylogenetically, as well as the small amplification rate of *D. mediopunctata* loci obtained by Trava and collaborators (2016) for species *D sturtevanti*, as they belong to different subgenera. The primers tested here could be useful for an investigation of the diversity and genetic structure of *D. austrosaltans* populations and their transferability could be evaluated for other species in the *Drosophila saltans* group. The anticipated success for these studies may encourage others of the same nature, with the advantages already mentioned.

Acknowledgments: to FAPESP (Fundação de Amparo à Pesquisa do Estado de São Paulo) (process 2014/14059-0 and 2016/11994-5) and CAPES for financial support.

References: Bicudo, H.E.M.C., 1978, Genet. 1: 11-27; Bicudo, H.E.M.C., 1973, Genet. 44: 313-329; Duda, O., 1927, Archiv fur Naturgeschichte 91: 1-228; Laborda, P.R., L.B. Klaczko, and A.P. de Souza 2009, Conservation Genet. Resour. 1: 281-296; Roman, B.E., 2018, Reconstrução filogenética do grupo *saltans* de *Drosophila* utilizando marcadores morfológicos e moleculares. 79f. Dissertação (Mestrado em Biociências) - Instituto de Biociências Letras e Ciências Exatas, Universidade Estadual Paulista "Júlio de Mesquita Filho", São José do Rio Preto, 2018; Spassky, B., 1957, Univ. Texas Publ. 5721: 48-61; Sanguinetti, C., E. Dias Neto, and A.J.G. Simpson 1994, Biotechniques 17: 209; Tractz, C.C., G.R. Salomon, S.V. Zorzato, L.P.B. Machado, and R.P. Mateus 2012, Dros. Inf. Serv. 95: 76-79; Trava, B.M., 2018, Estrutura populacional de *Drosophila sturtevanti* (subgrupo *sturtevanti*; grupo *saltans*) por meio de microssatélites espécie-específicos e biodiversidade de drosofilídeos em domínios da Mata Atlântica. 124f. Tese (Doutorado em Biociências) - Instituto de Biociências Letras e Ciências Exatas, Universidade Estadual Paulista "Júlio de Mesquita Filho", São José do Rio Preto, 2018. Trava, B.M.; L.P.B. Machado, R.P. Mateus, L. Madi-Ravazzi 2016, Dros. Inf. Serv. 99: 16-18; Zanella, C.M., C. Turchetto, C. Palma-Silva, and F. Sperb-Ludwig 2017, Sociedade Brasileira de Genética 94-117.

Microsatellites null alleles detection in species of *guarani* and *guaramuru* groups collected in Highland Araucaria Forest of Brazil.

Santos, K.A.V., S.V. Zorzato, G.R. Salomon, L.P.B. Machado, and R.P. Mateus*. Laboratório de Genética e Evolução, Departamento de Ciências Biológicas, UNICENTRO – Universidade Estadual do Centro-Oeste, Guarapuava-PR, Brazil; *Corresponding author: rogeriopmateus@gmail.com.

Introduction

Drosophila griseolineata and *D. maculifrons* are sister species from *guaramunu* group, while *D. ornatifrons* belongs to the *guarani* group, which is phylogenetically close to *guaramunu* (Yotoko *et al*., 2003; Robe *et al*., 2005, 2010a,b; Hatadani *et al*., 2009). These species are frequently found in areas of the Atlantic Forest, mainly in the South of Brazil (Medeiros and Klaczko, 2004; Gottschalk *et al*., 2007; Döge *et al*., 2008; Hochmüller *et al*., 2010; Cavasini *et al*., 2014). There are few studies of genetic structure and, so far, there is only one published work that analyzed *D. maculifrons* populations through microsatellite loci, aiming to know the distribution of interpopulation genetic variability (Silva *et al*., 2015). Studies with this scope are important because genetic variability within a population is the basis for changes over time, resulting in population

differentiation. *Drosophila* microsatellite loci described for a species can be applied to others, and transfer success seems to depend in some level of phylogenetical relationships among them (Laborda *et al*., 2009a; Tractz *et al*., 2012; Prestes *et al*., 2015; Trava *et al*., 2016). Nevertheless, these heterologous amplifications can often result in null alleles due to mutations in the flanking regions, which could, in case of high frequency of null alleles, end up underestimating the genetic diversity of natural populations (Waples, 2018, as example). This way, the goal of this work was to investigate, using pedigree analysis, the occurrence of null alleles in *D. griseolineata*, *D. maculifrons,* and *D. ornatifrons* using heterologous amplification of microsatellites described to *D. mediopunctata* (Laborda *et al*., 2009b).

Materials and Methods

Drosophilid surveys were performed according to dos Santos *et al*. (2010) in two biological conservation areas characterized by highland Araucaria Forest vegetation in Guarapuava-PR municipality, Brazil: 1) Parque Natural Municipal das Araucárias (PMA) (25°23'36" S, 51°27'19" W), and Parque Natural Salto São Francisco da Esperança (SSF) (25º03'49.1" S, 51º17'29.8" W). Collected flies were identified (Freire-Maia and Pavan, 1949; Vilela and Bächli, 1990), and isofemale lines of *Drosophila griseolineata*, *D. maculifrons,* and *D. ornatifrons* were obtained, which were maintained at 20ºC and natural photoperiod.

Several crosses were performed for each population (PMA and SSF) of each species. Seven to nine days old couples (one female and one male, both virgins) were placed in a vial containing standard *Drosophila* food (banana-agar), and after seven days, each couple was transferred to a new vial with food. After another seven days in this new vial, the parental couples were individually frozen at -20ºC in 1.5 mL microtubes containing absolute ethanol. Each vial was examined until F1 emergence, and the offspring were also individually frozen at -20ºC in microtubes with ethanol, marked in order to link to its respective parental flies. All flies were maintained at -20ºC for later pedigree analysis.

Eleven *D. mediopunctata* microsatellite loci (Laborda *et al*., 2009b) that showed positive amplification in individual samples of *D. griseolineata* (Prestes *et al*., 2015), *D. maculifrons,* and *D. ornatifrons* (Tractz *et al*., 2012) were amplified in the parental and their respective offspring (Table 1).

Table 1. Characteristics of eleven microsatellite loci described for *D. mediopunctata* (Laborda et al., 2009b) that were tested for the presence of null allele in heterologous amplification in *D. griseolineata* (Prestes et al., 2015), in bold, *D. maculifrons* and *D. ornatifrons* (Tractz et al, 2012). BP = locus size in base pair; AT = primer annealing temperature (°C) used in the PCR amplification: G = *D. griseolineata*, M = *D. maculifrons*, O = *D. ornatifrons*, were used to differentiate distinctive AT for the same locus.

Loci	BP	AT
Dmed^{UNICAMP}_SSR034	115	60 (M),56 (O)
Dmed^{UNICAMP}_SSR053	122	56
Dmed^{UNICAMP}_SSR054	**214**	**50**
Dmed^{UNICAMP}_SSR057	137	60 (M),58 (O)
Dmed^{UNICAMP}_SSR065	198	51
Dmed^{UNICAMP}_SSR079	**143**	**54 (G)**, 58
Dmed^{UNICAMP}_SSR087	**128**	**56 (G)**, 60
Dmed^{UNICAMP}_SSR096	**152**	**54 (G)**, 52
Dmed^{UNICAMP}_SSR107	**179**	**56 (G)**, 55
Dmed^{UNICAMP}_SSR118	**136**	**50 (G)**, 58
Dmed^{UNICAMP}_SSR126	**291**	**54 (G)**, 56

Results and Discussion

All microsatellite loci were detected in females, and heterozygote males were also observed in most of them, indicating that they are not located in sex chromosomes. Two loci, SSR079 and SSR107, which were amplified in *D. griseolineata* from Santa Catarina (Prestes *et al*., 2015), were not amplified in our pedigree analyses of the highland Araucaria Forest PMA and SSF populations. This result was detected even using a touchdown program for amplification in the PCR machine. Thus, it could be suggested that mutations in the flanking regions of these loci are fixed in the *D. griseolineata* populations from Guarapuava-PR, avoiding primer annealing, resulting in null loci. The detection of null loci is important information on population differentiation, because null alleles can over time become fixed in a population but not in the other of the same species, indicating these populations are differentiating. Furthermore, populations or species that share null alleles or loci are probably closer to each other than to any other,

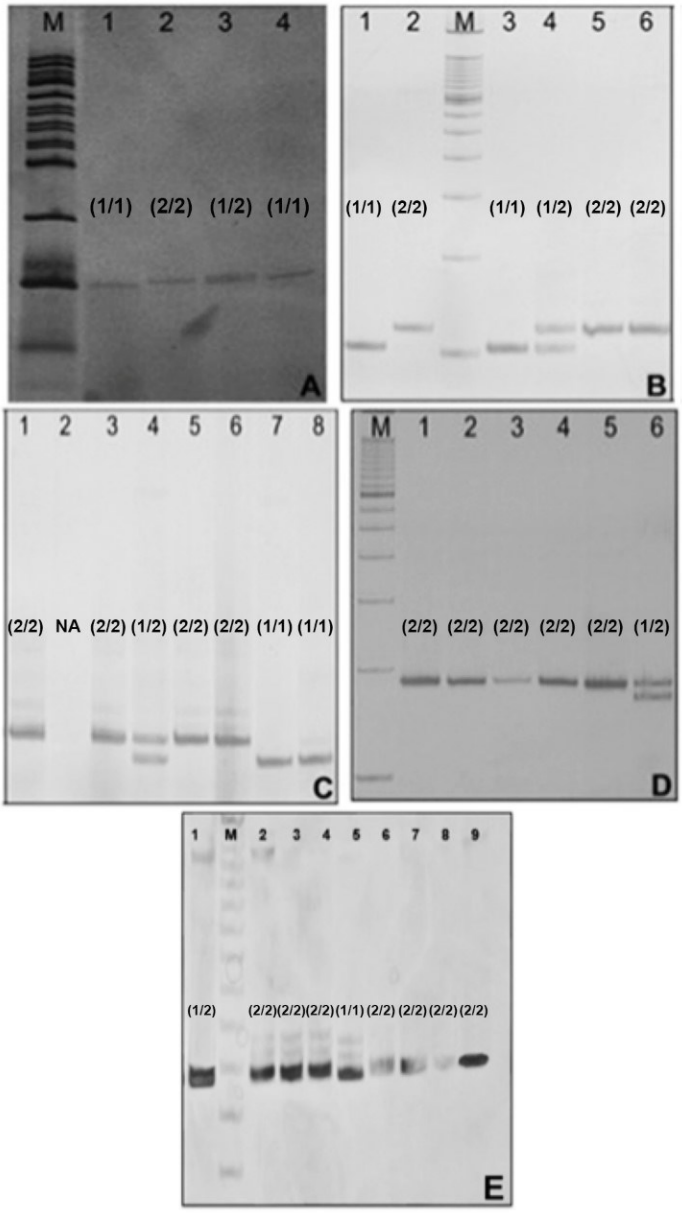

Figure 1. Visualization in 6% PAGE of microsatellite loci amplification from pedigree analyses of *Drosophila griseolineata*, *D. maculifrons* and *D. ornatifrons*. M = 100 bp ladder (1 μg/μL). A. SSR034 locus in *D. maculifrons*: 1 and 2 = parents; 3 and 4 = F1 descendants. B and C. SSR079 locus in *D. ornatifrons*: B. 1 and 2 = parents; 3 to 6 = F1descendants. C. 1 and 2 = parents; 3 to 8 = F1 descendants. D. SSR096 locus in *D. ornatifrons*: 1 and 2 = parents; 3 to 6 = F1 descendants. E. SSR126 locus in *D. griseolineata*: 1 and 2 = parents; 3 to 9 = F1 descendants. NA = no amplification.

or they could be the result of a previous population expansion (Callen *et al*., 1993).

Null alleles were detected in four microsatellite loci: SSR034 in *D. maculifrons*, SSR079 and SSR096 in *D. ornatifrons*, and SSR126 in *D. griseolineata*. In one cross of *D. maculifrons*, parents were genotyped as homozygotes for different alleles of SSR034, thus it was expected the whole offspring to be heterozygotes. However, one F1 descendant was homozygous for the allele of one of the parents. This indicated an absence of amplification (null allele) of the other parent allele in this F1 individual (Figure 1A).

It was possible to infer the presence of null alleles in SSR079 of *D. ornatifrons* through two crosses. In one, F1 flies were 1/1 or 2/2 homozygotes, and the parents were homozygotes for the same genotypes. Therefore, it was expected all offspring to be 1/2 heterozygote (Figure 1B). The fact that the majority of descendants were homozygotes for one or the other allele indicated that both parents had null alleles. In another cross, although the parental male showed no amplification, it was possible to observe that the female parent presented null allele because two F1 descendants did not show the maternal allele (Figure 1C). The pedigree analysis also showed the presence of a mutation in SSR096 of *D. ornatifrons*, as the parents and three of the four descendants were homozygotes for allele 2 and one F1 presented 1/2 genotype (Figure 1D).

For SSR126 of *D. griseolineata*, null allele was confirmed in the parental female, and it was transmitted to one F1 female (Figure 1E). The parental male was genotyped as heterozygote 1/2, the parental female as homozygote 2/2, and one F1 female was genotyped as a homozygote 1/1. If it is considered that the allele 1 of the F1 female had paternal origin, then the maternal allele was not represented (null allele). Thus, it can be concluded that neither the parental female nor the F1 female were homozygotes. The parental female

would have allele 2 and another non-amplified null allele in the homologous chromosome, and, therefore, the F1 female would have the paternal allele 1 and the non-amplified allele of maternal origin.

In cases where both parents and their F1 were homozygotes for the same allele, or even when a pedigree showed one parent to be homozygote and the other heterozygote, and the offspring did not present a different genotype than expected, the occurrence of null alleles could not be totally discarded. However, the absence of null alleles was confirmed in cases where both parents were heterozygotes, demonstrating that both alleles of the homologous chromosomes were amplified.

Null alleles can decrease the variability and diversity of microsatellite loci. However, its effects on the interpretation of Fis (inbreeding index) and Fst (population differentiation) must be done with caution (Waples, 2018). The analysis of population structure using microsatellite loci in some species of *Drosophila* and Coleoptera suggests low frequency of null alleles and, therefore, it may have little or no interference in population genetic data in the studied species (Machado *et al*., 2010; Marrec *et al*., 2014). The causes and consequences of null alleles in the analysis of population genetics seem to depend on the microsatellite motifs (repetition units), the organism, the mutation rates, and the frequency of these events (Angers *et al*., 2000; Estoup *et al*., 2002; Leblois *et al*., 2003; Adams *et al*., 2004; Navascues and Emerson, 2005; Machado *et al*., 2010; Marrec *et al*., 2014; Waples, 2018).

The results of the present study allowed us to infer a low frequency of null alleles, between 10 and 14% of the tested microsatellite loci, which suggests the other loci as suitable markers for population analyzes in the species *D. griseolineata*, *D. maculifrons,* and *D. ornatifrons*. However, due to the high homozygote proportion detected in pedigree analyses, a greater number of crosses would be necessary to further corroborate the low frequency of null alleles in these loci, and to discard their interference in case of heterozygote deficiency and/or non-amplification in population analyses. The detection of null loci, through heterologous amplification, in populations of *D. griseolineata* and *D. ornatifrons* indicates that the absence and presence of amplification may be good indicators of population differentiation in these species. Keywords: heterologous amplification, molecular marker, *D. griseolineata*, *D. maculifrons*, *D. ornatifrons*.

Financial support: Conselho Nacional de Desenvolviemnto Científico e Tecnológico (CNPq) and Fundação Araucária; Coordenação de Aperfeiçoamento de Pessoal de Nível Superior (CAPES) Brasil master degree scholarship for: KAVS, SVZ, and GRS.

References: Adams, R.S., K.M. Brown, and M.B. Hamilton 2004, Mol. Ecol. 13: 2579–2588; Angers, B., A. Estoup, and P. Jarne 2000, Mol. Biol. Evol. 17: 1926–1932; Callen, D.F., A.D. Thompson, Y. Shen, H.A. Phillips, R.I. Richards, J.C. Mulley, and G.R. Sutherland 1993, Am. J. Hum. Genet. 52: 922-927; Cavasini, R., M.L.T. Buschini, L.P.B Machado, and R.P. Mateus 2014, Braz. J. Biol. 74: 761-768; Döge, J.S., V.L.S. Valente, and P.R.P. Hofmann 2008, Rev. Bras. Entomol. 52: 615– 624; dos Santos, K., L.P.B. Machado, and R.P. Mateus 2010, Dros. Inf. Serv. 93: 185-188; Estoup, A., P. Jarne, and J.M. Cornuet 2002, Mol. Ecol. 11: 1591–1604; Freire-Maia, N., and C. Pavan 1949, Cultus 1: 3-66; Gottschalk, M.S., D.C. De Toni, V.L.S. Valente, and P.R.P. Hofmann 2007, Neotrop. Entomol. 36: 848–862; Hatadani, L.M., J.O. Mcinerney, H.F. Medeiros, A.C.M. Junqueira, A.M. Azeredo-Espin, and L.B. Klaczko 2009, Mol. Phylogenet. Evol. 51: 595-600; Hochmüller, C.J., M. Lopes-Da-Silva, V.L.S. Valente, and H.J. Schmitz 2010, Pap. Avulsos Zool. 50: 285-295; Laborda, P.R., L.B. Klaczko, and A.P. de Souza 2009a, Conservation Genet. Resour. 1: 281-296; Laborda, P.R., G.M. Mori, and A.P. de Souza 2009b, Conservation Genet. Resour. 1: 297-307; Leblois, R., A. Estoup, and F. Rousset 2003, Mol. Biol. Evol. 20: 491–502; Machado, L.P.B., R.P. Mateus, F.M. Sene, and M.H. Manfrin 2010, Biol. J. Linn. Soc. Lond. 100: 573-584; Marrec, R., S. Ruault, C. Ribout, M. Plantegenest, and B. Gauddre 2014, Eur. J. Entomol. 5: 726–729; Medeiros, H.F., and L.B. Klaczko 2004, Biota Neotrop. 4: 1-12; Navascues, M., and D.C. Emerson 2005, Mol. Ecol. 14: 1333–1341; Prestes, J.O., S.A. Beira, L.P.B. Machado, and R.P. Mateus 2015, Dros. Inf. Serv. 98: 35-37; Robe, L.J., V.L.S. Valente, M. Budnik, and E.L.S. Loreto 2005, Mol. Phylogenet. Evol. 36: 623-640; Robe, L.J., E.L.S. Loreto, and V.L.S. Valente 2010a, J. Zool. Syst. Evol. Res. 48: 310–321; Robe, L.J., V.L.S. Valente, and E.L.S. Loreto 2010b, Genetica 138: 725–735; Silva, D.C., L.P.B. Machado, and R.P. Mateus 2005, Braz. J. Biol. 75: 254-255; Tractz, C.C., G.R. Salomon, S.V. Zorzato, L.P.B. Machado, and R.P. Mateus, Dros. Inf. Serv. 95: 76-79; Trava, B.M., L.P.B. Machado, R.P. Mateus, and L. Madi-Ravazzi 2016, Dros. Inf. Serv. 99: 16-18; Vilela, C.R., and G. Bächli 1990, Mitt. Schweiz. Entomol. Ges. 63: 1–332;

Waples, R.S., 2018, J. Hered. 109: 457-461; Yotoko, K.S.C., H.F. Medeiros, V.N. Solferini, and L.B. Klaczko 2003, Mol. Phylogenet. Evol. 28: 614–619.

Life history traits and esterase activity of *Drosophila* species of the *tripunctata* and *guarani* groups in different food resources.

Domit, S.G., L.M.S. Baptista, B.M. Araujo, L.P.B. Machado, and R.P. Mateus*. Laboratório de Genética e Evolução, Departamento de Ciências Biológicas, UNICENTRO – Universidade Estadual do Centro-Oeste, Guarapuava-PR, Brazil. *Corresponding author: rogeriopmateus@gmail.com

Introduction

Drosophila mediostriata (Duda, 1925) of the *tripunctata* group has a Neotropical distribution. It can be found in several environments in Brazil, such as Atlantic Forest, urban areas, Cerrado and Amazon Forest (Schmitz and Valente, 2007). *Drosophila griseolineata* (Duda, 1927) belongs to the *guaramunu* group, which is closely related to the *tripunctata* group of *D. mediostriata* (Robe *et al*., 2010). It is generally found in humid areas of the Atlantic Forest, especially in the south and southeast of Brazil (Medeiros and Klaczko, 2004; Cavasini *et al*., 2014, as examples), and it is rarely collected in gallery forests of the Cerrado in Brazil (Tidon-Sklorz *et al*., 1994; Tidon, 2006). These species belong to groups of the most generalist Neotropical species and with high ecological versatility for breeding sites (Valadão *et al*., 2019).

The type and availability of food resources in nature can lead to changes in the organism fitness, mainly affecting life history traits such as viability and development time. The objective of this work was to evaluate the effect of different types of resources (standard *Drosophila* banana diet, and LPS, EPS, and HPS diets – Matzkin *et al*., 2011) on life history traits and the esterase activity, which are isozymes that, among other functions, play an important role in the insect digestive processes (Vogt and Riddiford, 1981; Karotam *et al*., 1993; Gu and Zera, 1994; Argentine and James, 1995; Feyereisen, 1995).

Material and Methods

Drosophila griseolineata and *D. mediostriata* larvae of strains from the Araucaria Forest highland area (Parque Natural Municipal das Araucárias), in the municipality of Guarapuava-PR, were transferred to 10 replicates (with 40 larvae each) with four types of diet: 1) BSM - banana standard medium; 2) HPS - High Protein Sugar, with a higher protein:sugar ratio; 3) EPS - Equal Protein Sugar, with an intermediate protein:sugar ratio; and 4) LPS - Low Protein Sugar, with a lower protein:sugar ratio. The last three diets were prepared according to Matzkin *et al*. (2011).

Viability was estimated as the average proportion of larvae transferred to each diet that survived to the adult stage. The development time was measured as the average time elapsed (in hours) between the transfer of the 1st instar larvae to the diet and the emergence of each adult fly. Esterase analyses were performed using electrophoresis on 10% polyacrylamide gel, as described by Mateus *et al*. (2011).

Results and Discussion

Drosophila griseolineata and *D. mediostriata* were not able to develop in the LPS and EPS diets. Thus, it was only possible to estimate the development time in BSM and HPS. It is worth mentioning that the viability of these species was also low in BSM, and even lower in HPS, with *D. griseolineata* showing higher viability in BSM and lower in HPS when compared to *D. mediostriata* (Table 1). These low viability values in HPS compromised a reliable analysis for the mean development time and the esterase activity in this diet for both species.

Table 1. Viability (VI - %) and Development Time (DT – h) of *Drosophila griseolineata* and *D. mediostriata* in different diets: Banana Standard Medium (BSM); Low Protein:Sugar (LPS); Equal Protein:Sugar (EPS); High Protein:Sugar (HPS). LPS, EPS and HPS according to Matzkin et al. (2011).

	Drosophila griseolineata				*Drosophila mediostriata*			
	BSM	LPS	EPS	HPS	BSM	LPS	EPS	HPS
VI	20	0	0	2,5	12,42	0	0	6,81
DT	490,35	-	-	435,00	415,50	-	-	444,80

Cactophilic *Drosophila* species that occur in xeric areas of the Nearctic have shown high viability in both standard diet and diets with variation in protein:sugar ratios (Matzkin *et al*., 2011). Flies of the *Sophophora* subgenus of *Drosophila* genus feed almost exclusively on microorganisms from fruits, consuming glucose and fructose in their natural environment. Thus, the use of these carbohydrates is probably more suitable for their development (Keller, 2007; Matzkin *et al*., 2009; Rovenko *et al*., 2015). However, generalist species of the *Drosophila* subgenus, such as *D. griseolineata* and *D. mediostriata*, feed on yeast of different parts of the plant, not only form fruits, requiring diets rich in yeast for optimal development. Therefore, their survival rates and reproduction increase when this component is provided (Good and Tatar, 2001; Keller, 2007; Matzkin *et al*., 2009; Rovenko *et al*., 2015; Valadão *et al*., 2019).

Drosophila mediostriata had slower development time for larvae that develop in HPS than in banana; the opposite was obtained for *D. griseolineata* (Table 1). This showed that, although the viability is similar among these closely related species, the resources provided for larval development affected differently in the development time, revealing that some species (populations or individuals) may be more vulnerable to dietary changes than others (Matzkin *et al*., 2011). The change in development time can have a direct consequence on fitness due to intra and interspecific competition, for example. Species with a longer development time are more susceptible to competition, while species with shorter development present greater competitive ability, since, in nature, the larvae explore scarce resources that rapidly deplete (Bakker, 1969; Zwaan *et al*., 1995; Nunney, 1996; Chippindale *et al*., 1997; Prasad *et al*., 2000; Wertheim *et al*., 2000; Krijger *et al*., 2001; Ghosh *et al*., 2019; Shrader *et al*., 2020).

The analysis of *D. griseolineata* esterase profile revealed the inactivation of the β-esterase (EST-5, arrow in Figure 1) in male adults obtained in HPS, which indicates the sensitivity of this enzyme whose expression occurs under a certain amount of sugar in the medium, or to another BSM component. However, in mammals, sugary diets can result in inactivation of esterase activity (Yan and Harding, 1999). For *D. mediostriata*, any other esterase enzyme detected in the adults (EST-1 and EST-6) showed change in HPS, when compared to the adults from BSM. Seven esterase loci (EST-1 to EST-7) were observed in adults from BSM. One was a β-esterase locus (EST-5) and all others were α-esterase (Figure 2). The esterase profile of individuals of this species from HPS diet showed the expression of EST-4 (arrow in Figure 2) only in some individuals, suggesting that the expression of this locus may be related to diets with a higher concentration of protein. Thus, it can be suggested that the response of a species to different diets depends on aspects related to the evolution of specific metabolic pathways for each evolutionary lineage.

The response to different resources on life history traits and isozyme activity was not similar, even in species of closely related groups such as those analyzed in this work. Therefore, future studies that analyze populational variation of the same traits under different conditions of energy resources will help to clarify the amplitude of the adaptive capacity of *Drosophila* species from Neotropical region.

Key words: Dietary, Isozymes, *D. griseolineata*, *D. mediostriata*.

Financial support: UNICENTRO, Conselho Nacional de Desenvolvimento Científico e Tecnológico (CNPq) - undergraduate research scholarship to S.G. Domit and L.M.S. Baptista, and Fundação Araucária - undergraduate research scholarship to B.M. Araujo.

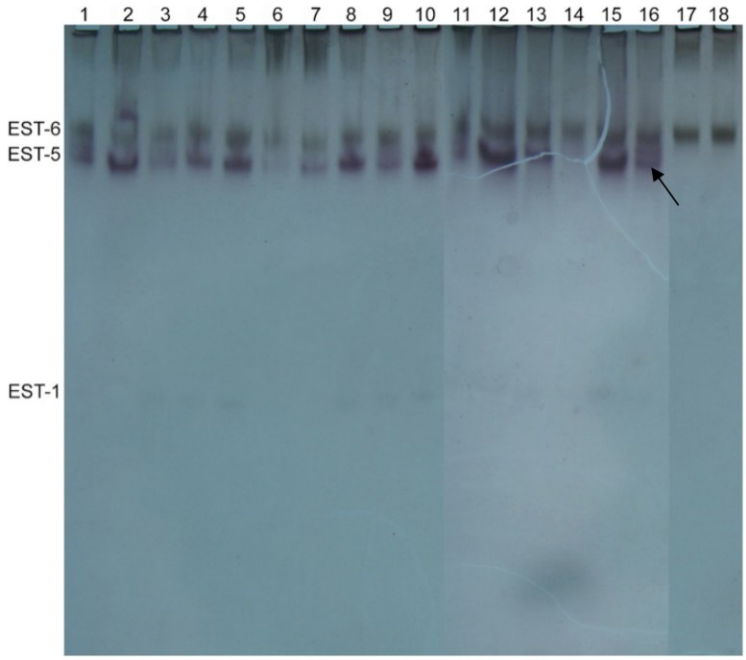

Figure 1. PAGE 10% of *Drosophila griseolineata* adults emerged from larvae that developed in BSM (1 to 10 – females; 11 to 16 – males;) and HPS (17 and 18). Arrow = β-esterase EST-5.

Figure 2 (below). PAGE 10% of *Drosophila mediostriata* adults emerged from larvae that developed in BSM (1 to 8 – females; 9 to 17 – males) and HPS (18 to 24 – females; 25 to 32 – males). Arrow = band obtained in individuals from HPS.

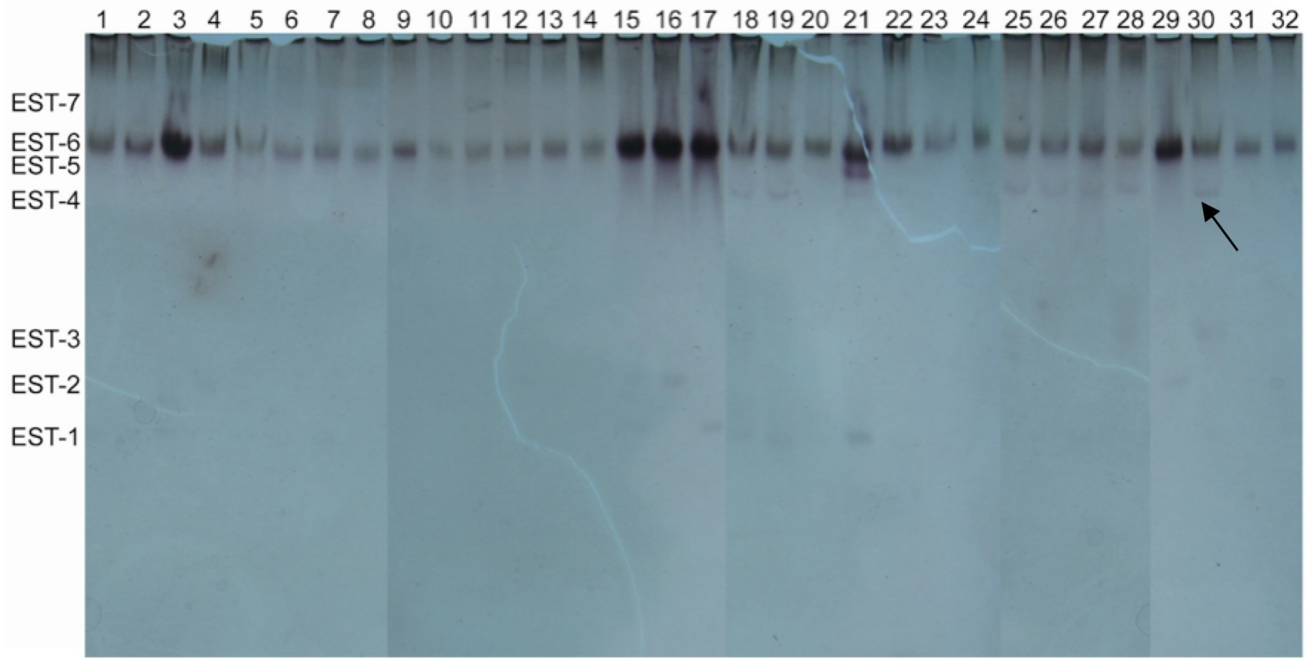

References: Argentine, J.A., and A.A. James 1995, Insect Biochem. Molec. Biol. 25: 621-630; Bakker, K., 1969, Neth. J. Zool. 19: 541-595; Cavasini, R., M.L.T. Buschini, L.P.B. Machado, and R.P. Mateus 2014, Braz. J. Biol. 74: 761-768; Chippindale, A.K., J.A. Alipaz, H-W. Chen, and M.R. Rose 1997, Evolution 51: 1536–1551; Duda, O., 1925, Arch. Naturgesch. 91: 1-228; Duda, O., 1927, Arten R Stricker; Ghosh, S.M., K.M. Satish, M. Jayaram, and A. Joshi 2019, Front Ecol. Evol. 7: 1-16; Good, T.P., and M. Tatar 2001, J. Insect Physiol. 47: 1467-1473; Feyereisen, R., 1995, Toxicol. Lett. 82/83: 83-90; Gu, X., and A.J. Zera 1994, Comp. Biochem. Physiol. B Biochem. Mol. Biol. 107: 553-560; Karotam, J., A.C. Delves, and J.G. Oakeshott 1993, Genetica 88: 11-28; Keller, A., 2007, Curr. Biol. 17: R77-R81; Krijger, C.L., Y.C. Peters, and J.G. Sevenster 2001, Oikos 92: 325-332; Mateus, R.P., L.P.B. Machado, and C.R. Ceron 2011, InTech p.353-372; Matzkin, L.M., S. Jhonson, C. Paight, G. Bozinovic, and T.A. Markow 2011, J. Nutr. 141: 1127-1133; Matzkin, L.M., K. Mutsaka, S. Johnson, and T.A. Markow 2009, J. Insect Physiol. 55: 1145–

1150; Medeiros, H.F., and L.B. Klaczko 2004, Biota Neotrop. 4: 1–12; Nunney, L., 1996, Evolution 50: 1193–1204; Prasad, N.G., M. Shakarad, V.M. Gohil, V. Sheeba, M. Rajamani, and A. Joshi 2000, Genet. Res. 76: 249–259; Robe, L.J., V.L.S. Valente, and E.L.S. Loreto 2010, Genetica 138: 725–735; Rovenko, B.M., N.V. Perkhulyn, D.V. Gospodaryov, A. Sanz, V. Lushchak, and V.I. Lushchak 2015, Comp. Biochem. Physiol. A Mol. Integr. Physiol. 180: 75- 85; Schimtz, H.J., and V.L.S. Valente 2007, Neotrop. Entomol. 36: 53-64; Shrader, M.E., H.J. Burrack, and D.G. Pfeiffer 2020, J. Econ. Entomol. 113: 230-238; Tidon, R., 2006, Biol. J. Linn. Soc. Lond. 87: 233–247; Tidon-Sklorz, R., C.R. Vilela, F.M. Sene, and M.A.Q.R. Pereira 1994, Rev. Bras. Entomol. 38: 627-637; Valadão, H., C.E. Proença, M.P. Kuhlmann, S.A. Harris, and R. Tidon 2019, Ecol. Entomol. 44: 721-737; Vogt, R.G., and L.M. Riddiford 1981, Nature 293: 161-163; Wertheim, B., J.G. Sevenster, I.E.M. Eijs, and J.J.M.Van Alphen 2000, J. Anim. Ecol. 69: 335-351; Yan, H., and J.J. Harding 1999, BBA-MOL BASIS DIS 1454: 183-190; Zwaan, B., R. Bijlsma, and R.F. Hoekstra 1995, Evolution 49: 635–648.

Modifiers of cell death in the *Drosophila* wing using sequenced strains of the *Drosophila melanogaster* Genetic Reference Panel (DGRP).

Lammons, John W., Kimberly A. Faria, and James N. Thompson, jr. Department of Biology, University of Oklahoma, Norman, OK 73019.

Using sequenced lines of the *Drosophila melanogaster* Genetic Reference Panel (DGRP), we are exploring genetic modifiers of cell death during development. In previous studies designed for a genetics laboratory course, we identified some key modifiers affecting the ommatidia number in males carrying the X-linked duplication Bar (*B*, 1-57.0; FlyBase, http://flybase.org). Precise counts of ommatidia in F1 Bar males heterozygous for known, sequenced genomes, followed by association mapping (GWAS; dgrp2.gnets.ncsu.edu) allowed the identification of some of the genes in the background that influenced the severity of cell death. In a companion study that compared the amount of cell death in the two compound eyes, however, we also explored a related, but independent trait, the maintenance of bilateral symmetry. This led to identification of genes influencing developmental homeostasis (Thompson *et al*., submitted). Deviation from symmetry (fluctuating asymmetry, FA) reflects the relative strength of developmental homeostasis, based on the formula: FA = |L-R| / [(L+R)*0.5], where L and R refer to the two sides of the bilateral trait, but not necessarily the anatomical "left" and "right" (Møller and Swaddle, 1997). Since it is the difference between the two sides of a bilateral trait, the anatomical units cancel out. FA simply measures the deviation from symmetry. In our present study, we use a similar approach to assess the modifiers of symmetry in amounts of cell death among 34 sequenced strains affecting a completely different trait: the amount of cell death as measured by the degree of notching of the wings of *Drosophila* carrying the dominant, sex-linked trait Beadex (Bx^2; 1-59.4).

Bx^2 females were crossed separately to males from sequenced strains of the DGRP collection (Mackay *et al*., 2012; obtained from the Bloomington *Drosophila* Stock Center). In each such cross, F1 offspring are genetically identical, being heterozygous for the known genome of a sequenced strain and for the inbred genetic makeup of the Bx^2 standard. In each screen of 34 DGRP genomes, both wings were removed from eight F1 male adults and mounted as pairs on a microscope slide with DePeX mountant (BDH Chemicals Ltd., Poole, England). Five wing pairs were traced for each DGRP cross. Images were taken using the CellSens program with an Olympus SZ61 microscope at 45×. Once the images were saved, they were analyzed with the program ImageJ (imageJ.nih.gov). The posterior area of the wing was outlined using the Polygon Selections feature (Figure 1). Two replicate tracings were done by each of two researchers for each wing to help assess measurement variance.

Areas of cell death are seen as cuts or notches along the edge of the wing, with the largest effects along the posterior margin. For this reason, our measurements focus on the posterior half of the wing, which is approximately equivalent to the posterior compartment of the *Drosophila* wing. Wings showed notable

symmetry within individuals (Figure 2). The asymmetry values of the five pairs from each DGRP cross were then averaged to create a single asymmetry value for each sequenced genotype. But symmetry remained stable across a wide range of wing areas (Figure 3).

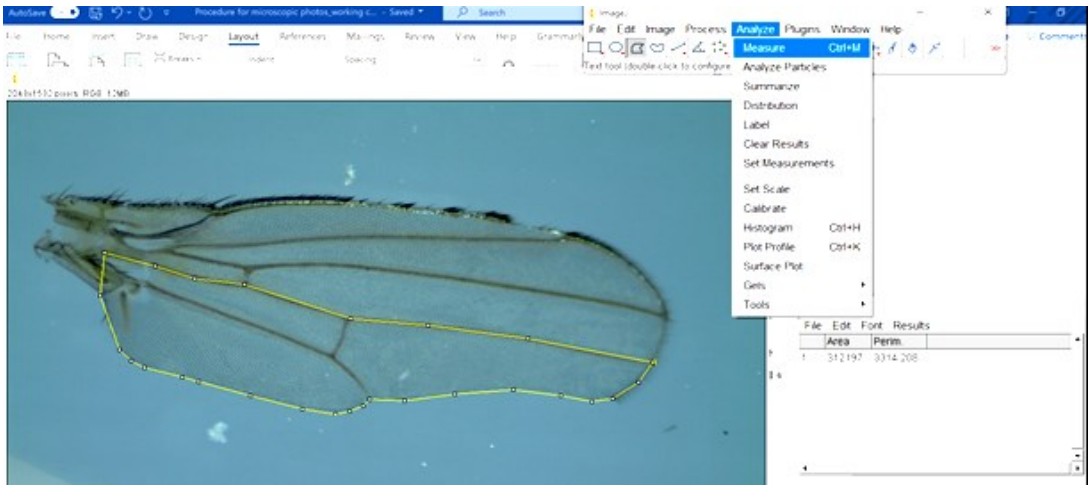

Figure1. Outline of the posterior area of the wing, measured along the length of the L4 vein to the tip and then along the posterior edge of the wing.

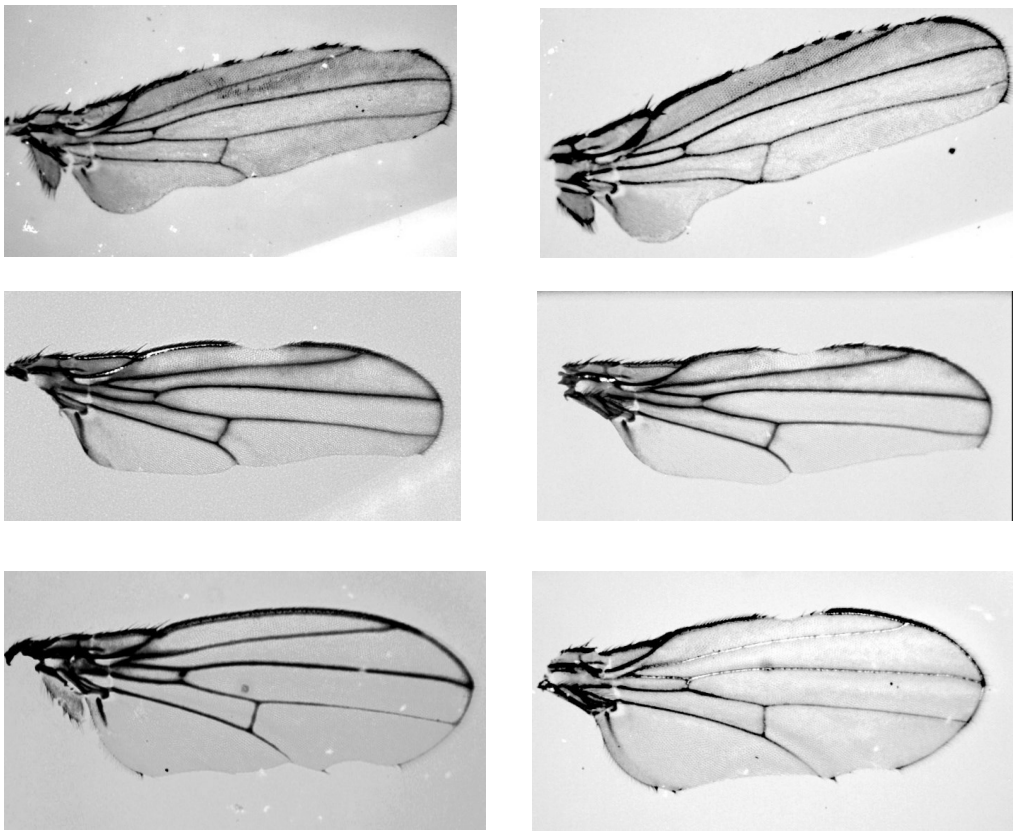

Figure 2. Representative pairs of wings showing the range of notching and the degree of symmetrical expression.

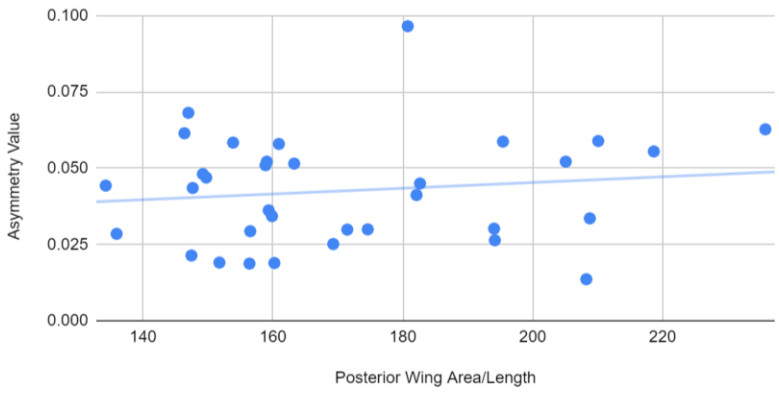

Figure 3. The degree of asymmetry does not change as a function of wing size (notching). Regression of asymmetry value on wing area scaled by wing length = 9.38E-05x + 0.0265 (not significant).

Table 1. Top-scoring loci associated with symmetry of wing cell death in Bx^2. Data from FlyBase.

p - value	FlyBase Gene	Gene
6.60E-07	FBgn0037783	Npc2c
6.60E-07	FBgn0037783	Npc2c
9.98E-07	FBgn0003747	Gr5a
1.22E-06	FBgn0037783	Npc2c
1.70E-06	FBgn0052333	CG32333
1.80E-06	FBgn0003747	Gr5a
1.80E-06	FBgn0003747	Gr5a
1.99E-06	///	
2.92E-06	FBgn0001085	fz
3.24E-06	FBgn0001085	fz
3.97E-06	FBgn0037720	CG8312
4.20E-06	///	
4.23E-06	FBgn0011656	Mef2
5.49E-06	FBgn0263102	psq
5.50E-06	FBgn0053519	Unc-89
7.04E-06	///	
7.20E-06	FBgn0037792	CG6241
7.20E-06	FBgn0261817	CG42759
7.31E-06	FBgn0052409	CG32409
8.34E-06	///	
8.79E-06	FBgn0052409	CG32409
9.73E-06	FBgn0021764	sdk
9.94E-06	FBgn0011656	Mef2

Single nucleotide polymorphisms (SNPs) linked to regions that segregate with loci that might be associated with degrees of symmetry were identified by genome-wide association mapping (GWAS; Table 1). There were 23 loci that were found to show a single mixed P value of less than 1×10E-6. Of these, four loci appeared more than once in the 23 most common gene associations: *Npc2c* (3 times), *Gr5a* (3 times), *fz* (2 times), and *Mef2* (2 times). *Npc2c* encodes for Niemann-Pick disease type C (NPC). In humans, this rare progressive genetic disorder is characterized by an inability of the body to transport cholesterol and other fatty substances inside of cells (*c.f.*, rarediseases.org). *Gr5a* is gustatory receptor 5a, which is involved in sweet taste receptor activity. Frizzled (*fz*) encodes for a family of receptors for *Wnt* ligands involved in signaling and planar cell polarity pathways. It is involved in processes like cell polarity, wing hair orientation, and other organ processes. Myocyte enhancer factor 2 (*Mef2*) encodes a protein that belongs to the MADS-box family of transcription factors and is required for muscle development. It directly activates a large number of muscle protein genes, and also regulates gene expression in other tissues, including the fat body and neural tissue. Among the other three candidate loci, *Unc-89* is also associated with muscle development. It codes for a protein needed for symmetrical formation of sarcomeres. The gene *sdk* (sidekick) is the protein-coding gene that is involved in several compound eye development events. Finally, pipsqueak (*psq*) codes for a transcription factor, whose effects include embryonic pattern formation and imaginal disc-derived wing morphogenesis. Thus, some of the most notable associations appear to have developmental roles one could hypothesize to be related to the wing, but further analysis and additional association mapping will be needed to clarify the developmental relationships uncovered by this approach. At this point, however, the functional connection between these effects, cell death homeostasis, and symmetry, if any, are not obvious.

References: Mackay, T.F.C. *et al*., 2012, Nature 482: 173-178; Møller, A.P., and J.P. Swaddle 1997, *Asymmetry, Developmental Stability, and Evolution*. Oxford University Press, Oxford; Thompson, J.N., jr., D.M. Tinney, and T. Holy (submitted); Thompson, J.N., jr., K. Faria, C.A. Delgado, A.W. Douglas, N.M. Henning, I. Jhingan, M.F. LaPorte, L.E. Longoria, J.R. McKinney, H.S. Park, S. Sowdagar, W. Xie, S. Zhang, and B. Safiejko-Mroczka 2019, Dros. Inf. Serv. 102: 91-93.

Gene duplication of the antimicrobial peptide attacin in Japanese populations of *Drosophila virilis.*

Kitagawa, Hiroko. Department of Chemistry, Faculty of Science, Josai University, Keyakidai 1-1, Sakado, Saitama 350-0295, Japan; E-mail: hkita@josai.ac.jp

Antimicrobial peptides play an important role in biological defense mechanisms, and seven distinct families have been identified in *Drosophila*. Defensin is produced in response to gram-positive bacteria (Dimarcq *et al.*, 1994), while cecropin, attacin, diptericin, and drosocin are produced in response to gram-negative species (Wicker *et al.*, 1990; Charlet *et al.*, 1996; Ekengren and Hultmark., 1999; Hedengren *et al.*, 2000). Drosomycin and metchnikowin are known to be produced in response to fungi (Bulet *et al.*, 1993; Levashina *et al.*, 1995). As indicated by Sackton *et al.* (2007), *Drosophila melanogaster* attacin is encoded by four genes; diptericin, by two genes; cecropin, by six genes (including pseudo-genes); and drosomycin, by seven genes. Analysis of the entire genome sequence of *Drosophila virilis* has shown that attacin is encoded by four genes; diptericin, by three genes; cecropin, by five genes (including pseudo-genes); and defensin, by two genes. Thus, the drosomycin and drosocin found in *D. melanogaster* differ from those found in *D. virilis*, indicating that each species of insect has different types of antimicrobial peptides and different numbers of underlying genes.

Drosophila species have adapted to a variety of environments. The main diet of *D. melanogaster* is fermented fruit, while *D. virilis*, which is native to forests, is known to feed mainly on tree sap and rotten wood (Throckmorton, 1975). Thus, it is believed that, for these types of antimicrobial peptides to adapt to the variety of microorganisms that grow in each environment, the composition and expression patterns of the genes change. Forest-dwelling *D. virilis* is thought to have resistance to fungi. With 67% of its land covered in forest, Japan is one of the few "forest nations" in the world. In addition, the Japanese islands stretch from north to south, and the country is split in the center by a mountain range that divides the country into the Sea of Japan and Pacific Ocean sides, creating a wide variety of forest types. Thus, it is likely that *D. virilis*, which inhabits forests throughout Japan, experienced evolutionary changes in its antimicrobial peptide genes to allow it to adapt to the microorganisms present in the different types of forests.

Attacins are glycine-rich antimicrobial peptides with similar biological activities. Attacin A and B genes are arranged in tandem. Attacin C is similar to the nearby attacin A and B genes. Attacin D gene is more divergent and located on a different chromosome (Hedengren *et al.*, 2000). Attacin genes retain high levels of polymorphism in *D. melanogaster* populations (Lazzaro and Clark, 2001).

In the present study I deal with the attacin genes of *D. virilis*. I report herein genetic variation in five lines derived from Japanese population.

Materials and Methods

D. virilis individuals were collected at five locations in Japan, maintained as isofemale lines listed in Table 1. A Mexican population of *D. virilis* was obtained from the National Drosophila Species Resource Center.

Genomic DNA obtained from adult flies was prepared, and the attacin genes were amplified using genomic PCR. Attacin A and B are structured so that primers AB-1 and AB-2 are positioned on the chromosome so as to sandwich the two genes, and attacin C and D primers C-1, 2 and D-1, 2 are structured by each of the genes (Table 2). PCR was performed using the PrimeSTAR HS (Takara Bio Inc. Japan) kit using the following protocol: 98°C for 10 s, 60°C for 5 s, and 72°C for 4 min. The size of the PCR products was confirmed using agarose gel electrophoresis. The PCR products were sequenced using a BigDye Terminator Cycle Sequencing kit (Applied Biosystems, USA) on an ABI PRISM 310 Genetic Analyzer. Phylogenetic trees were constructed using MEGA7 (Kumar *et al.*, 2016).

Table 1. Populations of *Drosophila* used in this study.

Population name	Collection location and year
KIBA	KIBA, JAPAN, 1979
MEX	MEXICO[a]
SAP	SAPPORO, JAPAN,
KYO	KYOTO, JAPAN, 2002
HO99	HORIOKA, JAPAN, 1999
HO83	HORIOKA, JAPAN, 1983
OM80	OMAEZAKI, JAPAN, 1980
OM78	OMAEZAKI, JAPAN, 1978

[a] Obtained from the National Drosophila Species Resource Center (stock numbers 15010-1051.48)

Table 2. Oligonucleotide primers used in genomic PCR.

Name	Sequence (5' - 3')
AB-1	GCAGATGTCCCAATCGAGTC
AB-2	GCTCGAAGTCGCGAGCTGAAC
C-1	CATCTGCGACTTCAGAACGTA
C-2	TGATCCACAGGCTTATCAGGA
D-1	ACTTATTTCAGATGCTAACGCA
D-2	ACTAAATAAGCCACATTGGAG

Results and Discussion

Agarose gel electrophoresis analysis of the genomic DNA PCR products of the seven lines in six populations are shown in Figure 1. In all lines, attacin C had a single band of 1.8 Kb, and attacin D had a single band of 1.5 Kb. The number of base pairs estimated based on the genome data was 1,775 bp for attacin C and 1,471 bp for attacin D, and, therefore, the band size was nearly consistent. Based on this analysis of the nucleotide sequences, I found that there is one gene each, and, as indicated by the genome data, attacin C has a 308-bp exon 1 and 400-bp exon 2, while attacin D has a 161-bp exon 1 and 385-bp exon 2. In contrast, however, analysis of the PCR products of attacin A and B indicated that band sizes differed by population. PCR fragment of KIBA population was approximately 6 Kb and those of the Mexico, Sapporo, Kyoto, and Horioka (total = 4) populations were 3.7 Kb, while those of the two lines from Omaezaki were 1.5 Kb. The

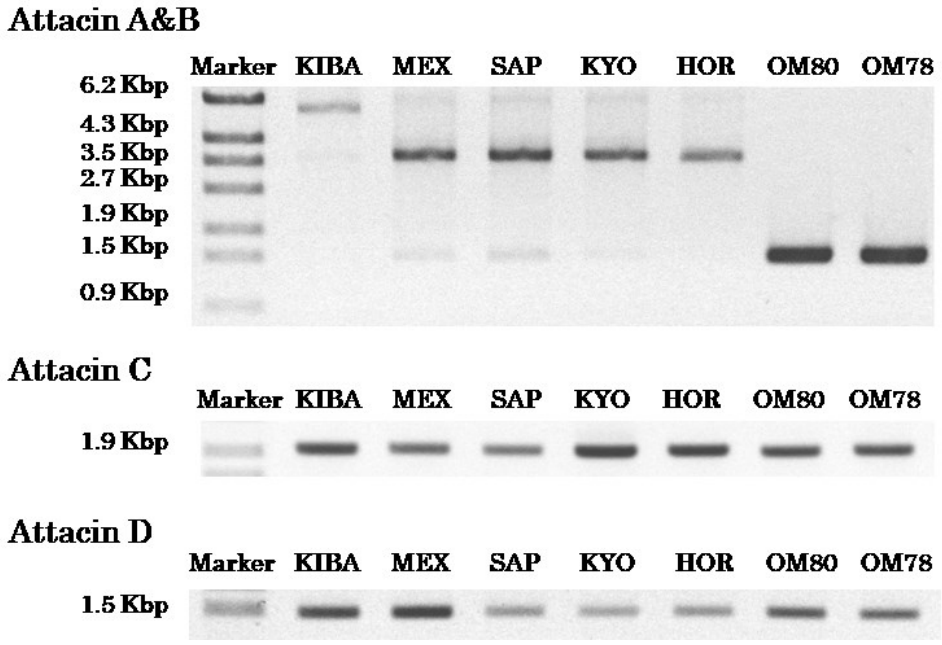

Figure 1. Agarose gel electrophoresis analysis of the PCR products of the attacin genes. See Table 1 for the names of the populations. The numbers on the left indicate the size of the marker DNA.

size of this region as estimated from the genome data was 3,679 bp. Based on correspondence to the 3.7-Kb fragments indicated in the four populations, I estimated that attacin A and B genes were present. I analyzed the nucleotide sequences for all the fragments in order to investigate the reasons for the differences in length. Our analysis of the nucleotide sequences showed that there were three attacin genes on the 6-Kb fragments of KIBA; two attacin genes on the 3.7-Kb fragments of the four populations of Mexico, Sapporo, Kyoto, and Horioka; and one attacin gene on the 1.5-Kb fragments of Omaezaki. Two attacin genes corresponded to A and B, and I named the upstream genes A and the downstream genes B. The three KIBA genes were named KIBA-1, 2, and 3.

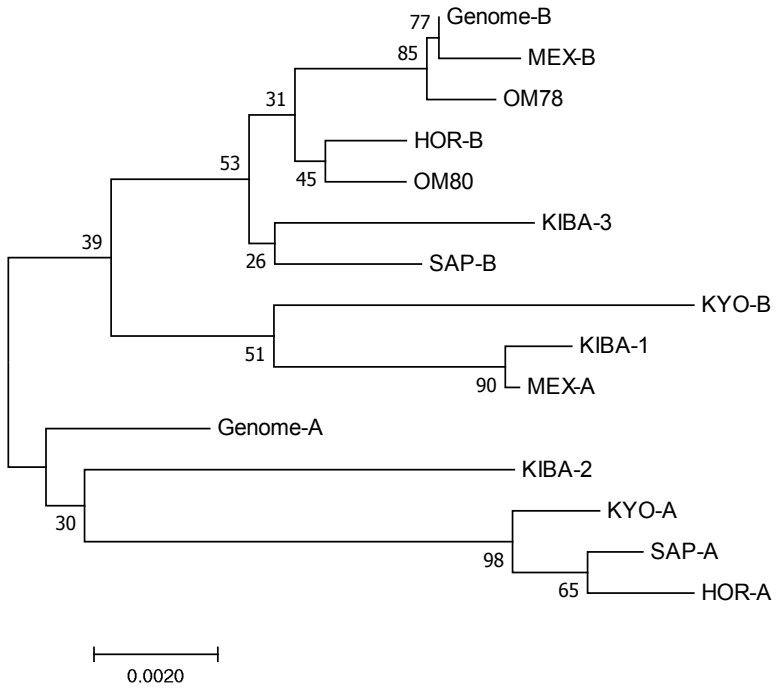

Figure 2. Molecular phylogenetic tree for the attacin gene. The evolutionary history was inferred using the Neighbor-Joining method (Saitou and Nei, 1987). The optimal tree with the sum of branch length = 0.05693157 is shown. The percentages of replicate trees in which the associated taxa clustered together in the bootstrap test (500 replicates) are shown next to the branches (Felsenstein, 1985). The tree is drawn to scale, with branch lengths in the same units as those of the evolutionary distances used to infer the phylogenetic tree. The evolutionary distances were computed using the Kimura 2-parameter method (Kimura, 1980) and are in the units of the number of base substitutions per site.

I created phylogenetic trees (Figure 2) of the eight lines, including genome data, from the region of exon 1, including an intron, to the region of exon 2 using the neighbor joining method (Saitou and Nei, 1987). The results indicated that they were broadly divided into two groups. Based on the fact that KIBA-2 was included in the same groups as attacin A of the genome and A in the three populations of Sapporo, Kyoto, and Horioka, I identified KIBA-2 as attacin A. Another group was divided into two sub-groups, with OM78, OM80, and KIBA-3 located in the same groups as attacin B of the genome and B of the four lines, and thus I identified them as attacin B. Therefore, the Omaezaki population had lost the attacin A. The other sub-group included KIBA-1. The KYO B gene was located in this group, but since there was a close relation to the A gene of Mexico, I inferred that KIBA-1 was the attacin A gene.

The gene composition of attacin A and B were shown in Figure 3. In the four populations of Mexico, Sapporo, Kyoto, and Horioka, attacin A and B are separated by approximately 1.4 Kb, which corresponds with the genome data (Figure 3 (B)). In KIBA, the three genes are nearly the same distance apart, at approximately 1.4 Kb (Figure 3 (A)). The heavy line in Figure 3 (B), from the nucleotide sequence and alignment of the genome data, inserts into the upstream side, which I believe indicates that attacin A has increased in size. Attacin A has been lost in the Omaezaki population. The heavy line in Figure 3 (B) from the nucleotide sequence and alignment of the genome data is lost at the position indicated by the arrow. Based on these data, I found that among the Japanese populations of *D. virilis*, there are those with different numbers of attacin A genes. It is interesting that although KIBA is geographically close to Horioka, their genetic compositions are different. Moreover, although the Omaezaki samples were collected during different years, the same genetic composition was observed, and thus, the genetic composition of this population might be fixed. In *D.*

melanogaster, attacin A and B genes have generated by paralogous gene conversion events (Lazzaro and Clark, 2001), similar to the results I found for *D. virilis* in the present study. Further studies to investigate other antimicrobial peptide genes in *D. virilis* are required to clarify the adaptive response to microbial environments.

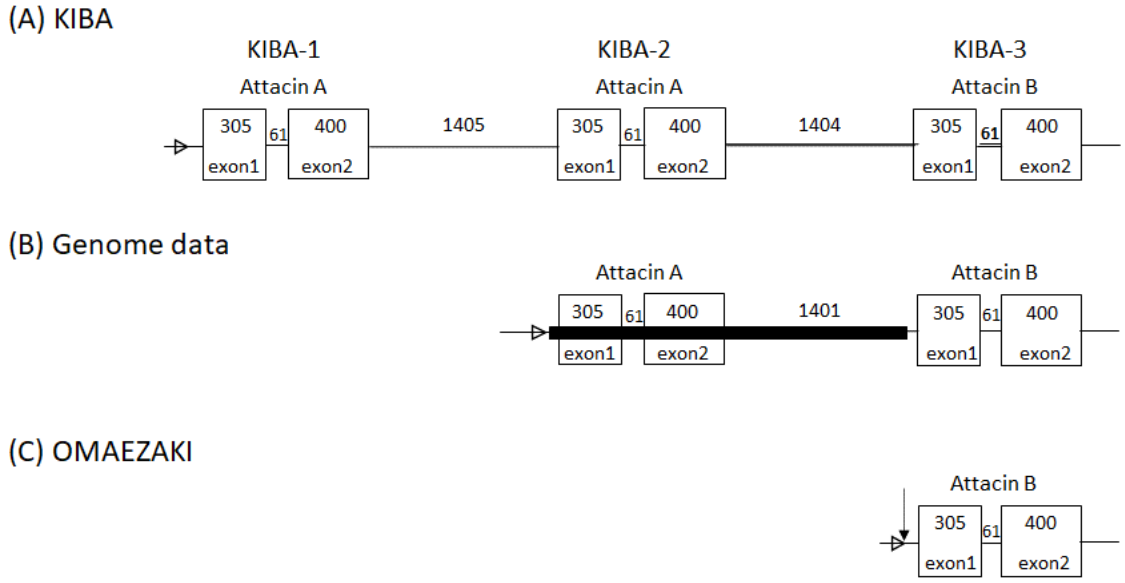

Figure 3. The gene composition of the attacin A and B. (A) shows the KIBA population, (B) shows the genome database, and (C) shows the Omaezaki population. The box indicates the exons; the numbers indicate the number of base pairs; and the triangle indicates the location of the PCR primer on the 5' side. The heavy line in the (B) indicates the size of the deletion/insertion. Arrow in the (C) indicates the location of the deletion/insertion.

References: Bulet, P., J.L. Dimarcq, C. Hetru, M. Lagueux, M. Charlet, G. Hegy, A. Van Dorsselaer, and J.A. Hoffmann 1993, J. Biol. Chem. 268: 14893-14897; Charlet, M., M. Lagueux, J. Reichhart, D. Hoffmann, A. Braun, and M. Meister 1996, Eur. J. Biochem. 241: 699-706; Dimarcq, J., D. Hoffmann, M. Meister, P. Bulet, R. Lanot, J. Reichhart, and J.A. Hoffmann 1994, Eur. J. Biochem. 221: 201-209; Ekengren, S., and D. Hultmark 1999, Insect Biochem. Mol. Biol. 29: 965-72; Felsenstein, J., 1985, Evolution 39: 783-791; Hedengren, M., K. Borge, and D. Hultmark 2000, Biochem. Biophys. Res. Commun. 279(2): 574-581; Kimura, M., 1980, J. Mol. Evol. 16: 111-120; Kumar, S., G. Stecher, and K. Tamura 2016, Mol. Biol. and Evol. 33: 1870-1874; Lazzaro, B.P., and A.G. Clark 2001, Genetics 159: 659–671; Levashina, E., S. Ohresser, P. Bulet, J. Reichhart, C. Hetru, and J.A. Hoffmann 1995, Eur. J. Biochem. 233: 694-700; Sackton, T.B., B.P. Lazzaro, T.A. Schlenke, J.D. Evans, D. Hultmark, and A.G. Clark 2007, Nature Genet. 39: 1461-1468; Saitou, N., and M. Nei 1987, Mol. Biol. Evol. 4: 406-425; Throckmorton, L.H., 1975, *In*: *Invertebrates of Genetic Interest*. Plenum Press, New York, 421-469; Wicker, C., J.M. Reichhart, D. Hoffmann, D. Hultmark, C. Samakovlis, and J.A. Hoffmann 1990, J. Biol. Chem. 265: 22493-22498.

A Turing machine for the Life Sciences.

Spratt, Spencer J.[1,2]*. [1]Okinawa Institute of Science and Technology Graduate University 1919-1 Tancha, Onna-son, Kunigami-gun, Okinawa 904-0495; [2]Department of Electrical Engineering and Information Systems, The University of Tokyo, Tokyo 113-8656, Japan; *e-mail: ifxequals1minusxput0ifnotput1@gmail.com

Abstract

During the development of new medicines mutually exclusive specificity appears to be required but hitherto is most often included at the late clinical trial stage. Here, I describe the use of Hedgehog signalling in *Drosophila* as a model to represent a mutually exclusive relationship within the context and report the identification of *CG43658*, a putative Rho guanine nucleotide exchange factor and orthologue of the Charcot-Marie-Tooth disease associated gene *ARHGEF10*. Furthermore, a Computer that is able to consider the whole and describe the sum of everything in it absolutely in unambiguous terms is a useful tool. Here I describe such a computer with a suggestion for an application to examine any component in the context where a medicine is sought. Taken, together I would like to propose this method as a fundamental necessity and improvement upon current existing methods related not only to Hedgehog signalling but plausibly to life science research and the search for medicines in general. Keywords: Turing machine, *Drosophila*, Mutual exclusivity, Specificity, *In vivo* database searching, Machine learning, Philosophy of Science

Introduction

An introduction to the problem

Before a new medicine can be used, it needs to be tested in the context it has been developed for, very often a whole human. In principle this is to examine two things: 1/ that it is effective against the problem, for example a virus or cancer, and 2/ that it does not appear to cause harm. We might imagine two cell types: those afflicted or infected and those not. However, while this often appears to be an oversimplification, any medicine should function with specificity to a degree able to neutralize diseased cells or make them better while not affecting vital cells or tissue to any extent that could compromise viability of the organism. Thus, it can be seen that however which way we look at this type of problem when it comes to the consideration of the context and searching for medicines there is a mutually exclusive conditional requirement for specificity. And interestingly a *specific* we are informed is an outdated term for a medicine (OED, 1989).

This requirement is not a problem *per se* but hitherto the way to achieve this I believe does present a problem and helps to explain not only the lengthy and costly process of research and development (R&D) but also the fact that many potential medicines fail. Thus any method that can speed up this process and importantly enable a better determination of potential therapeutic targets and medicines and their potential for mutually exclusive specificity with respect to the context at an early stage in R&D does appear sought after and should be of high interest.

Some reasons for the problem: The consideration of the context, relationship and the use of scientific induction

Context can be everything including the cells and things (*e.g.*, components such as nucleotides, proteins, lipids, sugars etc. or any other functional entity) they consist of and their relationships with each other and the sum of this in space-time. Thus, context can be described by the sum of relationships or simply: context = relationship (Figure 1a). Therefore it seems apparent that any consideration of a context should include a corresponding relationship.

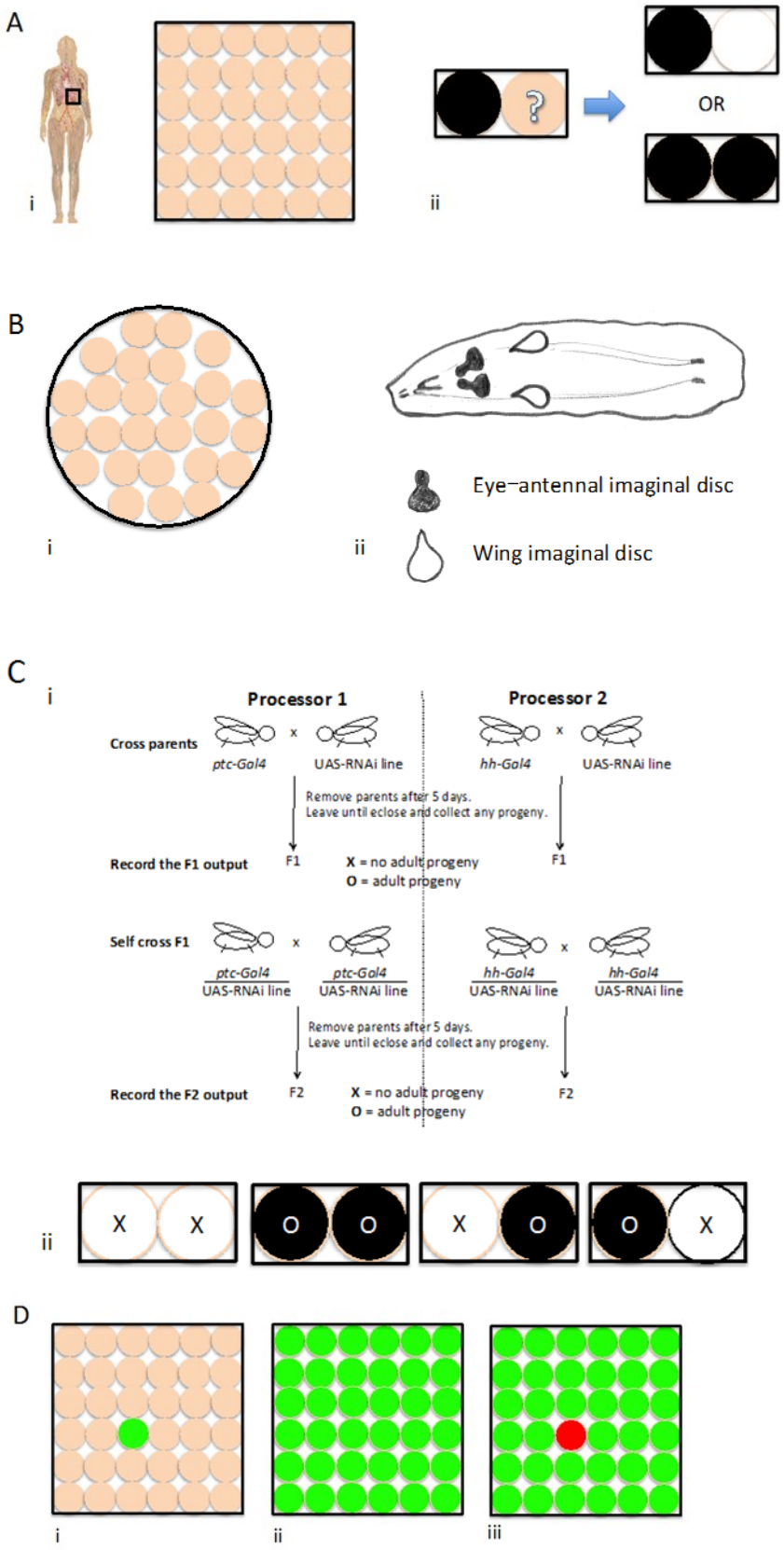

Figure 1. The consideration of context in the life sciences A) i: A schematic of a human body with a representation of a field of cells. ii: A system can be described by considering the relationship between two parts. B) i: A schematic of human cells in a cell culture dish. ii: a drawing of a *Drosophila* wandering 3rd instar larva with depictions showing the eye-antennae and the wing imaginal discs and their approximate positions. C) Fly mutually exclusive computing. i: Cross scheme. ii: A representation of the four possible results or outputs. D) A schematic representation of cells showing how directed expression (green) and the use of a repressor system (red) can be used to generate a complementary pattern.

Regardless of the number of units that make-up a system and the complex relationships that describe them, these can still be considered as few if considered together, even as few as one context of the whole organism. In terms of a relationship to describe any part of this space-time it can be summed up most simply as between two parts: the part in question and the rest. Therefore, if a difference between two parts of the system is the minimum required for a description (Figure 1a) or with the desired aim in mind to elucidate specificity, then it should become apparent that a mutually exclusive relationship is not only sufficient but required to meet our aim.

Thus, when it comes to studies in the life sciences that can be categorized as in the earlier stages of R&D, a reasonable question might be: what can we say with respect to the context studied in terms of the relationships they include (Figure 1b)? The Scientific method used in Life science relies heavily on a process of logic involving inductive reasoning, something that Alan Turing explains and terms Scientific induction (Turing, 1950). Essentially, any attempt at a conclusion is limited and can only be said to appear to be. In many instances, additional validation studies are essentially only a repeat of the first type of one-dimensional type of study, *i.e*., examination in another part of the organism or in a part or parts of different model systems generally accepted to resemble more closely humans. A mutually exclusive relationship in the context is often not considered in the study, until a clinical trial. Importantly, when it comes to consideration of the context, Scientific induction for the most part does not consider the whole and does not include a mutually exclusive relationship required to examine where a phenomenon does not occur – this I believe is the important limitation, not necessarily an oversight since previously technology has been lacking. Taken together, this I believe helps explain why on a higher proportion of occasions many potential therapeutics appearing to hold great promise, proceed to the later stages of R&D but fail.

A solution to the problem: Drosophila and mutually exclusive computation

The fruit fly *Drosophila melanogaster* is a powerful cost effective *in vivo* research tool with a quick generation time and technologies for controlling directed gene expression both endogenous and of exogenously introduced nucleotides (Spratt, 2013), not to mention a possibility to easily inject things (Garen and Gehring, 1972; Zalokar, 1971). Thus, the use of *Drosophila* as a general tool to assess things in real life is probably unsurpassed compared to the possibilities and practical limitations of other systems. In addition, the biology important for life is vital and therefore by definition is highly conserved meaning that most, if not all things or at least parts of the things involved in viability of the system will share a common history with all other life systems, *i.e*., there is commonality. Hence, the inexhaustible effort to record every nucleotide sequence possible and thus generating the consensus genome sequence for comparative genomics and traceability of things vital. This reasoning, allows us to use *Drosophila* as a model to study human disease, identifying interacting genes for things or components that translate directly to the physiological requirements for putative orthologous components in mammalian cells: for example for parts of a virus (Hao *et al.*, 2008; Merkling *et al.*, 2019) or genes implicated in cancer (Ingham, 2018).

To clarify what I am trying to ask here: if the context and relationship we have interest in, is the whole organism and a mutually exclusive conditional requirement for specificity, this often being the ultimate aim of many studies, then is there an ethical way to include this in our study at an early stage before clinical trials? Thus, with this question in mind I would like to highlight in this report an example of technology able to achieve this (Spratt, 2013) (Figure 1c, Here I also report the identification, of the putative protein encoding gene CG43658. I believe this emphasizes further the power of this, for the most part overlooked, Scientific method and its suitability for generating sufficient data to support the prioritization of things identified.

Materials and Methods

RNAi line with TRiP ID HMS00332 (*Drosophila* RNAi Screening Center). All other materials and methods are as described in Spratt (2013).

Results and Discussion

A Computer able to identify components with mutually exclusive specificity

In this instance, with respect to testing components in the context including a mutually exclusive relationship, this can be modeled by the use of two directed expression drivers describing the pattern of expression of the receptor Patched (*Ptc*) and the signal Hedgehog (*Hh*) for the highly conserved and medically relevant Hedgehog signaling - *ptc*-Gal4 and *hh*-Gal4, respectively (Figure 1c; Spratt, 2013). Briefly, this method is able to process nucleotides and does so in this instance using RNA interference (RNAi) and describes the context in terms of viability once processed through both parts, *i.e*., it can be said to consider the whole of the system giving an output or result to describe the sum of everything in it absolutely recorded using unambiguous terms: using X for non-viable and O for viable. The two parts share a relationship, enabling us to interpret something meaningful from the results. This can return four possible results XX, OO, XO, or OX, with the latter two being of interest with respect to specificity. Furthermore, I would like to reiterate because I find it striking that in this *Hh* signalling context that we know is used again and again throughout development and in the adult, sometimes the information or thing being processed causes the organism to be non-viable appearing to change the cell fate or is toxic when processed through one part of the system while in the complementary part, through two generations, the flies are viable or the information or thing being processed does not appear to change the cell fate or is not toxic to at least enough cells for the organism to be viable. I am always somehow humbled at the thought of this and it may be worth considering whether in all instances this can be explained sufficiently by a component sharing a relationship with *Hh* signaling or not.

Identification of CG43658

Previously this method identified *CG31522*, a putative Elongation of Very Long Chain fatty acids (ELOVL), whose protein is shown to physically interact with ATP synthase and protein encoded by its adjacent and highly similar sequence *CG31523* (see flybase.org). Interestingly, CG31523 has since been found to co-immunoprecipitate the *Hh* signalling component Rab23 (Cicek, *et al.*, 2016), a GTPase. Furthermore, ELOVL6 has been shown to regulate mitochondrial function and heat generation (Tan *et al.*, 2015) and *Hh* pathway activation can increases mitochondrial capacity (Yao *et al.*, 2017, Here, with the notion that I am describing to you a Computer able to identify things, beyond a reasonable doubt, relevant to the context and showing specificity, I would like to report the identification of *CG43658* a putative Rho guanine nucleotide exchange factor, not reported in the initial study because it was deemed to be insufficiently characterized, with an XO output (Table 1). Interestingly, *CG43658*`s orthologue *ARHGEF10* is an inherited peripheral neuropathy gene associated with Charcot-Marie-Tooth disease and *Drosophila CG43658* appears to offer an appropriate model (Yamaguchi and Takashima, 2018). Furthermore, Schwann cell derived Desert Hedgehog (*DHh*) controls development of the peripheral nerve sheath (Parmantier *et al.*, 1999) and *DHh* is associated with peripheral neuropathy (Umehara *et al.*, 2000).

Table 1. A record of the result for a computation using *ptc* and *hh* directed RNAi corresponding to *CG43658*.

Gene RNAi line	Directed expression				Signature	Additional information
	ptc		*hh*			
	F1	F2	F1	F2		
CG43658 HMS00332	O[a]	X	O	O	X, O	[a]Only female progeny.

A Turing machine able to consider the whole and describe it absolutely in unambiguous terms

This method can use other mutually exclusive relationships, for example using drivers representing other cell to cell communication mechanisms. Furthermore, by use of a repressor technology such as GAL80, a GAL4 repressor (Ma and Ptashne, 1987; Lee and Luo, 1999) in combination with a global driver, *e.g*., *tubulin*-GAL4 the method might be able to be used to study the context while including potentially all possible mutually exclusive relationships, at least as determined by the site of a driver`s insertion into the genome and

its particular expression pattern, *e.g.*, if a gene of interest, let`s call it *x* can drive the GAL80 repressor in a global GAL4 background then you can have the tools to direct the expression of things in those cells expressing *x*, *i.e.*, using *x*-GAL4 and also now have the ability to direct expression everywhere else or NOT *x* by using *x*-GAL80; *tubuli*n-GAL4 (Figure 1d; Spratt, 2013). This is how we might envisage that this target and potential therapeutic testing device will evolve, adjustable or tuned both on the level of the inputs and on the level of control according to the directed expression and with a possibility to adjust the background: an imaginable Computer able to search the context for mutually exclusive relationships of interest and use them to identify things with specificity.

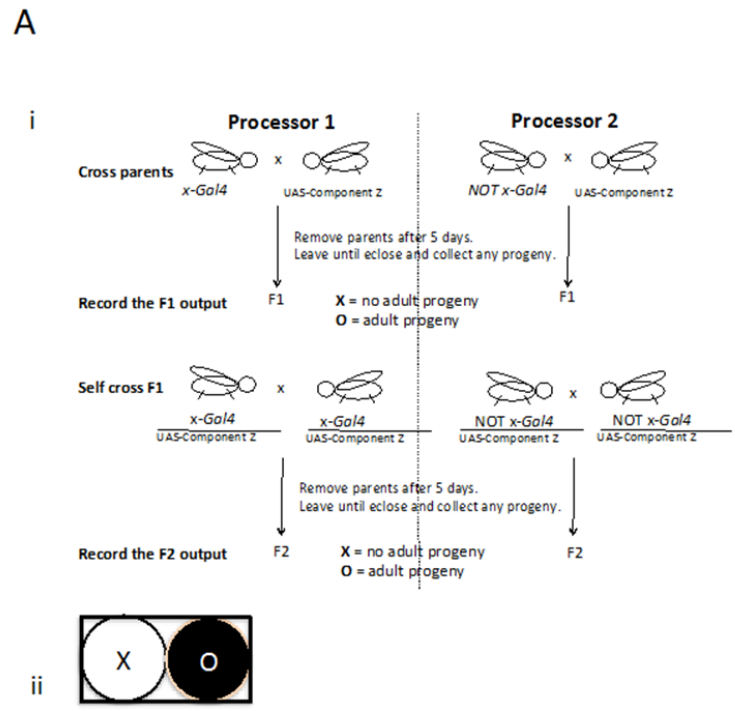

Figure 2. A hypothetical or imaginable Fly Computer. A) i: Mutually exclusive GAL4 drivers described by *x* and NOT *x* are used to interrogate a component Z to identify a relevant context. ii: If a computation represented in Ai generates an XO output, it can now be interrogated further. B) i: Component Z could now be investigated together with the directed expression of another functional entity, in this example an RNAi. ii: The idea being that a change in the XO output shown in Ai to OO would be of high interest.

Interestingly, with respect to finding new things and then feeding the information back to carry out new computations, what we can see is that this description is a Turing machine (Turing, 1936). I think also it is worth mention considering Alan`s comments when it comes to Scientific induction (Turing, 1950): this is not Scientific induction. This is a computer or more precisely, as Alan cleverly explains when it comes to definitions – this concept is a Turing machine. And a Turing machine or Computer that is able to consider the whole and describe the sum of everything in it absolutely in unambiguous terms is a useful tool, because it can tell you about things and not how things appear to be but how things really are according to the information available.

Further considerations and implications

Further interesting follow on ideas from this might be the use of a component known to generate an XO signature, and then process this type of control through the context using drivers with different mutually exclusive relationships until you find further XO or vice versa combinations. Another interesting question that springs to mind is could it be that there are certain combinations of mutually exclusive relationships for interrogating components in the context able to provide enough information with respect to any or at least many newly interesting targets or functional entities: for example, if we examine results for known approved medicines or their targets, that the results positively correlate, *i.e.*, with time, from this type of test and the data generated we might realize that the fly or a similar two-part test provides enough information to fast-track a candidate and potential therapeutic for drug development and ultimately clinical trials?

Recently, COVID-19 (Hu *et al.*, 2020; Sekhawat *et al.*, 2020) has highlighted the time it takes to find a solution and, together with the anticipation of emerging disease, questioned our security. Therefore with this imaginable Computer in mind, I would like to outline a hypothetical scenario: let`s imagine part of a virus, *e.g.*, SARS-CoV-2, is a timely example, but also any gene or mutation causing disease. Using molecular biology, this could be any part or combination, let`s call this component Z and imagine with the use of appropriate drivers this might generate an XO or vice versa output (Figure 2a: please allow for this conjecture based on prior knowledge and first principles that give us good reason to believe that an example may exist, The context can now be searched for, *e.g.*, a potential nucleotide candidate medicine that can bring about a change in the output (Figure 2b). Concerning potential medicines the use of nucleotides have progressed (for informative reviews concerning the state of the art please see, *e.g.*, Yoshioka *et al.*, 2019; Yamakawa *et al.*, 2019) so these, in addition to vaccines, should be considered. Interestingly, I must add that a number of viruses modulate Hedgehog signaling (Smelkinson *et al.*, 2017).

To end with. We are told, circa 330 BC, Aristotle said something like “To say that that which is, is not OR that which is not, is – is a falsehood and to say that that which is, is AND that which is not, is not – is true”.

Acknowledgments: I would like to thank everybody for making all this possible. Special mentions for Michael Ebenazer Kwadjo Omari Owuo Jr., Edward Christopher Sheeran, Damini Ebunoluwa Ogulu, Own it (Atlantic), Ariana Grande-Butera, Into you (Republic), Adam Richard Wiles and Samuel Frederick Smith, Promises (Columbia), Calvin Cordozar Broadus Jr. & Terius Youngdell Nash, Gangsta Luv (Priority), Andreas Kleerup and Ana Diaz, Trouble (U OK?), Lisa Fischer and the Rolling Stones, Gimme Shelter (Decca), Pharrell Williams, Freedom (Columbia), Kate Bush, Running Up That Hill (EMI), Peroulakis Nikos & Zinos, Olos o Kosmos Thalassa (Independent), Barry Gibb and to the late Robin & Maurice Gibb, Staying Alive (RSO), Leonard Cohen, Anthem (Columbia) and Johann Holzel, Out of the Dark (EMI Electrola).

References: Cicek, I.O., S. Karaca, M. Brankatschk, S. Eaton, H. Urlaub, and H.R. Shcherbata 2016, Genetics 202(3): 1167-1183. doi: 10.1534/genetics.115.185371; Garen, A., and W. Gehring 1972, Proc. Natl. Acad. Sci. USA. 69(10): 2982-5. doi: 10.1073/pnas.69.10.2982; Hao, L., A. Sakurai, T. Watanabe, E. Sorensen, C.A. Nidom, M.A. Newton, P. Ahlquist, and Y. Kawaoka 2008, Nature 454(7206): 890-3. doi: 10.1038/nature07151. Epub 2008 Jul 9; Hu, B., H. Guo, P. Zhou, and Z. Shi 2020, Nature Reviews Microbiology 6: 1-14.doi: 10.1038/s41579-020-00459-7; Ingham, P.W., 2018, Development 145(21): dev168898. doi: 10.1242/dev.168898; Lee, T., and L. Luo 1999, Neuron 22(3): 451-461. doi: 10.1016/s0896-6273(00)80701-1; Ma, J., and M. Ptashne 1987, Cell 50(1): 137-142. doi: 10.1016/0092-8674(87)90670-2; Merkling, S.H., H. Riahi, G.J. Overheul, A. Schenck, and R.P. van Rij 2019, Sci. Rep. 9(1): 2065. doi: 10.1038/s41598-019-38559-x; Oxford English Dictionary (OED) 1989, Second Edition revised. Oxford

University Press; Parmantier, E., B. Lynn, D. Lawson, M. Turmaine, S.S. Namini, L. Chakrabarti, A.P. McMahon, K.R. Jessen, and R. Mirsky 1999, Neuron 23:713-724. doi: 10.1016/s0896-6273(01)80030-1; Sekhawat, V., A. Green, and U. Mahadeva 2020, Diagn. Histopathol. Oxf, doi: 10.1016/j.mpdhp.2020.11.008; Smelkinson, M.G., A. Guichard, J.R. Teijaro, M. Malur, M.E. Loureiro, P. Jain, S. Ganesan, E.L. Zuniga, R.M. Krug, M.B. Oldstone, and E. Bier 2017, LoS Pathog. 13(8):e1006588. doi: 10.1371/journal.ppat. 1006588. eCollection 2017 Aug; Spratt, S.J., 2013, Front. Genet. 4: 284. doi: 10.3389/fgene.2013.00284. eCollection 2013; Tan, C.Y., S. Virtue, G. Bidault, M. Dale, R. Hagen, J.L. Griffin, and A. Vidal-Puig 2015, Cell Rep. 13: 2039-2047. doi: 10.1016/j.celrep.2015.11.004; Turing, A.M., 1936, Proc. Lond. Math. Soc. 42: 230-265. doi: 10.1074/jbc.M310529200; Turing, A.M., 1950, Mind 236: 433-460. doi: 10.1093/mind/LIX.236.433; Umehara, F., G. Tate, K. Itoh, N. Yamaguchi, T. Douchi, T. Mitsuya, and M. Osame 2000, Am. J. Hum. Genet. 67(5): 1302-1305. doi: 10.1016/S0002-9297(07)62958-9; Yao, P.J., U. Manor, R.S. Petralia, R.D. Brose, R.T.Y. Wu, C. Ott, Y-X. Wang, A. Charnoff, J. Lippincott-Schwartz, and M.P. Mattson 2017, Mol. Biol. Cell 28: 387-395. doi: 10.1091/mbc.E16-07-0553; Yamaguchi, M., and H. Takashima 2018, Adv. Exp. Med. Biol. 1076: 97-117. doi: 10.1007/978-981-13-0529-0_7; Yamakawa, K., Y. Nakano-Narusawa, N. Hashimoto, M. Yokohira, and Y. Matsuda 2019, Int. J. Mol. Sci. 20(17), Pii: E4224. doi: 10.3390/ijms20174224; Yoshioka, K., T. Kunieda, Y. Asami, H. Guo, H. Miyata, K. Yoshida-Tanaka, Y. Sujino, W. Piao, H. Kuwahara, K. Nishina, R.I. Hara, T. Nagata, T. Wada, S. Obika, and T. Yokota 2019, Nucleic Acids Res. 47(14): 7321-7332. doi: 10.1093/nar/gkz492; Zalokar, M., 1971, Proc. Natl. Acad. Sci. USA. 68(7): 1539-41.

Effect of population density on the development of Drosophila immigrans.

Del Pino, F., P. Espinoza, C. Pozo, F. González, M. Zamora, and E. Alvarez. Programa de Genética Humana, ICBM, Facultad de Medicina, Universidad de Chile. Independencia 1027, Santiago, Chile.

We have shown that social isolation in *D. melanogaster* larvae generates individuals that are lighter and smaller than group-reared pre-adults (Del Pino, 2018). In this work, we investigate the effect that population density has on the larval development of *D. immigrans*. For this, 4 types of groups were generated, all contained in Petri dishes of 4 cm in diameter with Burdick culture medium (Burdick, 1954). The types of groups sown were the following: i) 1 egg; ii) 10 eggs; iii) 20 eggs, and iv) 30 eggs. When the larvae of these groups reached 96 hours of age, their weight (mg) and size (mm) were recorded.

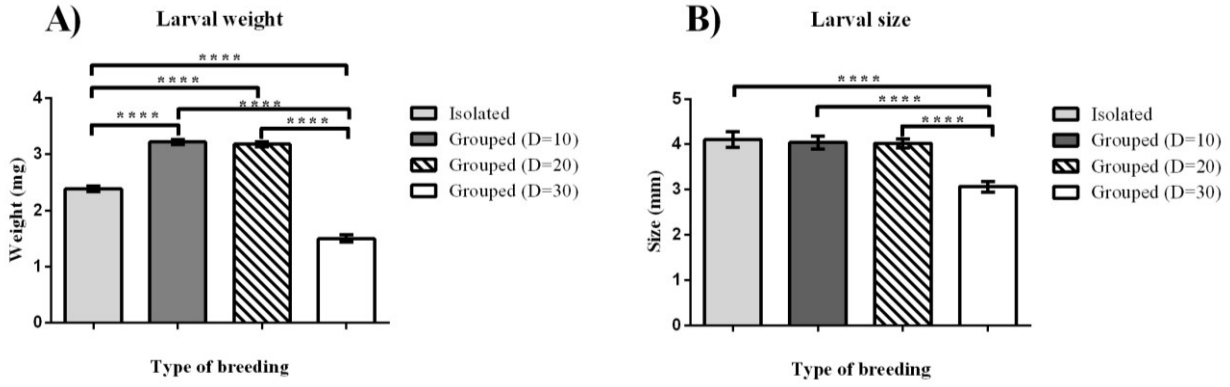

Figure 1. Comparison of results between grouped and isolated breeding. Results presented according to A) weight, and B) size at the end of the observation period. Bars represent mean ± SEM. Data analyzed with a 1-way ANOVA, *p < 0.05, **p < 0.01, ***p < 0.001, ****p < 0.0001.

The results related to larval weight show that groups of individuals of 10 and 20 are heavier than when they are isolated. However, the weight for the group of larvae of 30 decreases dramatically compared to the other groups (see Figure 1 A). For larval length, the groups of 1, 10, and 20 eggs show the same size. For its part, the group of 30 eggs shows a similar situation to that observed for weight. The larvae in this group are smaller compared to the rest of the groups (see Figure 1 B).

The results found in *D. immigrans* are opposite to those shown in *D. melanogaster* (Del Pino, 2018). The explanation for this phenomenon could be given by the difference in size of the larvae of both species. The *D. immigrans* larva is approximately 2.5 times larger than the *D. melanogaster* larva. This difference in size would have two consequences; i) *Immigrans* larvae have a greater capacity to break the culture medium and obtain the food necessary for their development, compared to *D. melanogaster* larvae, which, due to their size, could not do it alone; ii) *Immigrans* larvae reared in groups of 30 individuals would produce a greater amount of detritus than those of *melanogaster*, generating greater contamination in the culture medium, affecting the quality of the food and therefore its proper larval development.

References: Del Pino, F. *et al*., 2018, Dros. Inf. Serv. 101: 63; Burdick, A.B., 1954, Dros. Inf. Serv. 28: 170.

Effect of population density on the development of *Drosophila melanogaster*.

Del Pino, F., F. Claps, C. Gabilan, F. Santin, and E. Alvarez. Programa de Genética Humana, ICBM, Facultad de Medicina, Universidad de Chile. Independencia 1027, Santiago, Chile.

In *D. melanogaster*, social isolation generates lighter and smaller third instar larvae (Del Pino, 2018). Our team studied the larval development of *D. melanogaster* in groups formed by different numbers of eggs. For this, five types of groups were generated, all contained in Petri dishes of 4 cm in diameter with Burdick culture medium (Burdick, 1954). The types of groups sown were the following: i) 2 eggs; ii) 5 eggs; iii) 10 eggs; iv) 15 eggs; and v) 20 eggs. When the larvae of these groups reached 96 hours of age, their weight (mg) and size (mm) were recorded.

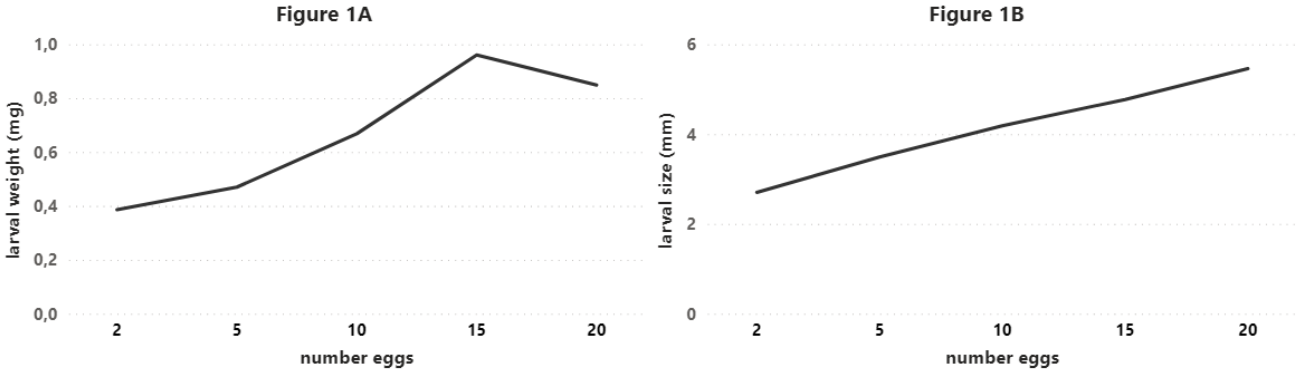

Figure 1.

The results show that the greater the number of individuals sharing the rearing environment, the weight and larval size increases (Figure 1 A, B). This suggests that the presence of congeners is an important factor for an adequate development of these pre-adults. The foregoing is in accordance with the phenomenon known as *quorum perception* (Vipin, 2015). In this publication, it is described that prokaryotic cells respond to congeners by releasing bioinducers that affect themselves and other individuals that form that community,

providing them with greater survival. Everything previously expressed teaches us that social relationships are present in all types of living beings, from prokaryotic organisms to multicellular eukaryotes.

References: Del Pino, F. *et al*., 2018, Dros. Inf. Serv. 101: 63; Burdick, A.B., 1954, Dros. Inf. Serv. 28: 170; Vipin, C.K., 2015, Quorum Sensing vs Quorum Quenching: A Battle With No End in Sight. Springer India. DOI: 10.1007/978-81-322-1982-8_1V.

Exact breakpoints of *In(1)w^{m4}* rearrangement.

Solodovnikov, A.A., and S.A. Lavrov. Institute of Molecular Genetics of National Research Centre «Kurchatov Institute», 123182 Moscow, Russia; Email: slavrov@img.ras.ru

Abstract

In(1)w^{m4} was known for decades as a classic example of position effect variegation-causing rearrangement and was mentioned in hundreds of publications. Nevertheless, the euchromatin breakpoint position of the rearrangement was not precisely localized. We performed nanopore sequencing of DNA from *In(1)w^{m4}* homozygous flies and determined the exact position of euchromatic (chrX:2767875) and heterochromatic breakpoints of the rearrangement.

Introduction

In(1)w^{m4} inversion represents the first described case of heterochromatin position effect (Muller 1930). An inversion with breakpoints near the *white* gene and in the heterochromatin of the left arm of chromosome X (Figure 1, A) results in a mosaic inactivation of *white* visible in the eyes of adult flies. The rearrangement is a classic model of PEV and has been mentioned in more than a hundred publications. In particular, in Vogel *et al.* (2009), the chromatin changes in case of *In(1)w^{m4}*-induces PEV were tracked using high-throughput methods (microarray hybridization and sequencing). In this paper, the euchromatin breakpoint position of inversion was determined with 1.5 kb accuracy (chrX:2766979-2768245, R6.22).

The heterochromatin breakpoint of *In(1)w^{m4}* was mapped to h28 block of X chromosome heterochromatin distal to rDNA cluster, and the sequence immediately near the breakpoint corresponds to R1 transposon (Appels *et al.,* 1982; Tartof *et al.,* 1984).

We decided to precisely map the positions of *In(1)w^{m4}* breakpoints to study the changes in chromatin organization immediately at the eu-heterochromatin border. The nanopore sequencing was applied to look deep into the heterochromatin beyond the breakpoint position. Nanopore sequencing is characterized by a significantly higher number of errors compared to traditional NGS approaches but has almost unlimited read length and is, thus, extremely helpful in assembly of repeat-rich regions of heterochromatin.

Materials and Methods

DNA isolation

DNA from *In(1)w^{m4}* flies was extracted using proteinase K treatment – phenol-chloroform extraction – ethanol precipitation protocol. 100 flies were disrupted in 1 ml of TET buffer (100 mM Tris pH 8.5, 50 mM EDTA, 0.2% Triton X-100) in ice by Potter homogenizer. Sodium sarcosylate was added to 1.5% and proteinase K to 100 µg/µl, the suspension was gently mixed and incubated for 1 h at 50°C. The mixture was extracted twice with phenol pH 8.0, once with the phenol-chloroform mix, and once with chloroform on Hula Mixer. The water phase after extraction was collected and sodium chloride was added to 100 mM. Then, 2 volumes of 96% EtOH were added and the tube slowly rotated until HMW DNA forms a tangle. DNA was washed once with 500 µl of 70% EtOH, dried, and dissolved in 100 µl of MilliQ water. DNA concentration

was measured using Qubit fluorimeter (DS DNA broad range kit). Liquid handling at every stage was performed gently and using cut off pipette tips.

MinIon sequencing

The sequencing library was prepared from 1.5 µg of DNA from homozygous *In(1)w^{m4}* flies according to the protocol recommended for Ligation Sequencing Kit (SQK-LSK109) from ONT (https://store.nanoporetech.com/us/media/wysiwyg/pdfs/SQK-LSK109/ Genomic_DNA_by_Ligation_SQK-LSK109_-minion.pdf). The prepared library was loaded to MinIon R 9.4.1. flowcell and sequenced without basecalling until ~4 Gb of data was obtained.

Data treatment

A set of .fast5 files from the sequencing run was basecalled on a standalone GPU-enabled server with Guppy Version 3.5.2 using dna_r9.4.1_450bps_hac profile. The resulting FASTQ files were loaded to the local Galaxy server for further processing. Quality checks using Nanostat (https://github.com/wdecoster/nanostat) and Nanoplot (https://github.com/wdecoster/NanoPlot) tools in Galaxy showed that ~2.4 Gb of reads (~20× genome coverage) with N50=14010 and Q>7 was received. Adapters were trimmed by Porechop (https://github.com/rrwick/Porechop) using default settings (reads with middle adapter were splitted).

Processed reads were mapped to r6.22 release of *D. melanogaster* genome using *Minimap2* software with Oxford Nanopore read to reference mapping profile (minimap2 -x map-ont) (Li 2018). The resulting .bam file was visualized in the local *UCSC Genome Browser* (Figure 1, B). FASTQ files with reads were also converted to FASTA using FASTQ to FASTA converter in Galaxy (Blankenberg *et al.,* 2010).

The euchromatin breakpoint was identified as a gap in aligned reads in the 2 kb region where *In(1)w^{m4}* breakpoint was located previously (Vogel *et al.,* 2009). The regions of 400 bp in size immediately upstream and downstream to the breakpoint (chrX:2767482-2767880 and chrX: 2767881-2768281) were blasted against sequencing reads in multifasta format to identify and extract reads overlapping breakpoint. 32 reads containing sequence near the breakpoint and unknown part corresponding to fused heterochromatin were identified. Two reads with the longest heterochromatin parts to the left and the right direction from the breakpoint were selected and their heterochromatin parts combined into one sequence. This sequence contains a region of heterochromatin ~80 kb in size, encompassing *In(1)w^{m4}* breakpoint (Figure 1, C).

The structure of heterochromatin near the *In(1)w^{m4}* breakpoint was analyzed using web application RepeatMasker (http://www.repeatmasker.org/cgi-bin/WEBRepeatMasker), which allows mapping of most types of *Drosophila* repeats. The output of RepeatMasker was manually converted to a .bed file, color information for different types of repeats added and the result visualized in IGV (https://software.broadinstitute.org/software/igv/) (Figure 1, C).

Data availability

Sequences mentioned in this work are available upon request.

Results

The results of sequences analysis are presented in Figure 1.

There is a gap in a reads coverage in the genome region chrX**:**2766979**-**2768245, which, as it was shown previously (Vogel *et al.,* 2009), contains *In(1)w^{m4}* breakpoint. The position of the gap is chrX:2767875-2767894 according to R6.22 release of *D. melanogaster* genome (Figure 1, B). We used BLASTN to extract reads containing sequences immediately near this gap and investigate their composition. All these sequences contain euchromatin part fused to *Drosophila melanogaster* type I transposable element *R1Dm*. The breakpoint position in *R1* is 2200 according to GenBank X51968.1 *R1* sequence.

Eventually, the position of euchromatin breakpoint of *In(1)w^{m4}* is chrX:2767875-2767894, the inversion is accompanied by a deletion of 20 nucleotides of euchromatin, and the breakpoint is 28.7 kb distal to *white* TSS (Figure 1, B).

A. *In(1)w^{m4}* structure

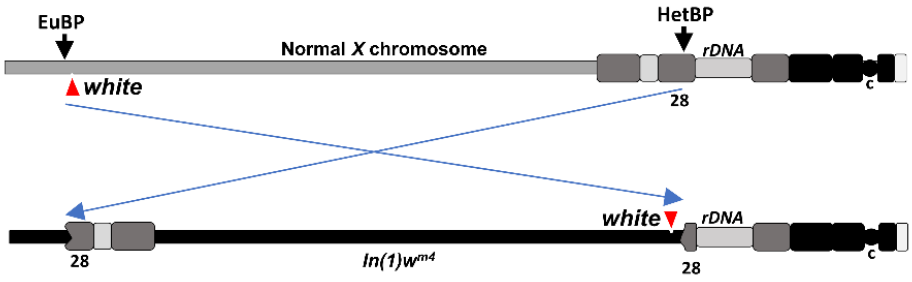

B. Euchromatin breakpoint

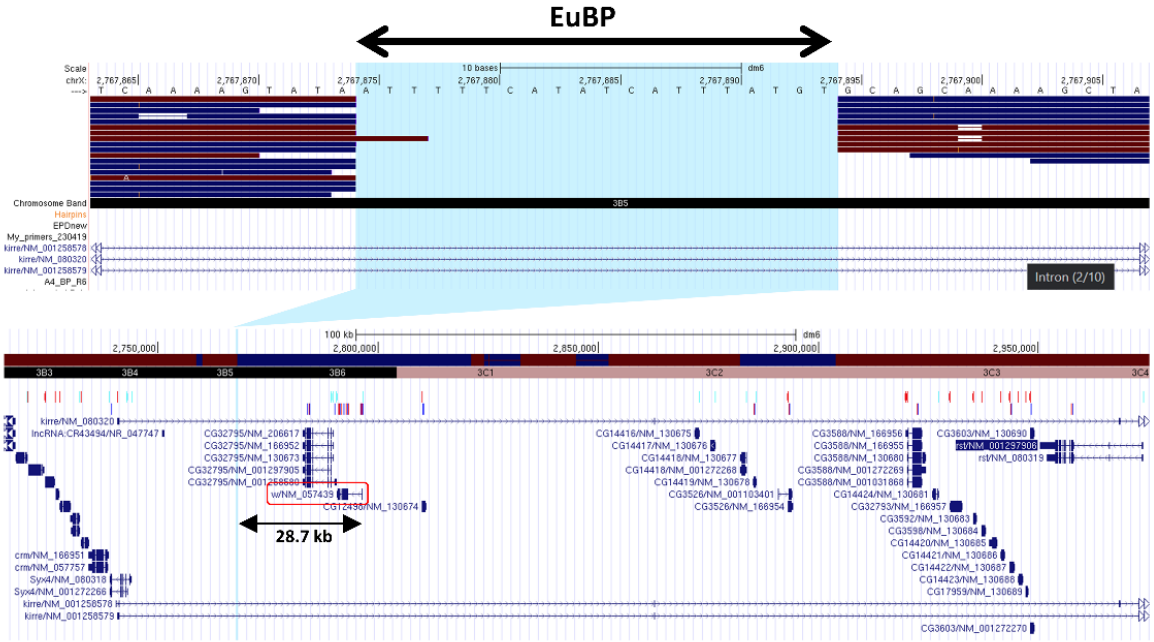

C. Heterochromatin breakpoint

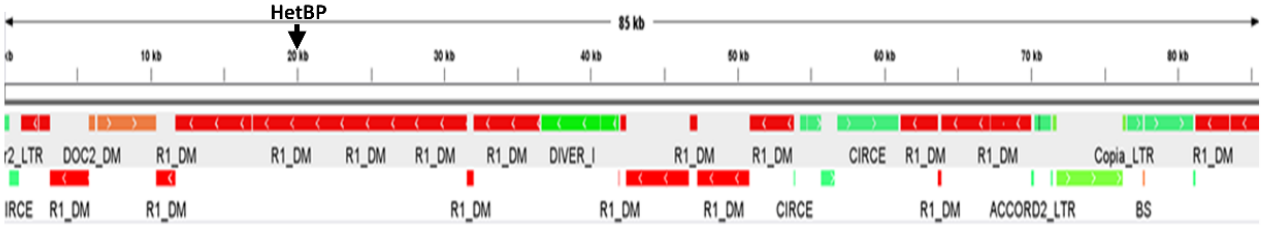

Figure 1. See next page for figure legend.

Figure 1. A. *In(1)w*^{m4} inversion scheme. EuBP – euchromatin breakpoint, HetBP – heterochromatin breakpoint, c – centromere, positions of h28 heterochromatin block and rDNA cluster are marked. Triangles denote the position of the *white* gene. B. Mapping of long reads to R6.22 *Drosophila* genome. The image is a collage of UCSC genome browser screenshots, the upper part is a close-up view of euchromatin breakpoint and reads mapped to this place, the lower part is an overview of 200 kb genomic region containing the breakpoint. The *white* gene is outlined, the arrow shows the distance between *white* TSS and the breakpoint. C. Heterochromatin breakpoint of *In(1)w*^{m4} inversion. The breakpoint in heterochromatin (HetBP) is in the element *R1* in the region, saturated with different types of mobile elements.

To identify sequences around the *In(1)w*^{m4} breakpoint in the heterochromatin, reads of maximum length containing the euchromatin regions closest to the breakpoint were extracted from the library of reads. Thus, the reads overlapping the breakpoint and containing ~80 kb of heterochromatin were detected. The structure of the heterochromatin was analyzed using the RepeatMasker. It was found that the heterochromatin breakpoint is in a region composed of fragments of different types of mobile elements (LINE (mainly R1) and LTR-containing), of different orientation and length. This type of organization resembles some piRNA-producing loci. Interestingly, the insertion of *I*-element in the h28 heterochromatin region leads to decreased reactivity in I-R hybrid dysgenesis system, pointing to the suppression of *I*-element transpositions (Dimitri *et al.,* 2005).

Acknowledgments: Authors are grateful to V.A. Gvozdev for his valuable comments and help in the preparation of this manuscript. The work was supported by the Russian Science Foundation (project No. 19-74-20178) and by the Russian Foundation for Basic Research (17-00-00282 KOMFI).

Conflict of interest. The authors declare no conflict of interest.

Compliance with ethical standards. This article does not contain any studies involving animals or human participants performed by any of the authors.

References: Appels, R., and A.J. Hilliker 1982, Genet. Res. 39: 149-156; Blankenberg, D., A. Gordon, G. Von Kuster, N. Coraor, J. Taylor, A. Nekrutenko, and T. Galaxy 2010, Bioinformatics 26: 1783-1785; Dimitri, P., and A. Bucheton 2005, Cytogenet. Genome Res. 110: 160-164; Li, H., 2018, Bioinformatics 34: 3094-3100; Muller, H.J., 1930, J. Genet. 22: 299; Tartof, K.D., C. Hobbs, and M. Jones 1984, Cell 37: 869-878; Vogel, M.J., L. Pagie, W. Talhout, M. Nieuwland, R.M. Kerkhoven, and B. van Steensel 2009, Epigenetics & Chromatin 2: 1.

GFP-RNAi* expression in dopaminergic neurons can reduce lifespan in *Drosophila melanogaster.

Jolfaei, Chavoshi, S. Mahin[1], and Brian E. Staveley. Department of Biology, Memorial University of Newfoundland, St. John's, Newfoundland & Labrador, Canada A1B 3X9; telephone (709) 864-4317; telefax (709) 864-3018; Corresponding author: Dr. Brian E. Staveley; email address: bestave@mun.ca; [1]Current address: Research School of Biology, Australian National University, Canberra, Australia AST 2600; email address: mahin.chavoshi.jolfaei@anu.edu.au

Introduction

The directed gene expression through the implementation of the *Gal4-UAS* system is comprehensively used for the expression of transgenes under a great number of scenarios in *Drosophila melanogaster* (Brand and Perrimon, 1993). In order to determine the consequences of specific loss of gene function, this approach can express select *RNAi* transgenes in order to post-transcriptionally silence endogenous genes (Perrimon *et*

al., 2010; Ni *et al*., 2011). While expression of *Gal4* can can result in an apoptosis-dependent "rough-eye" phenotype with *GMR-Gal4*^{12} homozygotes, one copy of the transgene produces a relatively normal phenotype under standard conditions (Kramer and Staveley, 2003). Maternally-inherited *arm-Gal4* directing *UAS-lacZ*$^{4-1-2}$ can reduce lifespan (Slade and Staveley, 2015). Although often utilized as a benign transgene in negative controls, expression of *UAS-GFP* can reduce lifespan and impair climbing ability over time when expressed in neuronal tissues (Mawhinney and Staveley, 2011). Ubiquitous expression of *GFP-RNAi* has been suggested to have a negative effect upon lifespan in RU48-induced experiments, although the activity of *Gal4* may have contributed to these results (Alic *et al.,* 2012). The activity of *Gal4* and the responding transgene each can influence the phenotypes such as ageing and age-related conditions in *Drosophila melanogaster*, that involve total or partial loss-of-function of specific genes using RNA interference, negative controls must be evaluated. One proposed control line for such experiments involves an *RNAi* for the green fluorescent protein, *UAS-GFP-RNAi*. Here we demonstrate that this transgene does not perform as a benign control for some experiments.

Material and Methods

Drosophila melanogaster stocks, media and culture

The GMR-Gal4^{12}; *UAS-lacZ*$^{4-1-2}$; *UAS-GFP-RNAi*^{142}, and *TH-Gal4*^{3} *(pale-Gal4)* lines were obtained from the Bloomington Stock Centre (University of Indiana, Bloomington). The stock of *ddc-Gal4*$^{4.3D}$ (Li *et al.,* 2000) provided by Dr. J. Hirsch of University of Virginia. The *Glass Multiple Reporter gene* (*GMR*)-*Gal4* transgene (Freeman, 1996), causes high levels of expression in *Drosophila* eye imaginal discs. Our research group described generation of *UAS-foxO*^{1} (Kramer *et al*., 2003) and the *GMR-Gal4 UAS-foxO* line was generated for overexpression of *foxO* in the developing eye by standard methods (M'Angale and Staveley, 2016). Flies were maintained on standard cornmeal, molasses, yeast and agar media treated with propionic acid and methylparaben to resist fungal growth.

Directed expression of the transgenes in the eye was accomplished by crossing virgin females bearing the *GMR-Gal4* transgene to responder males. The directed expression of transgenes in a subset of neurons including the dopaminergic neurons was achieved by crossing *Tyrosine Hydroxylase-Gal4 (TH-Gal4)* and *dopa decarboxylase-Gal4* (*ddc-Gal4*) virgin females to the responder lines. All crosses were done as per standard methods and male critical class flies were collected for assessment. Stocks were maintained at room temperature (22±3°C), whereas crosses and experiments were incubated at 25ºC.

Scanning electron microscopy and analysis

Critical class male progeny were isolated and allowed to age upon standard media at 25ºC for three to five days to achieve full phenotypic stabilization before storing at -80º C in 1.5 mL tubes. Frozen flies were examined under a dissecting microscope and mounted on aluminum studs with their left eye facing upward. Prepared studs remained under desiccation conditions for 24 to 48 hours. The eyes were scanned and imaged at 597× magnification, using a (MLA) 650FEG microscope (FEI in Hillsboro, Oregon, USA). Ten micrographs per genotype were analyzed using software ImageJ 1.42q (Abramoff *et al.,* 2004). To increase reproducibility, the area of the ommatidia was determined by measuring the area of a "floret" of ommatidia, consisting of a central unit surrounded by six others, then dividing by seven to obtain area per ommatidia. The number was determined by counting three florets per micrograph. Data was analyzed using GraphPad Prism 5 (Graphpad Software, San Diego California USA). An unpaired two-tailed t-test was used to decide significance at a level of $P < 0.05$.

Longevity and locomotor assays

The longevity assays were performed with approximately 200 male progeny of critical class isolated under carbon dioxide every 24 hours. Flies were transferred to fresh food without anesthesia frequently, three times a week, and maintained in numbers of no more than 20 per vial to prevent overcrowding. As they aged, flies were monitored for viability until all had perished according to our standard protocol (Staveley *et al*., 1990). The climbing (locomotor) assay was conducted following a standard climbing protocol (Todd and Staveley, 2004). Results were analyzed with the GraphPad Prism 5 software and Mantel-Cox test was used for longevity assay. For locomotor assay results an unpaired t-test was taken where significant differences

between means of groups and the slopes of the curves with non-overlapping 95% CI were considered significantly different.

Results and Discussion

The consequences of *GFP-RNAi* expression during development of the eye were investigated. Heterozygotes of the *GMR-Gal4* transgene, unlike homozygotes, do not display a severely abnormal eye phenotype at 25ºC (Kramer and Staveley, 2003). Our SEM micrographs reveal little to no differences between the morphology of the eyes, cultured at 25ºC, of *GMR-Gal4, UAS-lacZ* males, with mean values of 725.2 ommatidia, ommatidial area of 178.1 μm^2 and 535.2 interommatidial bristles, and the *GMR-Gal4, UAS-GFP-RNAi* flies, with mean values of 675.5 ommatidia, ommatidial area of 184.4 μm^2 and 519.5 interommatidial bristles (Figure 1). The presence of the *GFP-RNAi* gene products seems not to influence the relatively standard development of the eye as directed by *GMR-Gal4*.

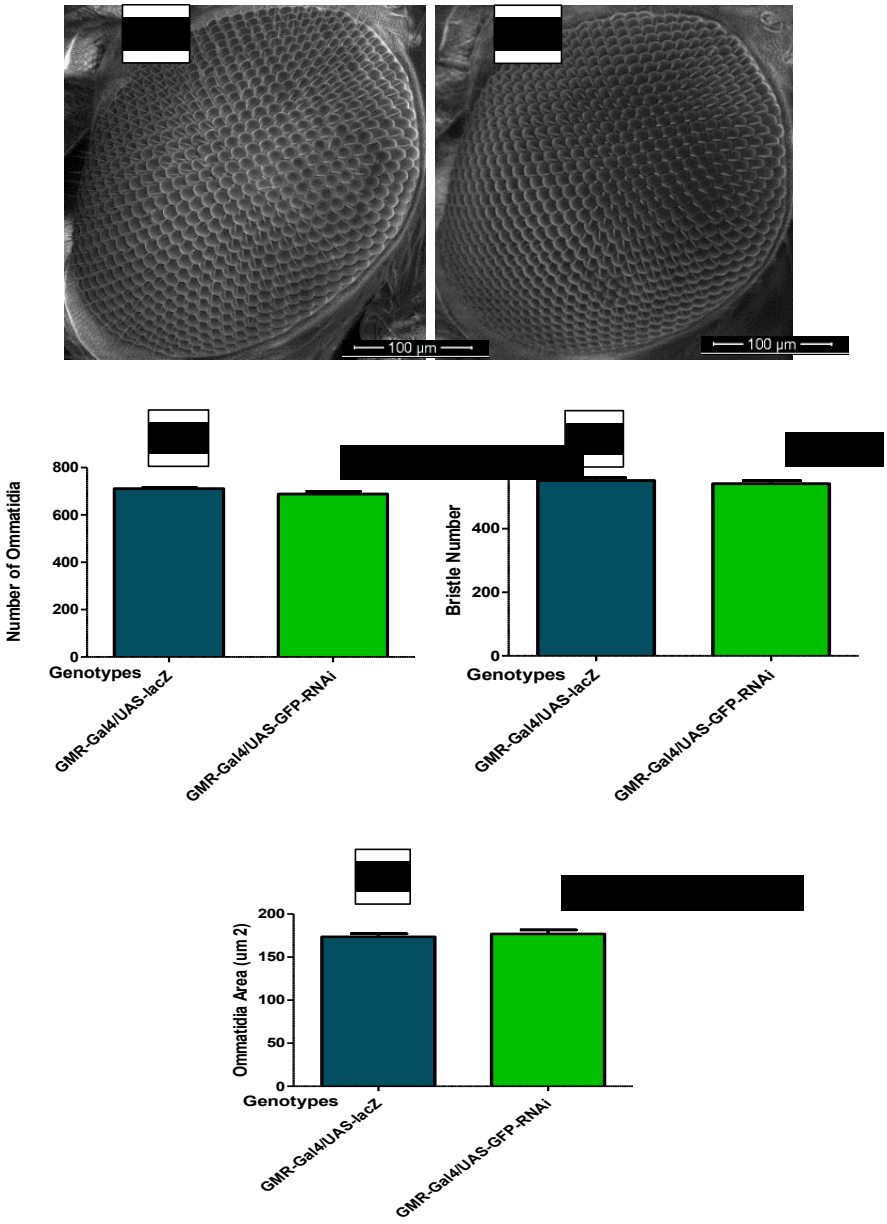

Figure 1. The expression of *GFP-RNAi* has little effect upon *D. melanogaster* eyes at 25ºC. Scanning electron micrographs of *D. melanogaster* eyes with the directed expression under the control of *GMR-Gal4* of *lacZ* (A) and *GFP-RNAi* (B). Genotypes are *GMR-Gal4/UAS-lacZ* (A) and *GMR-Gal4/UAS-GFP-RNAi* (B). *GFP-RNAi* does not alter ommatidia number compared to *GMR-Gal4/UAS-lacZ* (C). *GFP RNAi* does not influence the number of ommatidia (D) plus ommatidia area is not altered by *GFP-RNAi* (E). N-value is 10 for all and p-value of < 0.05 is considered significant. Error bars represent standard error of the mean (SEM). NS indicates not significant.

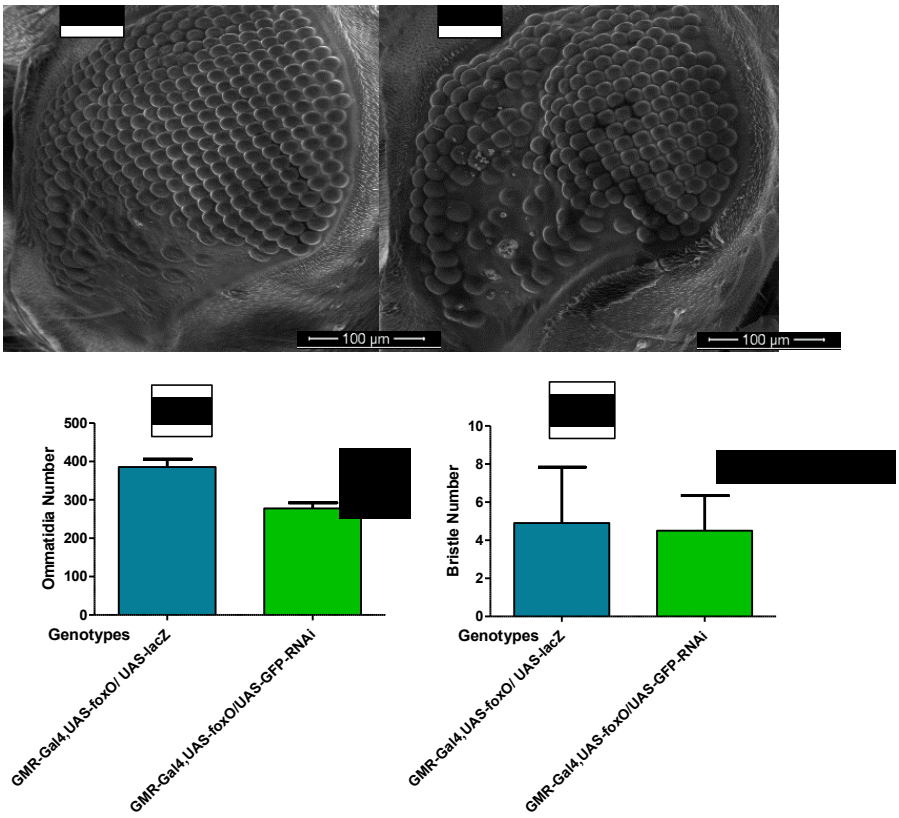

Figure 2. The expression of *GFP-RNAi* enhances the *GMR-Gal/UAS-foxO* phenotype at 25ºC. Scanning electron micrographs of *GMR-Gal4,UAS-foxO,UAS-lacZ* (A) and *GMR-Gal4,UAS-foxO,UAS-GFP-RNAi* (B). *GFP-RNAi* reduces ommatidia number (C) but does not alter ommatidia area (D) or bristle number (E). N-value is 10 for all and p-value of < 0.05 is considered significant. Error bars represent standard error of the mean (SEM). NS indicates not significant and the asterisk indicates a significant difference.

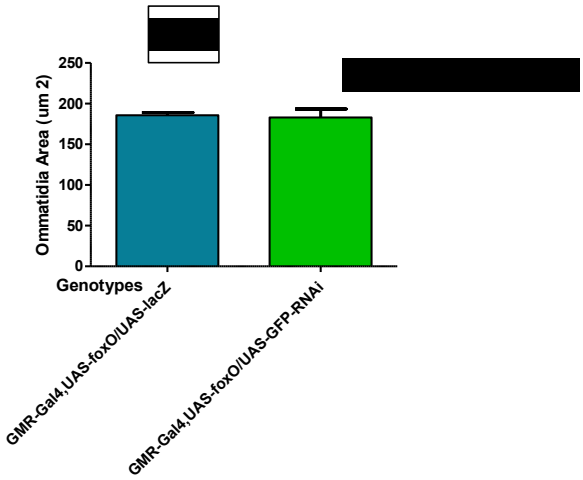

The expression of *foxO* in the *Drosophila* eye, directed by *GMR-Gal4,* produces an abnormal rough eye phenotype characterized by a reduced number of ommatidia, partial absence of bristles and a distorted eye periphery (Kramer *et al*., 2003). The expression of *GFP-RNAi* enhances the phenotype induced in *GMR-Gal4/UAS-foxO* flies (Figure 2). Although the size of the ommatidia and the absence of bristles does not differ much between *GMR-Gal4, UAS-foxO*/*UAS-lacZ* (with mean values of ommatidial area of 177.5 μm^2 and 4.7 interommatidial bristles), and *GMR-Gal4, UAS-foxO*/*UAS-GFP-RNAi* (with mean values of ommatidial area of 174.6 μm^2 and 4.5 interommatidial bristles) critical class males, biometric analysis reveals a significant reduction (p-value < 0.0001) in the number of ommatidia in flies that expressed *GFP-RNAi* (with mean of 263.6 ommatidia) compared to the *lacZ* (with mean of 372.7 ommatidia) control. Overall, while this *RNAi* does not alter standard development, the number of ommatidia can be greatly reduced under the non-standard development of *GMR-Gal4/UAS-foxO* individuals.

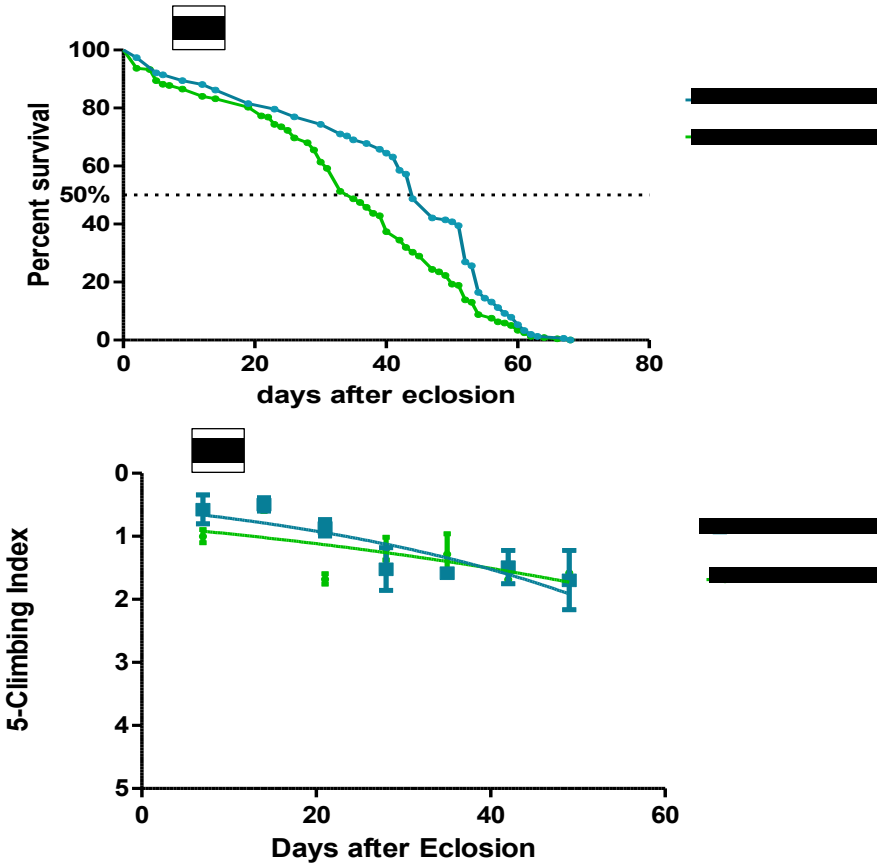

Figure 3. Ectopic expression of *GFP-RNAi* directed by *ddc-Gal4* reduces median lifespan but not climbing ability in *D. melanogaster* at 25ºC. (A) *GFP-RNAi* directed by *ddc-Gal4* in dopaminergic neurons decreases median lifespan (38 days) compared to the *ddc-Gal4/UAS-lacZ* control (47 days). *GFP-RNAi* lowers median lifespan according to Mantel-Cox test results. N-value is 200 for all. (B) Climbing ability is not significantly altered by *GFP-RNAi* directed by *ddc-Gal4* in neurons, including dopaminergic neurons.

To direct the expression of the *UAS-GFP-RNAi* transgene in the dopaminergic neurons of ageing *Drosophila*, two neuronal-specific *Gal4* lines, *ddc-Gal4* and *TH-Gal4* were selected with similar results being obtained. Expression of *GFP-RNAi* in a subset of neurons, including the dopaminergic neurons, directed by *ddc-Gal4* causes a decrease in median lifespan when compared to *ddc-Gal4/UAS-lacZ* controls (Figure 3). Median survival of *ddc-Gal4/UAS GFP-RNAi* flies is 38 days, much reduced when compared to the *ddc-Gal4/UAS-lacZ* controls of 47 days. When the *TH-Gal4* transgene was used to direct the *UAS-GFP-RNAi* responder to induce *GFP-RNAi* expression in dopaminergic neurons, the median lifespan was 38 days compared to 60 days for the *TH-Gal4/UAS-lacZ* controls (Figure 4). However, the climbing ability does not appear to be compromised among the survivors of either experimental critical class. The expression of *GFP-RNAi* directed to the dopaminergic neurons leads to a significant decrease in median lifespan.

In contrast to our initial hypothesis, *GFP-RNAi* inheritance in dopaminergic neurons can lead to diminished survivorship, which clearly indicates that *UAS-GFP-RNAi* may not be considered as a benign control. Ubiquitous and other modes of expression of *GFP-RNAi* has been demonstrated to have a negative effect upon lifespan in RU486-induced *Gal4* experiments (Alic *et al.,* 2012); however, the influence of *Gal4* gene expression products may have not received full consideration. This compromise in longevity demonstrates that RNAi transgenes can result in a decreased lifespan in *Drosophila*, especially when the dopaminergic neurons are targeted, as previously suggested. The reduced lifespan may indicate that activity of RNAi directed machinery may emerge as an enduring negative condition and that the probable "off-target" events may complicate experimentation and interpretation. To further investigate the influence of *GFP-RNAi,* future experiments could pursue the changes in the homeostatic baselines that lead to these altered phenotypes.

Acknowledgments: The authors wish to thank the Bloomington Drosophila Stock Center (University of Indiana, Bloomington, USA) for providing *Drosophila* lines. Our thanks go out to a recent anonymous reviewer of another manuscript for inspiration. This research was funded by Department of Biology of Memorial University of Newfoundland Teaching Assistantship and a MUN School of Graduate Studies

Fellowship to MSCJ and by a Natural Science and Engineering Council of Canada (NSERC) Discovery Grant to BES.

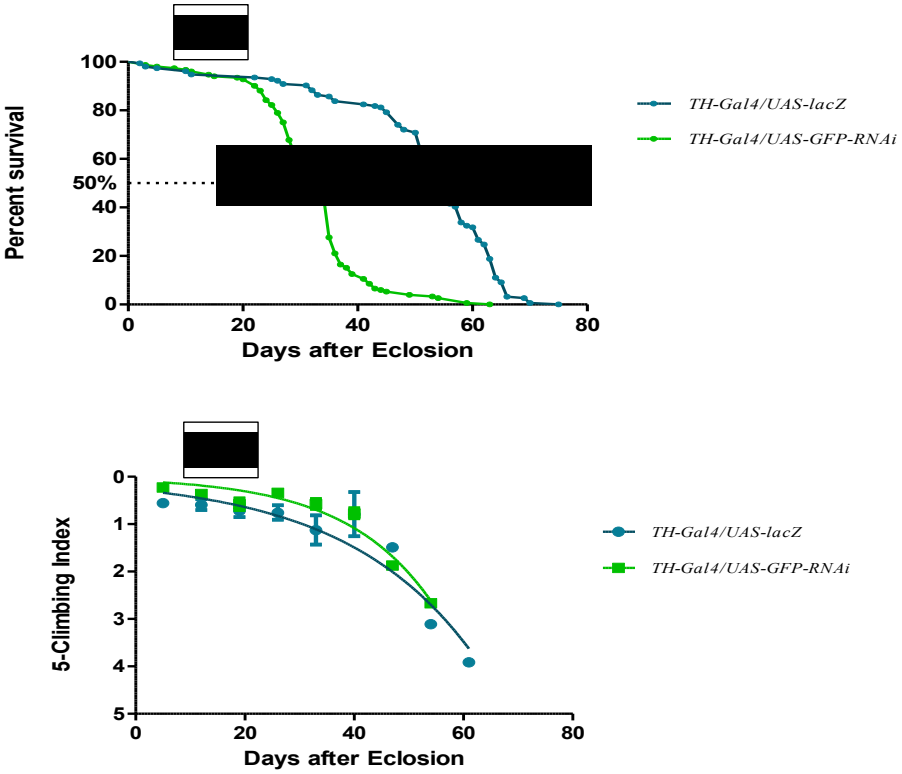

Figure 4. Ectopic expression of *GFP-RNAi* directed by *TH-Gal4* reduces median lifespan but not climbing ability in *D. melanogaster* at 25ºC. (A) *TH-Gal4/UAS-lacZ* flies show a median lifespan of 38 days whereas *TH-Gal4/UAS-GFP-RNAi* critical class males show median life span of 60 days. This *GFP-RNAi* lowers median lifespan very significantly according to Mantel-Cox test results (p-value < 0.0001). (B) Critical class males were chosen for the climbing or locomotion assay over time for two genotypes: the control *TH-Gal4/UAS-lacZ* and *TH-Gal4/UAS-GFP-RNAi* (initial n = 70). Non-linear regression fitted curves and statistical analysis show that there is no significant difference in the climbing abilities over time. Error bars represent standard error of mean and asterisk indicates significant difference.

References: Abramoff, M.D., *et al.*, 2004, Biophotonics Int. 11: 36–42; Alic, N., *et al.*, 2012, PLoS One 7: 45367; Brand, A., and N. Perrimon 1993, Development 118: 401-15; Freeman, M., 1996, Cell 87: 651-660; Kramer, J.M., and B.E. Staveley 2003, Genet. Mol. Res. 2: 43-47; Kramer, J.M., *et al.*, 2003, BMC Dev. Biol. 3: 5; Li, H., *et al.*, 2000, Curr. Biol. 10: 211–214; M'Angale, P.G., and B.E. Staveley 2016, PeerJ. 4: e2461; Mawhinney, R.M.S., and B.E. Staveley 2011, Genet. Mol. Res. 10: 494-505; Ni, J.Q., *et al.*, 2011, Nat. Methods 8: 405-407; Perrimon, N., *et al.*, 2010, Cold Spring Harb. Perspect. Biol. 2: a003640; Slade, F.A., and B.E. Staveley 2015, Genet. Mol. Res. 14: 12788-96; Staveley, B.E., *et al.*, 1990, Genome 33: 867-872; Todd, A.M., and B.E. Staveley 2004, Dros. Inf. Serv. 87: 101-108.

Guide to Authors

Drosophila Information Service prints short research, technique, and teaching articles, descriptions of new mutations, and other material of general interest to *Drosophila* researchers. The current publication schedule for regular issues is annually, with the official publication date being December. The annual issue will include material submitted during the calendar year. The submission deadline for each annual issue will be 31 December of the publication year except when special circumstances occur, but articles are accepted at any time. Submissions should be in MS Word. .

Submission: Proofs will not be sent to authors unless there is some question that needs to be clarified. The editor reserves the right to make minor grammatical, spelling, and stylistic changes if necessary to conform to DIS format and common English usage. Tables may be slightly reformatted to conform to DIS style. Color illustrations will appear black and white in the printed version but will be in color on our web site (www.ou.edu/journals/dis).

Citation of References: Citation should be by name and date in the text of an article (Smith, 1989; Jin and Brown, 1990; Waters *et al*., 1990). At the end of the article, references should be listed **alphabetically** by senior author, listing all authors with initials, date, journal, volume and page numbers. Titles will not be included except for books, unpublished theses, and articles in press. An example format is:

Green, R.L., 1998, Heredity 121: 430-442.
Waters, R.L., J.T. Smith, and R.R. Brown 1990, J. Genet. 47: 123-134.

Note the initials are before each name except for the senior author.

Manuscripts and inquiries should be sent to James Thompson, Department of Biology, University of Oklahoma, Norman, OK 73019. Telephone (405)-325-4821; email jthompson@ou.edu; FAX (405)-325-7560.

Technique Notes

A method using CO_2 anesthesia to collect embryos for microinjection in *Drosophila elegans.*

Massey, Jonathan H.[1], Jun Li[2], and Patricia J. Wittkopp[1,3]. [1]Department of Ecology and Evolutionary Biology, University of Michigan, Ann Arbor, MI; [2]Institute of Evolution and Ecology, School of Life Sciences, Central China Normal University, Wuhan 430079, China; [3]Department of Molecular, Cellular, and Developmental Biology, University of Michigan, Ann Arbor, MI 48109, USA.

Abstract

A key step for genetic transformation of animal hosts is collecting enough embryos for microinjection. In *Drosophila melanogaster*, fertile females will often lay hundreds of embryos when placed on a grape plate with yeast. In other *Drosophila* species, however, females typically lay few if any embryos under similar conditions, hindering efforts to inject genetic reagents to create new mutants or markers for downstream genetic analyses. Here, using the species *Drosophila elegans*, we describe a method using CO_2 anesthesia to collect embryos for microinjection. This technique allowed us to collect and inject enough embryos for CRISPR/Cas9 gene editing in this non-model species, resulting in a null allele of the *ebony* gene.

Required Materials

Grape Juice Agar (*e.g.*, Nutri-fly, Cat #: 47-102, Genesee Scientific)
Petri Dishes (Cat # 3050-00, Weber Scientific): 100 × 15 mm (83 mm Diameter)
Embryo Collection Cages - Small (Cat # 59-100, Genesee Scientific): 5.6 cm (D) × 7.6 cm (H)
Standard *Drosophila* media with added molasses (Wirtz and Semey, 1982)
At least 10 expanded vials of *Drosophila elegans* (~1000-2000 flies) on molasses media
Standard *Drosophila* CO_2 anesthesia equipment
Whatman 1004-042 Filter Circles, 42.5mm Diameter

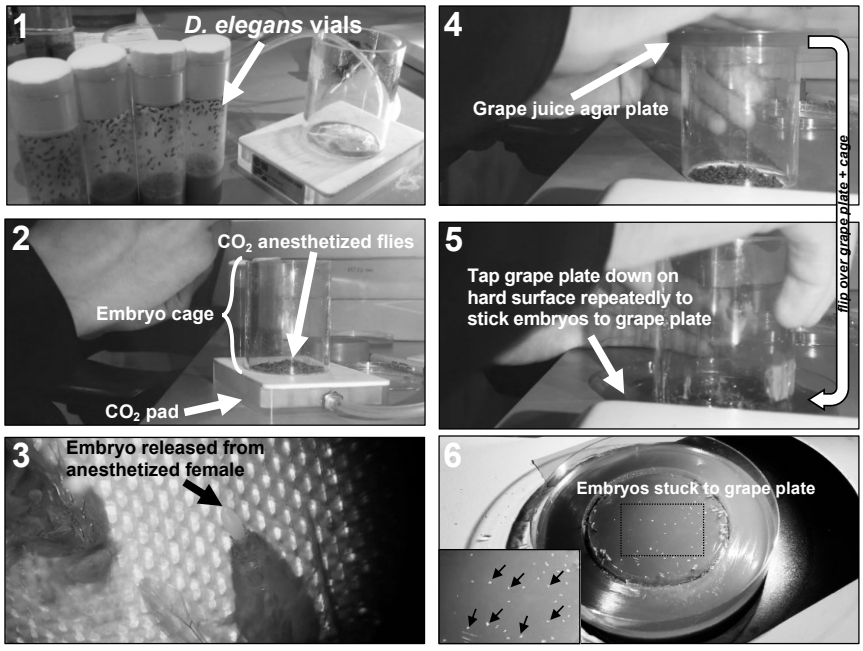

Figure 1. Steps for using CO_2 anesthesia to collect *Drosophila* embryos for microinjection.

Procedure

1. Prepare fresh grape juice agar plates following the Nutri-fly recipe from Genesee Scientific (Cat #: 47-102).

2. Expand *Drosophila elegans* population to at least ~1000-2000 flies. *D. elegans* have trouble pupating on the sides of the vials, so adding Whatman filter paper deep into the food of each vial once L3 larvae develop helps provide a greater surface area for larvae to pupate on, allowing adults to eclose (see Methods in Massey *et al*., 2020, for more details on rearing methods).

3. Age *D. elegans* males and females together in vials for ≥2 weeks (flipping to new food vials when L3 larvae develop) to give the adults enough time for multiple matings to occur and for embryos to develop.

4. Using CO_2 anesthesia, knock out at least 500 flies and dump them into an empty embryo collection cage (Cat # 59-100, Genesee Scientific) (Figure 1, Steps 1 and 2).

5. If the females have mated and are old enough (≥ 2 weeks), you should see several individuals begin to release an embryo from their ovipositor (Figure 1, Step 3).

6. Take a fresh grape juice agar plate at room temperature, flip it upside-down, and push the agar down hard enough onto the bottom of the embryo cage to puncture the agar and form a seal with the inside of the embryo cage (Figure 1, Step 4).

7. Flip the assembly (grape plate + embryo cage + anesthetized flies) over so that the flies come into contact with the grape agar. Next, tap the assembly down onto a hard surface repeatedly (~10 times) to force the released embryos to stick onto the agar (Figure 1, Step 5).

8. Flip the assembly back over so that the flies are again on the mesh ceiling of the embryo cage as in Figure 1, Step 4. Tap the assembly onto a hard surface to release any remaining adults stuck to the grape agar plate.

9. Place the assembly back onto the CO_2 pad to anesthetize the adults again before pulling the agar plate off of the embryo cage and dumping the adults back into their vials. We have found that adult females will continue to release embryos in this manner every 24 hours.

10. To facilitate larger (>1000) embryo collection procedures for multiple rounds of microinjection, repeat steps 2-9 in this procedure with a more expanded population of *D. elegans*. For our CRISPR/Cas9 experiment targeting the *ebony* gene (see Methods in Massey *et al*., 2021; Figure 2 below), we expanded our *D. elegans* population to ~10,000 flies and collected ~500 embryos a day to inject ~2000 embryos.

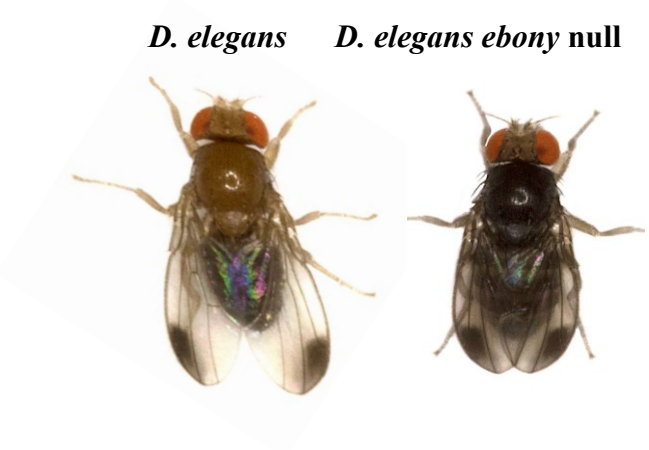

Figure 2. *Drosophila elegans* (Hong Kong strain) wild-type (left) and *ebony* knockout (right).

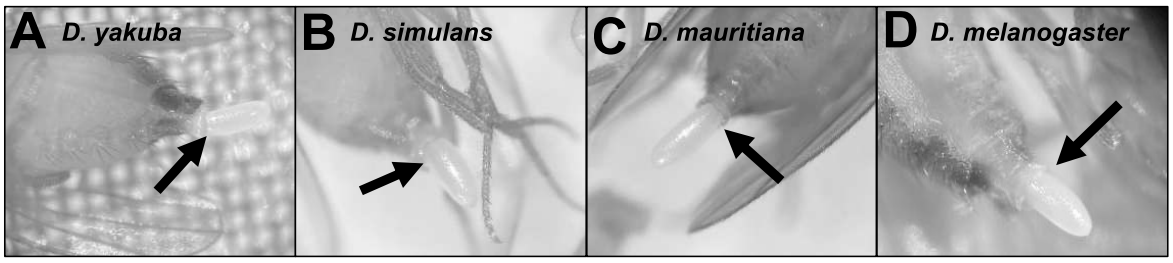

Figure 3. Embryo release from *Drosophila* species after CO_2 anesthesia.

Conclusion

Here, we present a method for collecting embryos from *D. elegans*. We also find that fertile females in other non-model species (*D. yakuba*, *D. simulans*, and *D. mauritiana*), as well as *D. melanogaster*, often release an embryo from their ovipositor when subjected to CO_2 anesthesia (Figure 3A-D). It is more difficult, however, to eject these embryos onto grape plates with the tapping method described in Step 8 above. Applying this technique to other *Drosophila* species for downstream microinjection applications, therefore, will likely require either using a paintbrush to remove individual embryos or a more forceful method to eject the embryos onto the grape plate. Finally, in our experience with *D. elegans*, we find that it is unnecessary to wash embryos in preparation of microinjection using the CO_2 anesthesia technique. Avoiding this step helped improve our embryo survival rates post injection.

References: Massey, J.H., G.R. Rice, A. Firdaus, C.Y. Chen, S.D. Yeh, D.L. Stern, and P.J. Wittkopp 2020, Evolution 74-6: 1098–1111; Massey, J.H., J. Li, D.L. Stern, and P.J. Wittkopp. Distinct genetic architectures underlie divergence in body, leg, and wing pigmentation between *Drosophila elegans* and *D. gunungcola*. *In revision* at Heredity; Wirtz, R.A., and H.G. Semey 1982, Dros. Inf. Serv. 58: 176–180.

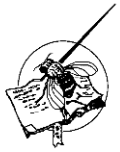

Lane-maze for behavioral tests in flies.

Eckert, Fabiola Boz[1, 4], Dhiozer de Brittos Valdati[2], José Marino Neto[2], Daniela Cristina de Toni[3], and Cilene Lino de Oliveira[1, 4]. [1] UFSC - Postgraduate Program in Pharmacology (Florianópolis, SC-Brazil), [2] UFSC - Institute of Biomedical Engineering (Florianópolis, SC-Brazil),[3] UFSC - Department of Cellular Biology, Embryology and Genetics (Florianópolis, SC-Brazil), [4] UFSC - Department of Physiological Sciences (Florianópolis, SC-Brazil); Corresponding Author: Cilene Lino de Oliveira, Departamento de Ciências Fisiológicas, Centro de Ciências Biológicas, Universidade Federal de Santa Catarina, Campus Universitário Trindade, 88049-900 – Florianópolis – SC – Brazil. Orcid: orcid.org/0000-0002-0627-530; cilene.lino@ufsc.br

Introduction

Behavior tests are useful tools to evaluate phenotypes, effects of drugs or other manipulations such as stressors on laboratory animals. These tests often consist of paradigms planned to obtain information on species-specific activities of an individual or group of animals under controlled conditions (Wang *et al*., 2013; Domingues *et al.*, 2019; Lin *et al*., 2016; Remus *et al*., 2015). Behavioral tests often involve direct observation of the subjects for a limited period in a structured arena where ongoing, stimulated, or disrupted activities may be registered (Zhou *et al*., 2014; Sequeira-Cordero *et al*., 2019). The integrity of the behavioral repertoire may allow for conclusions on the effects of relevant interventions.

In *Drosophila melanogaster* different aspects of motor activity, sexual, sleeping, feeding, drinking, or other motivated behaviors may be appraised by using distinct paradigms (Itskov *et al*., 2014; Murphy *et al.,* 2017; Neckameyer and Nieto-Romero, 2015). Levels of motor activity may be estimated by scoring the

exploring time or speed in an open field or registering the number of flies climbing a tube (Landayan *et al.*, 2017; Neckameyer and Nieto-Romero, 2015). Food intake or even preference for palatable food, for example, may be measured by estimating the fluid intake from a capillary (CAFE, Ja *et al*., 2007) or scoring frequency of proboscis extension towards food (Gordesky-Gold *et al.*, 2008) or detecting dyed abdomen after feeding with colored food (Deshpande *et al*., 2014). Additional tests to measure preference may include the latency to reach a sweet place (Thoma *et al.*, 2016) or "FLIC" (Ro *et al.,* 2014) and flyPAD (Itskov *et al*., 2014). Motivation to escape from a stressful situation may be measured by the time flies struggle in a forced swimming test (Araújo *et al*., 2018).

Each of the behavioral tests mentioned above requires specific devices and apparatuses to be performed. For example, "FLIC" (Fly Liquid-Food Interaction Counter) (Ro *et al.,* 2014) needs a hardware and software system for collecting and quantifying continuous measures of feeding, and flyPAD (Itskov *et al*., 2014) is a method that connects food to electrodes and measures the contact of flies with that based in changes in capacitance. Although useful, most of the apparatus mentioned above were developed to investigate a single experimental unit (an individual fly or a group of flies) at a time. In an interesting study, Murphy *et al.* (2017) created an apparatus allowing for the observation of motor activity and fluid intake of 30 individual flies simultaneously, named "Activity Recording Capillary Feeder" (ARC). ARC chambers containing 30 half-cylindrical-shaped wells, similar to the tubes used by Pfeiffenberger *et al.* (2010), were printed in acrylonitrile butadiene styrene or polylactic acid using a 3D printer. A 2-mm-thick clear plexiglass shield covered the arena and allowed the visualization of each fly during a behavioral test. Beneath the chamber, a base plate is used to keep the chamber upright. Above the wells, a gate containing regularly spaced 2.5-mm holes aligned with each well is inserted into the groove above the chamber and pushed into place. Then, each hole could receive a capillary kept straight by a support made using construction paper (Murphy *et al.,* 2010). This single capillary could be filled up with fluid for a fluid intake test.

Here, inspired by Murphy *et al.* (2017), an apparatus named lane-maze was projected, allowing for the insertion of two capillaries at each lane. This modification of ARC may provide conditions for the fluid assessment preference in flies, simulating preference tests as performed in rodents (Remus *et al*., 2015). Concomitant to the preference test, lane-maze allows for the assessment of motor activity similarly to Murphy *et al*. (2017). Besides, lane-maze accommodates up to 14 individual flies simultaneously.

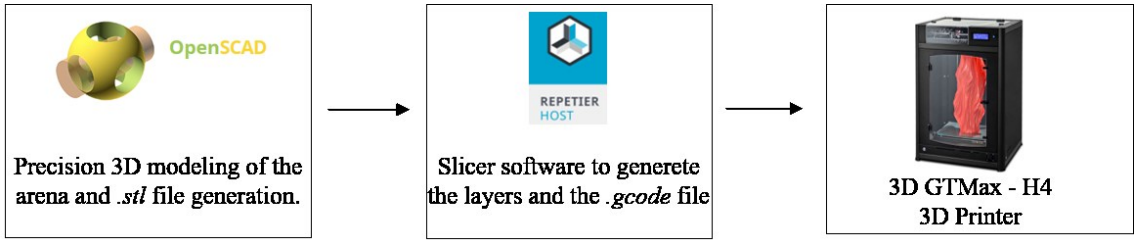

Figure 1. Process for printing the lane-maze.

Methods

Lane-maze apparatus was printed using acrylonitrile butadiene styrene filaments in a 3D printer (GTMax3D Pro Core H4). The arena was made using only open sources software. The precise 3D modelling was performed using the software OpenSCAD (https://www.openscad.org). After finished the 3D modelling and generated the *.stl* file in the OpenSCAD, the arena file was open in the software Repetier Host (https://www.repetier.com/download-software/). In this software, the *.stl* file was prepared to be printed. This process aims to layer through slicer software so that the 3D printer can print in layers. The Repetier Host has two slicer software, the Cura engine and the Slic3r (https://slic3r.org/download/). The software often used to slicer and made the layers to print in the 3D printer was the Slic3r, since this software can offer more options to change the way that the 3D printer printed. This software generates a file that the 3D printer can read. The extension of this file is *.gcode.* After generating the *.gcode* file of the arena, the new file was uploaded in the

3D printer and printed. The *.gcode* file of the lane-maze may be downloaded from the link https://osf.io/y46e9/files/osfstorage/5f6e0b0f9e9a3d02736e2d9a/. A flowchart of the process showing the primary goal of each process can be seen in Figure 1.

Lane-maze (Figure 2) consisted of a squared arena (external dimensions: 6.6 × 9.2 cm, internal dimensions: 5 × 5.5 cm) with 14 internal subdivisions (lanes) with identical dimensions (length: 5 cm, wide: 0.3 cm) covered with a transparent acrylic plate. In both extremities of each lane, a hole (diameter: 0.05 cm) allowed for the insertion of a glass capillary in an angle of 20 degrees provided by the inclined edges of the external arena. Glass capillaries allow access to palatable fluids during the lane-maze tests.

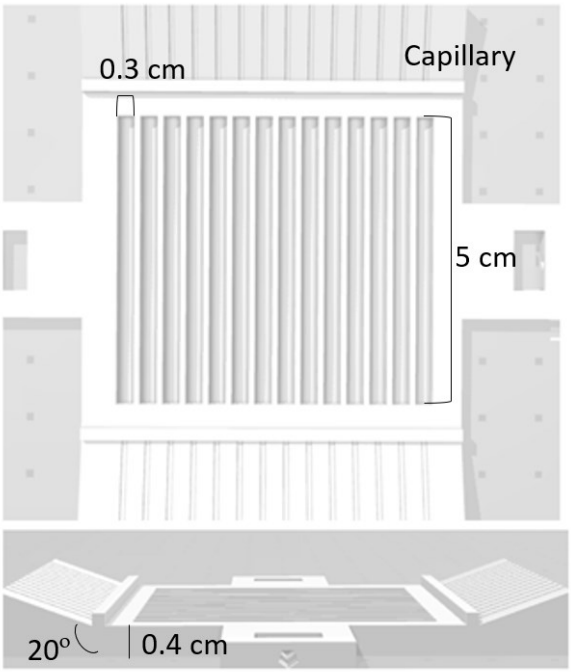

Figure 2. Lane-maze in a top view (upper figure) and a perspective view (lower figure).

Observations

Lane-maze and ARC are similar apparatuses allowing for the assessment of multiple experimental units simultaneously. However, lane-maze has two advantages over ARC: 1 – the possibility of using two capillaries may allow for a preference test performance; 2 – the inclined edges of the arena allows the insertion of the capillaries in inclined position decreasing the influence of gravity on the fluids, avoiding leaks, and contributing to the fluids to be accessed by flies during all the experiments. The advantage of the ARC over lane-maze is that it allows for testing of 30 flies simultaneously. However, the lane-maze allows adaptations to increase the number of lanes in the project, or more than one apparatus could be printed to perform experiments with more flies.

The pair of capillaries inserted at each lane of the lane-maze may be filled with fluids such as sucrose or vinegar offered as attractive stimuli in preference tests (Diegelmann *et al.* 2017; Ja *et al*., 2007). Slight modifications of the lane-maze apparatus may be useful to perform other behavioral tests. Indeed, by covering the lid with dark transparent film, a place preference test such as light-dark test (Araújo *et al*., 2018) may be performed. Negative geotaxis behavior (Bartholomew *et al.*, 2015; Neckameyer and Bhatt, 2016) could also be measured by laying down the apparatus on its lateral wall.

Acknowledgments: *Data sharing*: Data and other supplementary material are deposited at Open Science Framework in the following link: https://osf.io/pxad5/; *Funding***:** Fabiola B Eckert received fellowship from Conselho Nacional de Desenvolvimento Científico e Tecnológico, Brazil (140007/2016-4). This study was financed in part by the Coordenação de Aperfeiçoamento de Pessoal de Nível Superior – Brasil (CAPES) – Finance Code 001".

References: Araujo, S.M., M.R. Poetini, V.C. Bortolotto, *et al*. 2018, Behav. Brain Res. 351: 104–113; Bartholomew, N.R., J.M. Burdett, J.M. VandenBrooks, M.C. Quinlan, and G.B. Call 2015, Scientific reports 5: 15298; Deshpande, S.A., G.B. Carvalho, A. Amador, *et al*. 2014, Nature methods 11: 535; Diegelmann, S., A. Jansen, S. Jois, *et al*. 2017, J. Vis. Exp. 121: 55024; Domingues, K., F.B. Lima, A.E. Linder, *et al*. 2019, Synapse 74: e22130; Gordesky-Gold, B., N. Rivers, O.M. Ahmed, *et al*. 2008, Chemical senses 33: 301-309; Itskov, P.M., J.M. Moreira, E. Vinnik, *et al*. 2014, Nature communications 5: 1-10; Ja, W.W., G.B. Carvalho, E.M. Mak, *et al*. 2007, Proceedings of the National Academy of Sciences 104: 8253–8256; Landayan, D., D.S. Feldman, and F.W. Wolf 2018, Sci. Rep. 8: 5777; Lin, C.C., O. Riabinina, and C.J. Potter 2016, J. Vis. Exp. 114: e54346; Murphy, K.R., J.H. Park, R. Huber, 2017, Nature Protocols 12: 2355; Neckameyer, W.S., and P. Bhatt 2016, *Drosophila*: Human Press 303-320; Neckameyer, W.S., and A.R. Nieto-Romero 2015, Stress 18: 254-266; Pfeiffenberger, C., B.C. Lear, K.P. Keegan, and R. Allada 2010, Cold Spring Harbor Protocols 11: 5518; Ro, J., Z.M. Harvanek, and S.D. Pletcher 2014, PloS one 9: 101107; Remus, J.L., L.T. Stewart, R.M. Camp, *et al*. 2015, Behav. Neurosci. 129: 321; Sequeira-Cordero, A., A. Salas-Bastos, J. Fornaguera, and J.C. Brenes 2019, Scientific reports 9: 1-21; Thoma, V., S. Knapek, S. Arai, *et al*. 2016, Nat. Commun. 7: 10678; Zhou, J., X. Cao, A.C. Mar, Y.Q. Ding, X. Wang, Q. Li, and L. Li 2014, Psychopharmacology 10: 2067-2075.

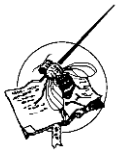

Efficient screening of CRISPR/Cas9 genome editing in *Drosophila* without a visible marker.

Graham, Patricia L. Matthew D. Fischer, and Leslie Pick. Department of Entomology and Program in Molecular & Cell Biology, University of Maryland, College Park, MD 20742, USA

Abstract

CRISPR/Cas9 genome editing is now widely used by *Drosophila* researchers to generate targeted mutations in genes of interest. In most cases, researchers are making use of the insertion of fusion genes encoding visible markers, such as GFP, to identify genome editing events. While this approach greatly facilitates the identification of CRISPR-induced mutations, there are situations in which insertion of a new gene into the genome is disadvantageous. For example, the inserted gene might disrupt coding regions or cis-regulatory elements and obscure interpretations of results. We have set up a lab pipeline for screening CRISPR-induced mutations by PCR that allows for effective and efficient identification of mutations without reliance on a visible marker. Mutations are identified within 3 to 4 weeks from the time injected (G0) flies eclose. This procedure was established by one of us (PLG) and has been replicated by another (MDF), suggesting that, as written, it can be easily adapted in any fly lab.

Protocol

Preparation

1) Prepare the guide RNAs (gRNA) and templates for Homology Directed Repair (HDR) as needed for the target of interest. We have been using Rainbow Transgenic Flies, Inc. for microinjection into flies carrying *nos-Cas9 (*BL54591 (*y[1] M{w[+mC]=nos-Cas9.P}ZH-2A w[*]*). We have found it useful to include a co-CRISPR gRNA as in Kane *et al.* (2017), that targets a different gene and acts as a positive control for Cas9 activity. This facilitates the identification of G0 lines that are most likely to have progeny carrying the genome edit of interest. In this strategy, a previously validated gRNA targeting a gene encoding a visible marker is injected along with gRNAs targeting the gene of interest. G0 lines that produce progeny with the visible marker are significantly more likely to also produce progeny that contain the desired genome edit than

those that do not produce such progeny. For example, we used the *ebony* gRNA from Kane *et al.* (2017), which causes a recessive mutation that darkens the cuticle. To see this phenotype in the F1, we crossed the G0 to *Dr/TM3Sb,e* flies. If a mutation is present in the *ebony* gene of the F1, the *Sb* progeny will also be ebony.

2) 1-2 weeks before mailing the DNA to Rainbow Transgenic Flies (or injecting on-site), start to build up the stock that will be used for outcrosses. For insertions on chromosome III, we have been using *Dr/TM3Sb,e* for outcrossing and balancing. Begin by setting up 3-4 vials 2×/week. After sending the DNA out, set up 3 bottles 2×/week. If many virgins are desired, set up new bottles twice a week. Allow the flies to lay for a week at room temperature, then toss them. This prevents overcrowding. It is advisable to set up bottles at the latest when the G0 crosses are established. Note that many vials will be required when the F1 start to eclose since 4-8 single crosses per G0 should be made.

Initial crosses (takes about 2-3 weeks until screening starts), all at 25°C

1) When the G0 eclose (occurs over 2-3 days), cross each G0 to three flies from the outcross stock. Establish as many crosses as possible.

For example, in one experiment ~120 G0 larvae were viable after injection. This yielded 38 G0 viable adults, 23 of which were fertile. The eclosion and fertility rates have varied for different CRISPR experiments, but appear to be generally lower than for other types of genetic manipulation.

2) Check the crosses after 3-5 days. Transfer adults from crosses that have progeny to a new vial. This provides a back-up vial in case something goes wrong or in case it is necessary to spread the screening out over a longer period.

3) When the F1 start to eclose (about 9-11 days from when the cross was set up at 25°C), establish 6-8 crosses using individual F1 from each fertile G0. Cross each F1 to three flies from the outcross stock.

- Use male F1 when possible - there are usually plenty available since they do not need to be virgin and you can use either balancer or non-balancer males (no crossing over in male flies). If F1 males are used, the outcross females to whom they mated can be transferred to a fresh vial when the F1 male is harvested for screening. The females will produce more progeny, giving extra time to get F2 from the ones that screen positive.
- If injecting into the strain BL54591 (*y[1] M{w[+mC]=nos-Cas9.P}ZH-2A w[*]*) where nos-Cas9 is located on the X chromosome, it is particularly advantageous to use male F1 in order to eliminate the *nosCas9* chromosome as soon as possible.
- Since progeny with the Cas9-induced genome editing event are often observed in the first 4-6 F1 screened, we set up 4-5 F1 crosses from each G0 as soon as possible, then set up more a few days later. We screen the first set of 4 from each G0, and only if there are not enough candidate lines will we go back to screen the second set.

4) Once it is clear that the F1 have progeny (~ 2-3 weeks after the G0 started to eclose), start the single fly PCR screen. This will take 3-6 days depending on how many can be done at once, how many G0 there were, and whether the desired genome edit is detected in the first round. If screening results are desired or needed faster than this time frame, it can be accomplished within 2-3 days (see "accelerated screening" below).

General strategy for PCR screening

Day 1: Make first set of single fly preps (protocol below), filling 4 PCR strips (8 tubes/strip, one fly/tube)

Day 2: Set up the PCR with the day 1 single fly preps as templates; pour the gel for day 3; and do another set of 4 strips of single fly preps.

Day 3: Run out the PCRs from the day 1 fly preps on the pre-poured gel; set up the PCR on day 2 fly preps; pour a gel for day 4; and do a 3rd set of single fly preps.

Continue this cycle, repeating as long as needed to detect desired number of CRISPR events.

It is crucial to keep careful track of the F1 crosses and corresponding DNA preparations. One possible system is to give each G0 a number. Each F1 is then named with the G0 number and a letter (*e.g.*, 2A, 2B etc.). Both the vial with the initial F1 cross and the vial to which the females are transferred are labeled with the F1 designation. The PCR tube into which you place the F1 is also labeled with the F1 name. Since sharpie often gets rubbed off, we usually label both the top and the sides of each tube. We found it best to screen 4 F1 from a given G0 on a group (*i.e.*, set up single fly preps from a given G0 only when there were 4 fertile F1 progeny available). This means that each PCR strip has F1 from 2 G0 lines, making it easy to keep things in order. We generally tried to go in sequence (1, 2, 3 …) as much as possible, and keep careful notes when this was not possible. If the tubes are loaded into the gel lanes in the same order, it is easier to identify the correct F1. In general, it is likely that a genome edited line will be found in the first 4 F1 samples if there is going to be a CRISPR/Cas9-induced event at all from that G0 parent.

For accelerated screening, condense the steps in Days 1 – 3 outlined above into one day. Set up the first set of single fly preps using 4 PCR strips and use the samples to immediately set up the PCR afterwards. While this reaction runs, cast the gels necessary for electrophoresis. Set up the second set of single fly preps and again immediately set up the second PCR. At this point, run the first PCR on the gel. While the gel electrophoresis is running, set up the third set of single fly preps and immediately set up the PCR. If timed effectively and efficiently, it will be possible to seamlessly obtain results from three full sets of screens in one workday by one scientist. It should be emphasized that caution should be taken for the accelerated screening to ensure there are no mix-ups or mistakes, as the high volume of processed samples can be easily confused without extra care.

Protocol for single fly preps

This protocol was based on Gloor and Engels (1992), with minor modifications.

1) Prepare stock of squishing buffer (10mM Tris-HCl pH8.2, 1mM EDTA, 25mM NaCl, 200µg/ml proteinase K) and keep it on ice. 50 µl/fly will be necessary.

2) Collect individual F1 flies and place each in a separate PCR tube. It is most efficient to first collect all the F1 that will be harvested on a given day (and if they are male, transfer the females that were with them to a new vial) and put them on ice before starting to squish any of them.

- Keep tubes on ice. If kept on ice, the flies do not wake up, and the DNA is stable. When each fly is put in the tube, be sure that the fly ends up on or near the bottom of the tube (gently tapping the tube(s) to get them down works fine).

3) Collect 50µl of squishing buffer in the pipet tip, but **do not** expel it until after the fly is squished. It is much more difficult to squish the fly when there is a lot of liquid in the tube. Squish the flies by mashing them with the pipet tip. If possible, use a 30-300 µl multichannel pipette to squish 8 flies at once. If a multichannel pipette is not available, use a normal 20-200 µl pipette. When using the multi-channel pipette, it is important to move slowly and keep an eye on all 8 tips to be sure that all 8 flies get at least a little bit squished. Having had success with single leg preps in beetles (although we did need to use 2 µl rather than 1 µl as template for the PCR), we conclude that as long as the flies are a little squished there will be plenty of DNA for PCR. We also amended the original protocol to use 85°C to heat inactivate the proteinase K, as opposed to 95°C. That helped when we wanted to do longer PCRs for sequencing or cloning reactions.

4) It is advisable to make a single fly prep of the out-cross strain to use as a negative control/marker for the screening PCRs.

PCR screening and next crosses

1) Set up PCRs with appropriate screening primers. Use 1µl of single fly prep for template.
We suggest setting up the following 3 control reactions for each set of PCRs:

- A single fly prep of the outcross strain to visualize the wildtype band.
- Water (no-template) to test for contaminants in the reagents.
- If appropriate, the HDR template diluted to 1ng/µl to visualize the band reflective of a genome edit.

2) Run out the PCRs on a gel and identify F1 that might have the genome edit mutation.

It may be possible to get decent sequence from a PCR reaction done on the single fly prep even though the F1 is heterozygous (*i.e.*, two templates for PCR and sequencing in the same tube). If the products of the normal and genome edited template are different enough in size, the edited fragment can potentially be gel purified away from the wildtype fragment. If this is not the case, sometimes sequence from the desired PCR product can be obtained even from the mix of templates.

Outcrossing and establishing lines

Once a possible genome edited mutant fly line has been identified, its offspring need to be outcrossed to eliminate the other chromosomes from the mutant that might carry second-site mutations (note: second-site mutations linked to the genome edited mutation are possible, and those will remain). The chromosome with the genome edit will be from the *nosCas9* strain, but the other copy of that chromosome will be replaced by a balancer from the outcross stock. Since the *nosCas9* transgene is marked with mini-white, progeny with white eyes should be selected to ensure elimination of the *nosCas9*-containing chromosome. This leaves just one chromosome to worry about. We recommend at least three generations of outcrosses using single flies from genome edited strains (1/8 chance of the other chromosome still remaining at the end). Each generation of outcrossing will decrease the chance of the other chromosome still remaining by a factor of two.

In each generation, we pick one outcross vial and start 3 single fly crosses from that vial. Each outcross is a single progeny fly crossed to 3 of the outcross stock. Since there is a single CRISPR fly in each cross, the cross will fail if that fly dies, so back-up crosses are suggested. Starting with F2, repeat for 3 generations to get to F5, then set up sibling crosses to generate a balanced line. If the induced mutation is homozygous viable, create homozygous lines by crossing siblings.

We suggest starting the outcrossing and simultaneously setting up an F2×F2 using F2 that harbor the desired genome edit over the balancer chromosome. The F2×F2 cross will allow observation of the possible phenotype as soon as possible, though the phenotype may be influenced by second site mutations.

References: Kane, N.S., M. Vora, K.J. Varre, and R.W. Padgett 2017, Efficient Screening of CRISPR/Cas9-Induced Events in *Drosophila* Using a Co-CRISPR Strategy. G3 Genes|Genomics|Genetics 7: 87-93; Gloor, G.B., and W.R. Engels 1992, Single fly DNA preps for PCR. Dros. Inf. Serv. 71: 148-149.

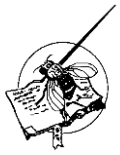

Fly transcriptomics uncovers the molecular signature of cellular and tissue-specific function.

Jain, Divyanshi, and Sujata Mohanty[#]. Department of Biotechnology, Jaypee Institute of Information Technology, A-10, Sector 62, Noida, Uttar Pradesh – 201 309; #Corresponding author, Fax: 0120-2400986; Email: sujata.mohanty@jiit.ac.in

Abstract

The central dogma of molecular biology explains the way the genetic information flows within a biological system: DNA transcribes to RNA and RNA translates into Protein. Therefore, the key player is

RNA which deciphers the message encoded in DNA. Transcriptome analysis identifies the genes in action through RNA profiling of cells or tissues at certain condition and/or a given time point. Thus, in the last few decades, transcriptomics has become one of the powerful technologies dramatically revolutionizing the health and agriculture sectors. The fruit fly *Drosophila* has been a versatile model organism since last century in providing significant insights in order to advance our understanding on biological processes. In this review, we summarize the contribution of *Drosophila* in understanding the potential candidate genes associated with organismal biology. Key words: Transcriptomics, *Drosophila*, Candidate genes, Organismal biology

Introduction

Transcriptomics has turned out to be one of the most popular and extensively used approaches for exploring and interpreting a vast range of research on prediction of key functional elements from genome and molecular mechanism behind diverse metabolic pathways and diseases (Wang *et al*., 2009; Evans, 2015). Transcriptome represents the complete sets of RNA transcript being produced by an individual cell which comprises of both coding RNAs (mRNA) and non-coding RNAs (tRNA, rRNA, siRNA, snRNA and lncRNA) (Kukurba and Montgomery, 2015; Manzoni *et al*., 2018). Transcriptomic studies suggest that mostly eukaryotic genomes get transcribed into RNAs. It is believed about 93% of human genome gets transcribed into the RNAs and out of this only 2% represents coding region (Dong and Chen, 2013).

Whole Transcriptome analysis began during early 1990s and since then it has been undergoing through various modifications (Lowe *et al*., 2017). The two key techniques with potential of capturing the nearly whole transcriptome are- i) microarray (chemical labelling-hybridization of cDNA on chip through the probes and requires pre-determined sequence knowledge), ii) RNA-seq (fragmentation of cDNA and generation of library to sequence through synthesis – the high throughput advanced sequencing method which does not require any prior knowledge of sequences) (Lowe *et al*., 2017; Manzoni *et al*., 2018). RNA-seq illustrates a broader range in comparison to microarray, allows detection of abundant lower transcripts, differentiation among critical biological isoforms, identification of more genetic variants and expressed genes possessing higher fold changes (Zhao *et al*., 2014) and also enable new routes for advancement in strategizing the areas of personalized medicine (Rathke *et al*., 2013).

Analysis at the transcriptome level provides researchers the new hopes to identify the gene "on" or "off" mechanism in different conditions and locations of cells and tissues. It enhances the possibilities of predicting the exact number of transcripts so that gene activity and expression can be quantified and highlights the activity level of genes at different stages (Adams, 2008). This approach provides strong support and evidence for studying vast gene regulatory networks and, simultaneously, also promotes the identification of novel networks in complex systems (Lowe *et al*., 2017; Gasser *et al*., 2007). Further, transcriptomics has also emerged as an inspiring field for the research sector of proteomics which serves as the initial point for studying and understanding translational mechanisms as well as widely supports the explanation of coding gene numbers inconsistency with the number of proteins being translated (Dong and Chen, 2013).

Here, in this review we highlight at different transcriptomic studies through the context of versatile experimental model species: *Drosophila,* which shares about 60% of its genomic homology with humans (Mirzoyan *et al*., 2019), 75% homology of its disease related genes with humans, and also their basic cellular and biological processes are found to be conserved among them (Pandey and Nichols, 2013; Ugur *et al*., 2016). Therefore, these studies will provide great scope for understanding different gene regulating mechanisms, expression levels, complex networks of diverse diseases, their associated pathways and evolutionary patterns among humans.

Conclusion

Transcriptomics is the most promising approach of elucidating differential biological, cellular and molecular mechanisms. It provides novel opportunities to identify the biomarkers for early detection, diagnosis and therapy set ups for treatment on time. It works as active drivers for genomic events and further needs to be constantly explored. Transcriptome analysis in *Drosophila* no doubt has fuelled our understanding

of key genetic elements regulating various cellular and metabolic activities and paving the way towards their application in agriculture and medical sciences.

Table 1. Transcriptomic studies conducted on *Drosophila* model.

S. No	*Drosophila* sp.	Study and its Significance	Citation
1.	*D. melanogaster*	Gene expression profiling of adult flies performed transcriptomically in response to fungal pathogen *Aspergillus flavus* which provides information of expressed gene levels with respect to innate defensive mechanism for viruses, bacteria, fungi and diseases among higher animals.	L. A. Ramírez-Camejo and P. Bayman, "A transcriptome-level view of Drosophila's immune response to the opportunistic fungal pathogen Aspergillus flavus," *Infect. Genet. Evol.*, vol. 82, Aug. 2020, doi: 10.1016/j.meegid.2020.104308.
2.	*D. melanogaster*	Combinatorial approach of GWAS and transcriptomics to determine the genes linked with thermal tolerability in response to effective stress and preparatory conditions. The functional analysis of SNPs related to thermal tolerability enables the identification of thermal sensitive candidate genes for further studies.	M. C. Lecheta *et al.*, "Integrating GWAS and Transcriptomics to Identify the Molecular Underpinnings of Thermal Stress Responses in Drosophila melanogaster," *Front. Genet.*, vol. 11, Jun. 2020, doi: 10.3389/fgene.2020.00658.
3.	*D. sechellia* (females)	Identification of Octanoic acid resistance genes, which helps in understanding of varying ecological adaptations depending upon the host need. It primarily highlights toward candidate genes, their evolutionary patterns for resistance to host-plant toxin.	"Transcriptomic analysis of octanoic acid response in Drosophila sechellia using RNA-sequencing." https://www.cabdirect.org/cabdirect/abstract/20183194219 (accessed Dec. 14, 2020).
4.	*D. melanogaster*	Identification of genetically different metabolites and metabolomics in context to varying organism's phenotype which helps in understanding the interconnection among genetic variations, metabolites, metabolomics and organism's phenotype.	S. Zhou, F. Morgante, M. S. Geisz, J. Ma, R. R. H. Anholt, and T. F. C. Mackay, "Systems genetics of the Drosophila metabolome," *Genome Res.*, vol. 30, no. 3, pp. 392–405, 2020, doi: 10.1101/gr.243030.118.
5.	*D. melanogaster*	Profiling of FACS sorted hemolectin positive cells which enables new insight to hemocyte functionology and also contributes toward understanding of host defense mechanism and wound healing metabolism.	E. Ramond, J. P. Dudzic, and B. Lemaitre, "Comparative RNA-Seq analyses of Drosophila plasmatocytes reveal gene specific signatures in response to clean injury and septic injury," *PLoS One*, vol. 15, no. 6 June, p. e0235294, Jun. 2020, doi: 10.1371/journal.pone.0235294.
6.	*D. melanogaster*	Demonstration of wild type populations with different geographical origin showing different expression of genes even when maintained under same environmental conditions for about a decade which provides the valuable insight toward the local adaptation processes to varying environmental parameters.	M. Zarubin, A. Yakhnenko, and E. Kravchenko, "Transcriptome analysis of *Drosophila melanogaster* laboratory strains of different geographical origin after long- term laboratory maintenance," *Ecol. Evol.*, vol. 10, no. 14, pp. 7082–7093, Jul. 2020, doi: 10.1002/ece3.6410.
7.	3 - *Drosophila* sp. (*D. melanogaster, D.pseudoobscura* and *D. simulans*)	Identification of Adenosine-to-inosine RNA-edited sites of brain among males and females of three Drosophila species at varying temperature ranges. The study also highlights the expression of Adar gene along with expression profiling of full set of genes with edited sites being favored by the phenomenon of natural selection- serves globally an important role for editomes at different development stages of *D.*	P. Bansal, J. Madlung, K. Schaaf, B. Macek, and F. Bono, "An interaction network of RNA-binding proteins involved in Drosophila oogenesis," *bioRxiv*. bioRxiv, p. 2020.01.08.899146, Jan. 09, 2020, doi: 10.1101/2020.01.08.899146.

		melanogaster which brings insight towards evolutionary concepts and functional significance to RNA editing.	
8.	*D. melanogaster*	Analyses the gene expression profiling towards insecticides which facilitates the prediction of binding sites for xenobiotic and cap-n-collar transcriptional regulator and also, the identification of regions with flanking transposable elements insertion signifying the contributive role of transposable elements on the expression pattern of genes in response to the exposure of insecticides through rewiring of cis-regulatory networks.	J. Salces-Ortiz, C. Vargas-Chavez, L. Guio, G. E. Rech, and J. González, "Transposable elements contribute to the genomic response to insecticides in Drosophila melanogaster," *Philos. Trans. R. Soc. B Biol. Sci.*, vol. 375, no. 1795, Mar. 2020, doi: 10.1098/rstb.2019.0341.
9.	*D. suzukii* (females)	Inter-disciplinary approach of transcriptomics and proteomics study aims to identify the adult reproductive genes and proteins related to "diapause" which provides platform for future research on molecular mechanisms regulating reproductive process of diapause in economically key insects.	Y. Zhai *et al.*, "Quantitative proteomic and transcriptomic analyses of metabolic regulation of adult reproductive diapause in Drosophila suzukii (Diptera: Drosophilidae) females," *Front. Physiol.*, vol. 10, no. APR, 2019, doi: 10.3389/fphys.2019.00344.
10.	5 - *Drosophila* sp. (*D. melanogaster, D. simulans*, *D. sechellia*, *D. erecta* and *D. elegans*)	Nutritional profiling, larval growth patterns and also, on their transcriptional and metabolic profiling w.r.t to different feeding patterns among five species which are further subdivided under two categories: i) generalist-capable to adapt at different food resources and includes *D. melanogaster, D. simulans* ii) specialist-capable to adapt at only specific diets and includes *D. sechellia*, *D. erecta* and *D. elegans* which signifies that during course of evolution, individuals have gained varying feeding habits which leads to differences in their adaptability patterns in response to diverse ranges of nutrient balance.	K. Watanabe *et al.*, "Interspecies Comparative Analyses Reveal Distinct Carbohydrate-Responsive Systems among Drosophila Species," *Cell Rep.*, vol. 28, no. 10, pp. 2594-2607.e7, Sep. 2019, doi: 10.1016/j.celrep.2019.08.030.
11.	*D. melanogaster*	Sexual traits possessing expression dependency on heightened conditions which provides support and proves the concept of condition dependency that acts as functional unit for genetic quality.	A. Malacrinò, C. M. Kimber, M. Brengdahl, and U. Friberg, "Heightened condition-dependence of the sexual transcriptome as a function of genetic quality in *Drosophila melanogaster* head tissue," *Proc. R. Soc. B Biol. Sci.*, vol. 286, no. 1906, p. 20190819, Jul. 2019, doi: 10.1098/rspb.2019.0819.
12.	*D. melanogaster*	Demonstrate the molecular atlas of first instar larval brain cells and larval brain neural circuits, their biological and developmental organizations. This serves as an important tool for exploring cell diversity and accessing their genetic, molecular and behavioral profiles.	C. B. Avalos, R. Brugmann, and S. G. Sprecher, "Single cell transcriptome atlas of the drosophila larval brain," *Elife*, vol. 8, Nov. 2019, doi: 10.7554/eLife.50354.
13.	*D. melanogaster*	The study uncovers normal ageing phenomenon and age-linked changes of gene expressions in brain and sets base for studies related to ageing and cognitive declination.	R. Pacifico, C. M. MacMullen, E. Walkinshaw, X. Zhang, and R. L. Davis, "Brain transcriptome changes in the aging Drosophila melanogaster accompany olfactory memory performance deficits," *PLoS One*, vol. 13, no. 12, p. e0209405, Dec. 2018, doi: 10.1371/journal.pone. 0209405.
14.	*D. melanogaster* (males)	Functional and anatomical aspect of different parts of the testis which provides complete understanding for coding and non-coding genes involved in the pivotal	V. Vedelek *et al.*, "Analysis of Drosophila melanogaster testis transcriptome 06 Biological Sciences

		stages of spermatogenesis.	0604 Genetics," *BMC Genomics*, vol. 19, no. 1, Sep. 2018, doi: 10.1186/s12864-018-5085-z..
15.	14 - *Drosophila* sp. (*D. sechellia, D. yakuba*, *D. virilis, D. bipectinata, D. biarmipes, D. simulans, D. erecta, D. kikkawai, D. ananassae, D. saltans, D. willistoni, D. mojavensis D. melanogaster D. austrosaltans)*	Examination of life history traits and exploration of transcriptomic analysis for divergent expression patterns, genes identification and processes that co-relates with longevity which enables understanding that lifespan is governed by complex system levels and is controlled globally through their overall gene expression levels rather than expression levels of individual gene.	S. Ma *et al.*, "Comparative transcriptomics across 14 Drosophila species reveals signatures of longevity," *Aging Cell*, vol. 17, no. 4, Aug. 2018, doi: 10.1111/acel.12740.
16.	9 - *Drosophila* sp. (*D. yakuba, D. ananassae, D. persimilis, D. willistoni, D. mojavensis, D. virilis, D. melanogaster, D. pseudoobscura D. grimshawi*)	Vast expression profiling dataset for 9 Drosophila species and to train the assembly of RNA genome through *D. melanogaster* with best matched approach of curated annotation which provides inter-disciplinary approach for understanding key similarities and differences among important model organisms group. Also, emphasizes on significance of annotation through the perspective of future genomes w.r.t tree of life.	H. Yang *et al.*, "Re-annotation of eight Drosophila genomes," *Life Sci. Alliance*, vol. 1, no. 6, Dec. 2018, doi: 10.26508/lsa.201800156.
17.	*D. melanogaster*	Profiling and characterization of three groups of different circardian brain neurons and their molecular contents on basis of: what they comprise and how they differentiate. The findings allow understanding for expression analysis and regulatory principles governing distinct transcript oscilliations including both known and assumed novel neural peptides.	K. C. Abruzzi *et al.*, "RNA-seq analysis of Drosophila clock and non-clock neurons reveals neuron-specific cycling and novel candidate neuropeptides," *PLOS Genet.*, vol. 13, no. 2, p. e1006613, Feb. 2017, doi: 10.1371/journal.pgen.1006613.
18.	*D. melanogaster*	Identification of differential expression patterns and edited sites among flies in response to different microclimates causing genetic differences and emphasizes on the use of CRISPR mutagenesis technology for validating the intronic SNP at edited levels of prominin gene. Also, the study represents the temperature effects on edited levels other than the sites with genetic differences and shows inter-connection	A. L. Yablonovitch *et al.*, "Regulation of gene expression and RNA editing in Drosophila adapting to divergent microclimates," *Nat. Commun.*, vol. 8, no. 1, Dec. 2017, doi: 10.1038/s41467-017-01658-2.

		among genetics, gene expression patterns and RNA edited levels providing a platform for future researches working on adaptive patterns for gene regulation and differences in RNA edited levels.	
19.	*D. melanogaster*	Determination of the splicing rates genome wide and to understand how splicing depends upon exon-intron length and recognition modes for splicing sites through RNA-seq/metabolic labelling and mathematical advanced models which sets platform for future studies based on splicing rates and splicing machinery focusing on cells with developmental cellular shifts and responses mounting on transcriptional productions.	A. A. Pai, T. Henriques, K. McCue, A. Burkholder, K. Adelman, and C. B. Burge, "The kinetics of pre-mRNA splicing in the Drosophila genome and the influence of gene architecture," *Elife*, vol. 6, Dec. 2017, doi: 10.7554/eLife.32537.
20.	*D. melanogaster*	Highly expressed, long and heavily spliced genes show a bias towards downregulation while circRNA levels increase strongly with age, suggesting that other gene expression mechanisms become altered with age.	Hall, H., Medina, P., Cooper, D.A. et al. Transcriptome profiling of aging Drosophila photoreceptors reveals gene expression trends that correlate with visual senescence. BMC Genomics 18, 894 (2017). https://doi.org/10.1186/s12864-017-4304-3
21.	*D. melanogaster*	Analyses about the differential developmental patterns and roles of the ring gland. Particularly focusses on pathways of gene which were not so far linked to ring gland w.r.t immune system and fatty acid metabolism which enables the valuable insight towards identification of novel roles being played by ring gland in diverse insect developmental signaling and processing.	D. Christesen *et al.*, "Transcriptome analysis of Drosophila melanogaster third instar larval ring glands points to novel functions and uncovers a cytochrome p450 required for development," *G3 Genes, Genomes, Genet.*, vol. 7, no. 2, pp. 467–479, 2017, doi: 10.1534/g3.116.037333.
22.	*D. melanogaster* (males)	Estrogenic effects of ethylparaben (EP) on development, lifespan and reproduction which provides future insights into the cellular, molecular and biochemical assays in response to different toxicity levels of EP among humans.	P. Xue, X. Zhao, M. Qin, Z. Shi, M. Zhang, and W. Gu, "Transcriptome Analysis of Male Drosophila melanogaster Exposed to Ethylparaben Using Digital Gene Expression Profiling," *J. Insect Sci.*, vol. 17, no. 4, Jul. 2017, doi: 10.1093/jisesa/iex050.
23.	Group of *Drosophila* females	Identification of novel genes in memory and learning regulation among mushroom body through single cell-type RNA-seq effective method which provides support for further understanding of varying patterns of memory and learning regulation in respect to varying expression levels of genes among particular neurons.	A. Crocker, X. J. Guan, C. T. Murphy, and M. Murthy, "Cell-Type-Specific Transcriptome Analysis in the Drosophila Mushroom Body Reveals Memory-Related Changes in Gene Expression," *Cell Rep.*, vol. 15, no. 7, pp. 1580–1596, May 2016, doi: 10.1016/j.celrep.2016.04.046.
24.	*D. melanogaster*	Identification of extracellular vesicles and defining of ex-RNA associated repertories among human and *Drosophila* which reveals significant similarities throughout extracellular vesicles among distant metazoans and provides platform for future studies on "loss of function".	F. A. Lefebvre *et al.*, "Comparative transcriptomic analysis of human and Drosophila extracellular vesicles," *Sci. Rep.*, vol. 6, Jun. 2016, doi: 10.1038/srep27680.
25.	*D. melanogaster*	Molecular and biological analysis of changes with respect to gravity at pupal stage which provides better vision for future studies on understanding the mechanism of gravity in basic patterns of developmental biology.	S. Hateley, R. Hosamani, S. R. Bhardwaj, L. Pachter, and S. Bhattacharya, "Transcriptomic response of Drosophila melanogaster pupae developed in hypergravity," *Genomics*, vol. 108, no. 3–4, pp. 158–167, Oct. 2016, doi: 10.1016/j.ygeno.2016.09.002.

26.	*D. melanogaster* (females)	Profiling of lncRNA and mRNA transcriptome at i) dietary restricted conditions and ii) fully-fed conditions which emphasizes towards close association among dietary patterns and lncRNAs. The study also highlights the important role of lncRNAs in ageing and age-linked diseases.	D. Yang *et al.*, "LncRNA mediated regulation of aging pathways in Drosophila melanogaster during dietary restriction," *Aging (Albany. NY).*, vol. 8, no. 9, pp. 2182–2203, 2016, doi: 10.18632/aging.101062.
27.	*D. pseudoobscura*	Identification and annotation of the intergenic long non-coding RNAs. Also, sex-specific lncRNAs were characterized throughout entire genome. Lastly, identified lncRNAs of *D. pseudoobscura* cross-referred to *D. melanogaster* and homologous lncRNAs which directs upon evolutionary theorems and facilitates the genus-based comparisons.	K. G. Nyberg and C. A. Machado, "Comparative expression dynamics of intergenic long noncoding RNAs in the genus drosophila," *Genome Biol. Evol.*, vol. 8, no. 6, pp. 1839–1858, 2016, doi: 10.1093/gbe/evw116.
28.	*D. melanogaster*	Analyze the different set of development stages, dissected organs and environmental changes in context to their ploy A+ RNA seq data which enables understanding on complexity level of transcriptomics w.r.t mRNA and ncRNA of different tissues and their specific conditions. Also,the study highlights on metazoan biology.	J. B. Brown *et al.*, "Diversity and dynamics of the Drosophila transcriptome," *Nature*, vol. 512, no. 7515, pp. 393–399, Aug. 2014, doi: 10.1038/nature12962.
29.	*Drosophila* stocks	Prediction of the insulin producing cells component of the brain that regulates the production of insulin like peptides (ILPs) which emphasis on the important aspect of ILPs in growth patterns and metabolic regulations. Flies ILPs works as functional analogous for mammalian insulin like growth factors and parameters.	J. Cao *et al.*, "Insight into insulin secretion from transcriptome and genetic analysis of insulin-producing cells of Drosophila," *Genetics*, vol. 197, no. 1, pp. 175–192, 2014, doi: 10.1534/genetics.113.160663.
30.	*D. melanogaster*	Functional interaction of mechanisms involved in RNAi with polycomb group pathways and shows that RNAi (Dicer-2/Argonaute-2) pathway is replaceable for polycomb regulated silencing of bithorax complex which signifies that mechanisms linked to RNAi in drosophila does not required mainly in regulating gene silencing for endogenous polycomb target position.	F. M. Cernilogar, A. M. Burroughs, C. Lanzuolo, A. Breiling, A. Imhof, and V. Orlando, "RNA-Interference Components Are Dispensable for Transcriptional Silencing of the Drosophila Bithorax-Complex," *PLoS One*, vol. 8, no. 6, Jun. 2013, doi: 10.1371/journal.pone.0065740.
31.	*D. melanogaster* Natural variants (females)	Identification of the candidate gene markers and processes involved behind the cause of extended longevity among starvation resistance flies which enables better knowledge towards changes at transcriptional level due to nutritional effects at diverse ageing lines with diverse age-related phenotypes.	A. Doroszuk, M. J. Jonker, N. Pul, T. M. Breit, and B. J. Zwaan, "Transcriptome analysis of a long-lived natural Drosophila variant: a prominent role of stress- and reproduction-genes in lifespan extension," *BMC Genomics*, vol. 13, no. 1, p. 167, May 2012, doi: 10.1186/1471-2164-13-167.
32	*D. melanogaster*	Transcriptional profiling of brain associated circardian rhythms among wild type and mutant period-null animals which highlights toward regulation of ncRNA expression levels through control mechanism of circardian machinery. Also, further illustrates towards novel splicing events, RNA editing and genome broad mapping of splicing mechanism in brain.	M. E. Hughes, G. R. Grant, C. Paquin, J. Qian, and M. N. Nitabach, "Deep sequencing the circadian and diurnal transcriptome of Drosophila brain," *Genome Res.*, vol. 22, no. 7, pp. 1266–1281, Jul. 2012, doi: 10.1101/gr.128876.111.
33.	*D. melanogaster*	Inspection of 30 different developmental stages which emphasizes towards highly magnified transcriptomic analysis of throughout developmental stages in drosophila and additionally provides an insight to unexplored metazoan development.	B. Graveley, "The developmental transcriptome of Drosophila melanogaster," *Genome Biol.*, vol. 11, no. S1, p. I11, Nov. 2010, doi: 10.1186/gb-2010-11-s1-i11.

34.	*D. melanogaster*	Detailed profiling of transcriptome through advanced RNA-seq technology which signifies on importance of ongoing transcriptomics annotation attempts.	B. Daines *et al.*, "The Drosophila melanogaster transcriptome by paired-end RNA sequencing," *Genome Res.*, vol. 21, no. 2, pp. 315–324, Feb. 2011, doi: 10.1101/gr.107854.110.
35	*D. melanogaster*	In silico analysis of transcriptome of fat body of the flies on the basis of expressed sequence tags (ESTs) which provides understanding for gene expression patterns, functions and possible pathways linked to fats deposit. Through genomics and bioinformatics inter-disciplinary approach *Drosophila* serves as model for studying obesity in humans.	Z. Jiang, X. L. Wu, J. J. Michal, and J. P. McNamara, "Pattern profiling and mapping of the fat body transcriptome in Drosophila melanogaster," *Obesity Research*, vol. 13, no. 11. North American Assoc. for the Study of Obesity, pp. 1898–1904, 2005, doi: 10.1038/oby.2005.233.

Acknowledgment: The authors thank the Vice Chancellor, JIIT for extending facilities for carrying out the present work.

References: Adams, J., 2008, Nature Education 1(1): 195; Dong, Z., and Y. Chen 2013, Sci. China Life Sci. 56(10): 960-7; Evans, T.G., 2015, J. Exp. Biol. 218(12): 1925-35; Gasser, B., *et al*., 2007, Appl. Environ. Microbiol. 73(20): 6499-507; Kukurba, K.R., and S.B. Montgomery 2015, Cold Spring Harb. Protoc. 11: 951-69; Lowe, R., *et al*., 2017, PLoS computational biology 13(5): 1-23; Manzoni, C., *et al*., 2018, Briefings in Bioinformatics 19(2): 286-302; Mirzoyan, M., *et al*., 2019, Front. Genet. 10(51): 1-16; Pandey, U.B., and Charles D Nichols 2011, Pharmacol. Rev. 63(2): 411-36; Rathke, A.P., *et al*., 2013, Pacific Symposium on Biocomputing 150-70; Ugur, B., *et al.*, 2016, Disease Models & Mechanisms 9: 235-44; Wang, Z., *et al*., 2009, Nat. Rev. Genet. 10: 57-63; Zhao, S., *et al*., 2014, PLoS One 9(1): 1-13.

Assessment of *Drosophila* muscle elasticity using dual Brillouin-Raman microspectroscopy.

Cheburkanov, Vsevolod[1*], Paulino Alicia[2*], Andrew Doan[2*], Vladislav V. Yakovlev[1#], and Vlad Panin[2#]. [1]Departments of Biomedical Engineering and [2]Department of Biochemistry and Biophysics, Texas A&M University, College Station, TX 77843. *Equal contribution authors. [#]Corresponding authors: yakovlev@tamu.edu and panin@tamu.edu

Abstract

Muscular dystrophy is a genetic disorder associated with the degeneration of skeletal muscles. *Drosophila* has been used as a model to study pathogenic mechanisms caused by defects in homologues of human genes affected in muscular dystrophies. One of the sensitive parameters of muscle physiology that can potentially be used to assess the muscular dystrophy phenotype is tissue elasticity. However, previously used approaches provided only indirect information about that characteristic. Here we describe the analysis of the muscle elasticity of live third instar *Drosophila melanogaster* larvae. We developed a method to image larval muscles using a dual Raman and Brillouin spectroscopy technique. Our experiments provided proof-of-principle results that demonstrated that the method can be applied for live analysis of muscle elastic properties without significant damage to the organism. Our new approach can be used in further studies to analyze muscle elasticity phenotypes in *Drosophila* models of muscular dystrophy and other neuromuscular abnormalities that may affect muscle physiology.

Introduction

Drosophila melanogaster is commonly used as a model organism to study pathogenic mechanisms of human disorders, including various forms of neuromuscular diseases, such as muscular dystrophy. Our

previous studies demonstrated that defects in protein O-mannosylation that cause most severe forms of muscular dystrophy termed dystroglycanopathies could be modelled and investigated using mutations in fly orthologues of human genes affected in these congenital disorders (Nakamura *et al.,* 2010). Although muscle degeneration is not the most prominent phenotype in *Drosophila* models of dystroglycanopathies (Baker *et al.,* 2018), mutations in *Dystroglycan* and *Drosophila Protein O-Mannosyltransferase* (*POMT*) genes, *rotated abdomen* and *twisted*, appear significantly to affect muscle elastic properties. Muscle stiffness was assessed in these mutants using fluorescent microscopy of fixed larval muscles based on the size of phalloidin-stained sarcomeres (Haines *et al.,* 2007). However, this approach showed variable genotype-phenotype correlation, suggesting that muscle fixation may have caused possible artifacts. Furthermore, that method did not provide direct information on muscle elasticity, and the relationship between the sarcomere size and muscle stiffness remains not fully understood. Thus, with the goal to examine muscle elastic properties *in vivo* and more directly, we decided to develop a method using Brillouin spectroscopy that was shown to be useful for the analysis of elasticity of live tissues and cells (Prevedel *et al.,* 2019).

Brillouin scattering is a phenomenon of non-linear interaction between incident electromagnetic radiation and acoustic phonons in the material of interest. This process yields a frequency shift in the incident electromagnetic wave of a magnitude directly proportional to the speed of sound in the medium. Elastic modulus (also known as Young's modulus) of the medium is directly related to the speed of sound, making it possible to determine the former by measuring the Brillouin shift in the spectrum. Materials of greater stiffness are known to display higher speed of sound in their bulk, meaning that Brillouin shift value is greater for such samples. In our previous experiments, we analyzed tissue elasticity of melanoma (Troyanova-Wood *et al.,* 2019) and adipose tissues (Troyanova-Wood *et al.,* 2017). Here we describe the adaptation of our approach to the analysis of *Drosophila* muscles.

Materials and Methods

Drosophila *strain*

We used a fly strain with transgenically expressed Myosin Heavy Chain–GFP (MHC-GFP) that has GFP expression in all muscles (Figure 1) (Hughes and Thomas 2007).

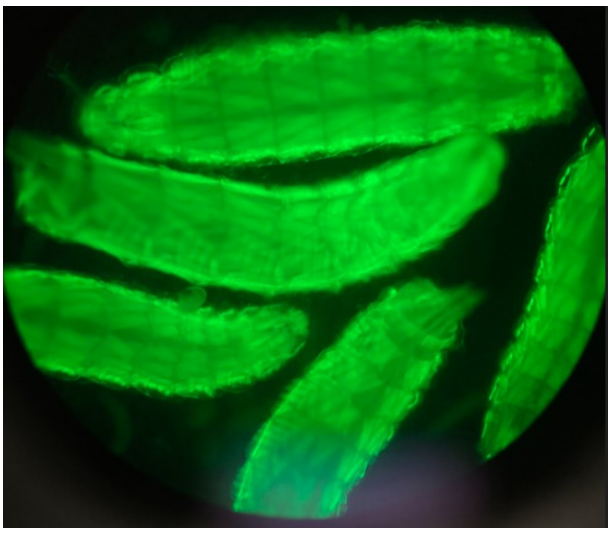

Figure 1. Fluorescent image of live third instar larvae with MHC-GFP expression that labels all body wall muscles.

Immobilization of larvae

FlyNap was purchased from Carolina Biological Supply Company, NC. Chloroform vapor method was developed based on previously described protocol (Cevik *et al.*, 2019).

Fluorescent microscopy and detection

Live imaging of GFP-expressing muscles was carried out using Zeiss Axioplan 2 fluorescent microscope equipped with Axiocam MRM-HR digital camera (Figure 1). GFP fluorescence was detected in custom-made Raman-Brillouin instrument by a fluorescence module using a 473 nm DPSS laser for excitation and a 482 nm long-pass filter (Semrock Inc., BLP01-473R-25) for emission detection (Figure 2).

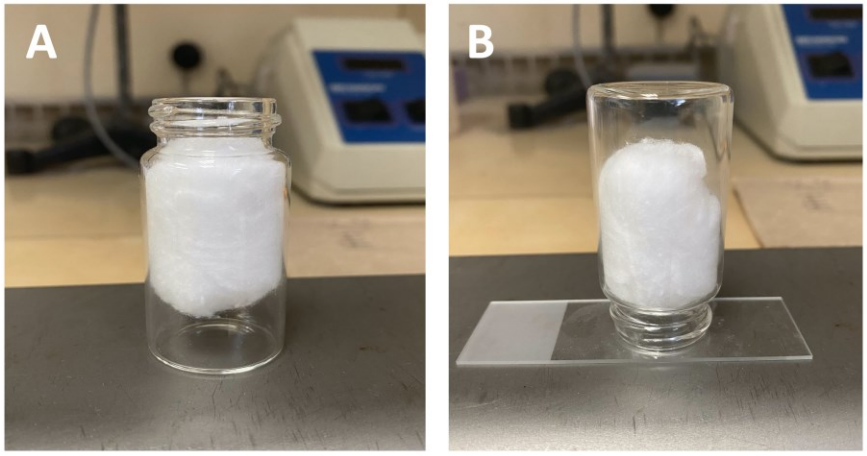

Figure 2. Chloroform vapor chamber. A, a scintillation vial with cotton ball inside was used to expose larvae to chloroform vapor. B, exposing larvae on a slide to chloroform vapor.

Raman and Brilouin spectroscopy

A custom-made instrument was assembled and used essentially as described before (Ballmann *et al.,* 2015) with some modification.

Results and Discussion

Immobilization of larvae

With the goal to immobilize *Drosophila* third instar larvae without affecting their viability and further development, we tested several methods, including cooling to 0^{o}C (ice-cold temperature), FlyNap anesthetizer, and chloroform vapor. Only the latter method developed based on previously published protocol (Cevik *et al.,* 2019) with some modifications provided satisfactory results, reliably eliminating muscle contractions for up to 40 minutes without causing significant post-assay mortality or noticeable developmental defects. In our experiments, we isolated several late-third instar larvae from food medium by washes in ice-cold PBS, placed one to four larvae on a PBS-wetted glass slide, and then quickly pipetted 500 µL of chloroform onto a pre-assembled vapor chamber made of a scintillation vial with an inserted cotton ball positioned 12 mm away from the opening (Figure 2A). The vapor chamber is then immediately placed upside down onto the slide to cover the larvae (Figure 2B). We tried different exposure times and combinations of exposures to chloroform vapor. After trial and error, we settled on the optimized protocol with an intermittent exposure, including placing the scintillation vial with the chloroform over the larvae for 30 seconds and then letting larvae to recover without chloroform for 3 seconds, while repeating this for a total of five times.

Dual Brillouin-Raman confocal spectrometer

To determine elastic properties of the larvae muscles a special optical setup was assembled (Figure 3). Laser radiation was generated using subassembly A , where 1 is a 532 nm composite laser source, 2 is a half wave plate, 3 is a polarizing beam splitter cube and 4 is a quarter wave plate. Rotation of 2 allows for power adjustment at the sample stage. And part 4 allows backscattered light to be diverted to the confocal pinhole part of the setup. Subassembly B is a periscope that delivers laser radiation to the sample plane, and doubles as a widefield microscope with the blue (473 nm) laser 5 acting as a light source, and CMOS 8 acquiring the image. Scattered light from the sample is collected using the objective 6 and is split on a dichroic mirror 7. Collected signal is then directed to the confocal pinhole assembly C, where out-of-plane scattered light is blocked by means of a spatial filter. Dichroic mirror 10 splits signal at 550 allowing for 532 nm component to

be processed in the Brillouin spectrometer 11 of module D, and components beyond 550 nm to be processed in a Raman spectrometer 12 of module E.

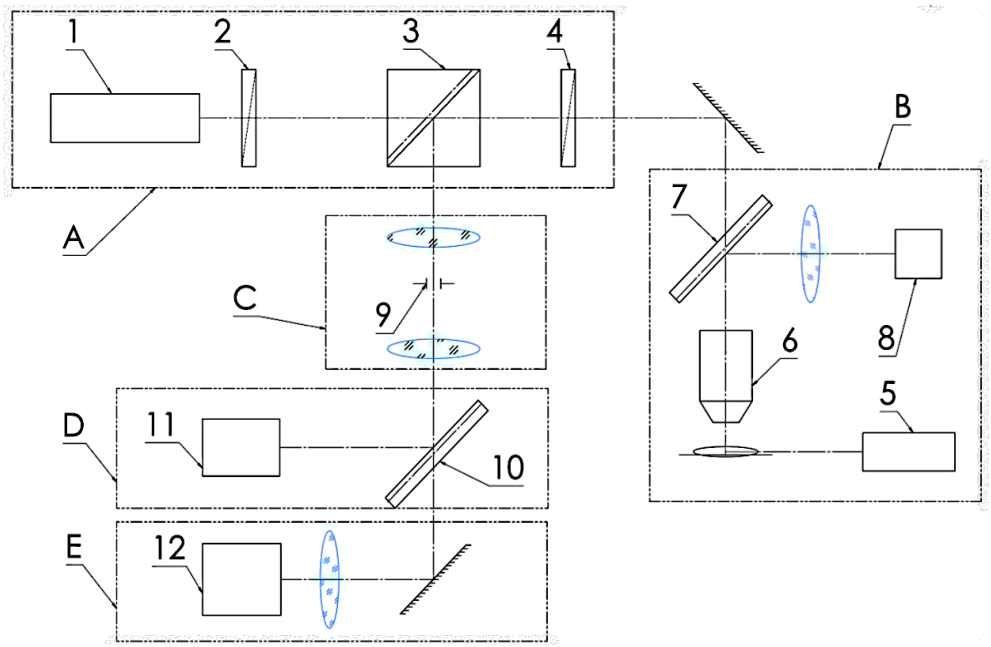

Figure 3. Schematic of dual Brillouin-Raman confocal spectrometer. The instrument consisted of five major modules: a 532 nm laser (A), an objective arm for recording epi-fluorescence images (B), a confocal pinhole assembly (C), a custom built VIPA-based spectrometer for Brillouin spectra acquisition (D), and a commercial spectrometer for Raman spectra acquisition (E).

Our dual confocal spectrometer system provides an important advantage over a single-channel Brillouin instrument by allowing to monitor the position inside the organism by Raman spectroscopy that can discriminate between different tissues based on their composition (Meng *et al.,* 2016). For example, muscles and cuticle can be easily distinguished based on their Raman spectra.

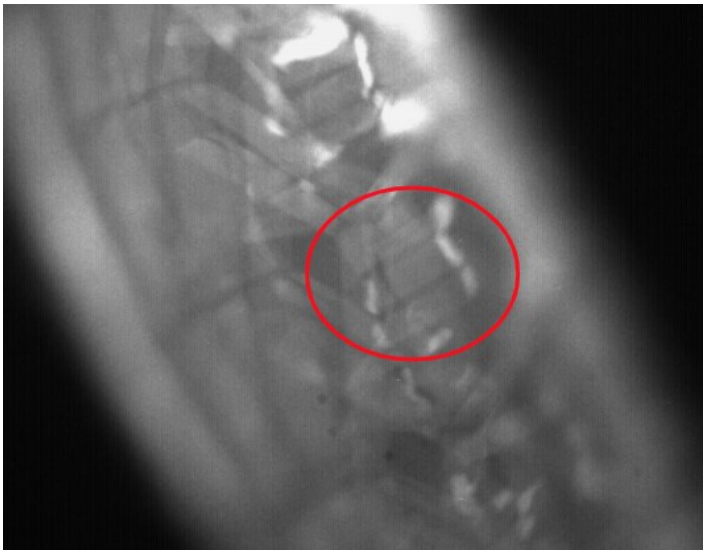

Figure 4. Muscles visualized in live larvae using GFP fluorescence. The image was obtained using low magnification (3.3×). Lateral transverse muscles 1-3 are circled.

Data acquisition and analysis

Chloroform-anesthetized larvae were placed on the 3-axis scanning table and illuminated with 473 nm laser. A low magnification objective was used first for adjusting the sample Z-position to bring muscles into the focal plane for spectral analyses. We focused on lateral transverse muscles 1-3 in abdominal segments 2-5 (Figure 4), as they are relatively big and located closely to the body wall, which makes them readily available

for spectral analyses. These muscles are easy to identify as they appear as stereotypically repeating bands perpendicular to the larvae's long axis located at the lateral sides of abdominal segments. To verify position on the muscle both Raman and Brillouin spectra were acquired simultaneously and later processed together (Figure 5).

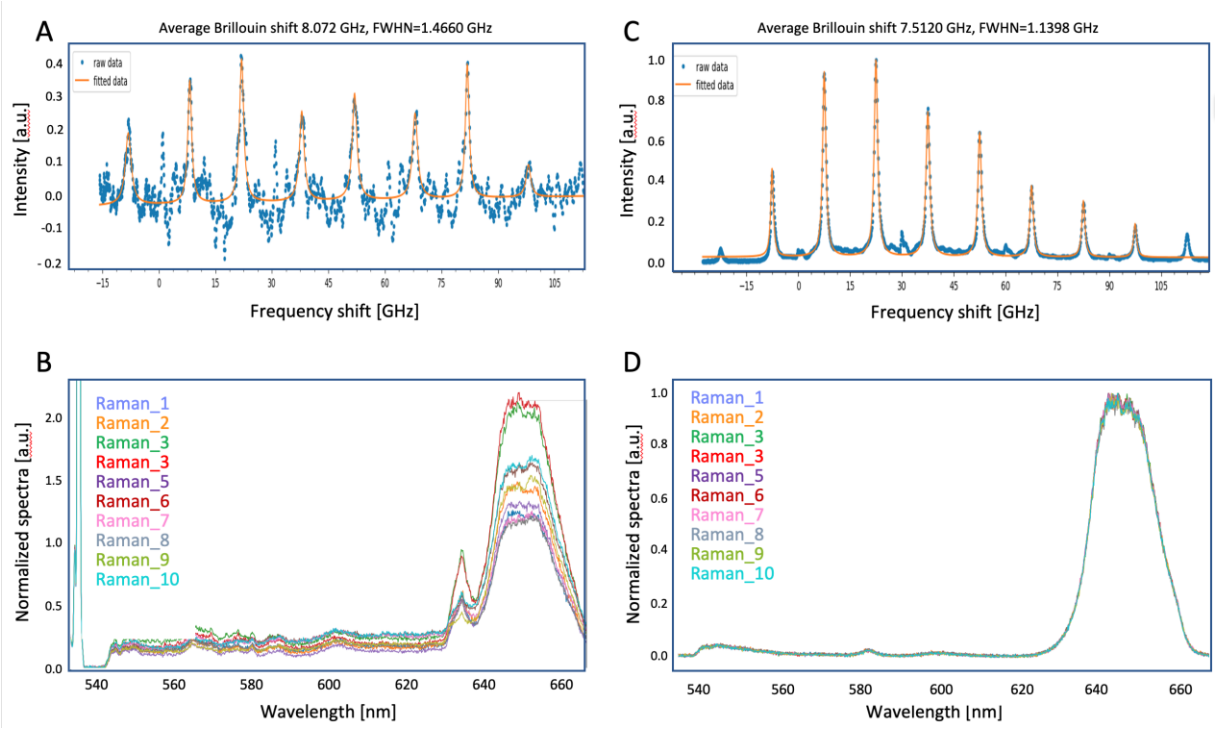

Figure 5. Examples of Brillouin (A, C) and Raman (B, D) spectra that were acquired from an abdominal lateral transverse muscle (A, B) and PBS (C-D) as a control. (A, C) Spectra were acquired at 2 sec acquisition time. Baseline removal (resulted in negative values in A) and Lorentzian fit were applied, and pixel values were converted to frequency shift units. Increased Brillouin shift in (A) indicates higher stiffness of muscles as compared to surrounding saline. (B, D) Raman spectra were acquired at 10 sec acquisition time using a 10× objective with 2 µm axial resolution/ 6 µm step size. Raman spectra 3 and 4 in (B) correspond to the same muscle analyzed for elasticity in (A). 10× magnification objective with 0.25 NA was used in all experiments, however, spatial resolution can be further increased by using a higher magnification objective (*e.g.*, 20× with 0.5 NA).

Concluding remarks

Here we designed and tested an approach to examine muscle elasticity of live *Drosophila* larvae. The approach is based on Brillouin spectroscopy that can provide a non-invasive and non-contact approach for fast and accurate volumetric elasticity mapping. In our proof-of-principle experiments, we used larvae with the transgenic expression of GFP that facilitated focusing on specific muscles. The method can be adjusted for analyses of muscles without GFP labeling as muscles can be visualized using regular light microscopy techniques, while finding a desired focal plane can be facilitated by confocal Raman spectra providing information on tissue composition. Our larva immobilization protocol eliminates muscle movements without noticeable side effects, such as abnormal contractions or twitching. However, currently we cannot exclude some conceivable side effects of chloroform vapor exposure on muscle physiology that may affect elasticity. Thus, additional experiments are needed to test for these potential artifacts. Finally, our method could provide very consistent measurements of muscle elasticity, with the variability of Brillouin shift obtained from 10 different larvae was found to result in the standard error of the mean of 2.24%. While this approach is

expected to be sensitive enough to analyze changes in muscle elasticity caused by degeneration, further studies are required to determine the correlation between elasticity and congenital muscle abnormalities.

Acknowledgments: We are grateful to Cynthia Hughes for MHC-GFP flies. The authors wish to thank Dr. Ishita Chandel for sharing expertise in immobilization and live imaging of *Drosophila* larvae. This work was funded in part by a grant from NIH (NS099409) and NIFA (TEX0-1-8950) to VP and from NSF (DBI-1455671, ECCS-1509268, CMMI-1826078), AFOSR (FA9550-15-1-0517, FA9550-18-1-0141, FA9550-20-1-0366, FA9550-20-1-0367), Army Research Laboratory (ARL) (W911NF-17-2-0144), the Office of Naval Research (ONR) (N00014-16-1-2578), NIH (1R01GM127696-01), AFRL SFFP, and the Cancer Prevention and Research Institute of Texas (RP180588) to VVY, and a T3 grant from TAMU (246491) to VP & VVY.

References: Baker, R., N. Nakamura, I. Chandel, B. Howell, D. Lyalin, and V.M. Panin 2018, J. Neurosci. 38(7): 1850-1865; Ballmann, C.W., J.V. Thompson, A.J. Traverso, Z. Meng, M.O. Scully, and V.V. Yakovlev 2015, Sci. Rep. 5: 18139; Cevik, D., M. Acker, P. Arefi, R. Ghaemi, J. Zhang, P.R. Selvaganapathy, I. Dworkin, and J.R. Jacobs 2019, J. Insect Physiol. 117: 103900; Haines, N., S. Seabrooke and B.A. Stewart 2007, Mol. Biol. Cell 18(12): 4721-4730; Hughes, C.L., and J.B. Thomas 2007, Mol. Cell. Neurosci. 35(2): 383-396; Meng, Z., S.C. Bustamante Lopez, K.E. Meissner, and V.V. Yakovlev 2016, J. Biophotonics 9(3): 201-207; Nakamura, N., D. Lyalin. and V.M. Panin 2010, Semin. Cell Dev. Biol. 21(6): 622-630; Prevedel, R., A. Diz-Munoz, G. Ruocco, and G. Antonacci 2019, Nat. Methods 16(10): 969-977; Troyanova-Wood, M., C. Gobbell, Z. Meng, A.A. Gashev, and V.V. Yakovlev 2017, J. Biophotonics 10: 1694; Troyanova-Wood, M., M. Zhaokai, and V.V. Yakovlev 2019, Biomed. Opt. Express 10: 1774-1781.

New Book Announcement

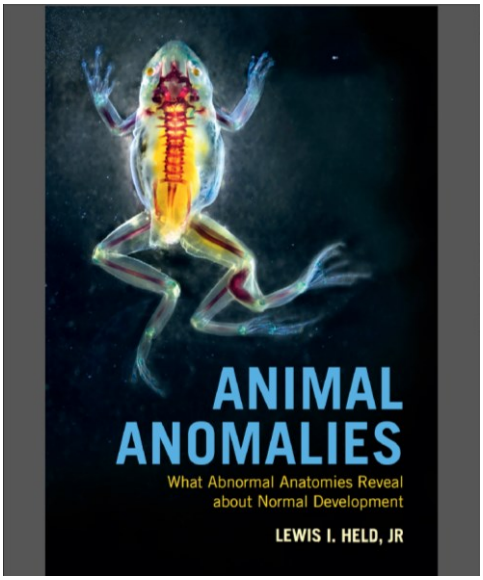

Animal Anomalies: What Abnormal Anatomies Reveal about Normal Development

Held, Lewis I., Jr. 2021. Cambridge University Press. ISBN 978-1-108-83470-4 Hardback; ISBN 978-1-108-81974-9 Paperback

Geneticists should be familiar with the approach of learning about normal gene function by studying mutations. We deduce normal function by studying the consequences of things going wrong. But it is easy to forget the power of insight that comes from that simple perspective. In this wonderful exploration of development, Lewis Held uses both familiar and less-well-known examples of frogs, flies, dogs, and cats to delve deeply into the underlying biological principles their traits can illustrate.

Let's look at an example or two. Rather than overwhelming the reader with a lot of technical terminology, the primary light is directed on key principles. But scientific precision is not traded for ease of accessibility. The focus is the connections that are made. For example, the four wings in flies carrying *bithorax* led to discovery of the Hox gene complex that defines anterior-posterior body axis throughout the animal kingdom. It is hard to predict where an interesting anomaly might lead. Held also describes the genetic basis of traits that pet-owners find endearing. Short legs of the Dachshund, the bulldog's underbite, a Dalmatian's spots, and the loss of hair in Mexican hairless dogs show the power of selective breeding, a process that differs from natural selection primarily due to the intentions, or perhaps sometimes the sense of humor, of the breeder. In addition to this fascinating exploration of genetic mechanisms and their outcomes is another idea that I have always valued in Lewis Held's work: the respect for pioneering insights and discoveries by earlier researchers like Curt Stern, Walter Gehring, Ernst Hadorn, and others. I remember hearing a faculty advisor once criticize a new graduate student for planning to cite a research article that was more than a couple years old as being irrelevant to "modern research". Thankfully, writers like Held remind us that the story of discovery is a long one, and critical insights can come from anywhere.

Jim Thompson, Editor, DIS

Teaching Notes

Influence of stress on the somatic movement of the *mariner* DNA element in *Drosophila simulans*: II. Crowding with *Drosophila melanogaster*.

Borowski, Nicole M., Michael A. Balinski, and R.C. Woodruff. Department of Biological Sciences, Bowling Green State University, Bowling Green, Ohio 43403.

The transposable *mariner* DNA element can move in *Drosophila simulans* causing mosaic spots in the eyes of flies that have the *mariner*-inserted w^{pch} (white peach) X-chromosome mutation (see reviews of this topic in Hartl, 1989; Chakrani *et al*., 1993; Nikitin and Woodruff, 1995; Robertson, 1995; Russell and Woodruff, 1999; Woodruff and Thompson, 2001; Pereira *et al*., 2018). In this study, we sought to determine if crowding of w^{pch} *D. simulans* with *D. melanogaster* increases the movement of the *mariner* DNA element. Crowding has been observed to affect life-history traits and fitness (Hoffman and Parsons, 1991; Imasheva and Bubliy, 2003; Klepsatel *et al*., 2018; Miller *et al*., 2019). Other stressors, such as increased temperature and irradiation, have also been shown to increase the rate of movement of DNA elements like *mariner* (Eeken and Sobels, 1986; Hoffman and Parsons, 1991; Arnault and Dufournel, 1994; Giraud and Capy, 1996; Vasilyeva *et al*., 1999; Capy *et al*., 2000; Belyayen, 2014; Piacentini *et al*., 2014; Fitzerald *et al*., 2017; Loreto and Pereira, 2017; Pereira *et al*., 2018; Borowski *et al*., 2019).

To measure the influence of interspecies crowding of w^{pch} *D. simulans* with *D. melanogaster* on the excision rate of *mariner* from the w^{pch} mutation, we performed the following crosses. The OK1 *D. simulans* line was established from isofemales collected at the University of Oklahoma Biological Station in May of 2019. The w^{pch} *D. simulans* mutation is caused by a 1,300 base-pair insertion of the *mariner* element, which can be excised out of the white locus by *mariner* transposase (see references and photographs of mosaics in Hartl, 1989; Pereira *et al*., 2018). OBL1&2 is a natural population line derived from *D. melanogaster* females collected in Perrysburg, Ohio on July 30, 2020.

To establish a baseline for the movement of *mariner* in the absence of crowding, we performed the following cross as a control.

P w^{pch} / w^{pch} virgin females × OK1 males

The eyes of F1 w^{pch} males from the P crosses were screened for red mosaic spots in a white-peach background, which are caused by the excision of the *mariner* DNA element from the w^{pch} mutation. It has been previously observed that the w^{pch} stock is stable; no mosaic spots were observed at room temperature among 449 flies (216 w^{pch}/w^{pch} females and 233 w^{pch}/Y males), but that the w^{pch} mutation was very unstable when mated with natural population lines of *D. simulans* (from 30 to 42 percent of progeny had mosaic eye spots) (Borowski *et al*, 2019).

To measure the influence of interspecies crowding on the rate of *mariner* movement, we again performed the above cross, with the addition of four females and four males of the *D. melanogaster* OBL1&2 stock to each vial. The only vials that were counted were those with both *D. simulans* and *D. melanogaster* F1 adults, indicating crowding.

In the control cross without interspecies crowding, we observed 74 males with no mosaic spots and 60 with spots in at least one eye (45% of flies showed spots). In the crowding experiment with *D. melanogaster*, we observed 23 flies with no spots and 41 with spots in at least one eye (64% of flies showed spots). The number of spot-displaying flies in the interspecies crowding experiment was significantly higher (P = 0.006) compared to the non-crowded control.

Hence, we have observed that the stresses of temperature (Borowski *et al,*.2019) and crowding (this study) increases the rate of somatic movement of the *mariner* DNA element from the w^{pch} mutation of *D. simulans*.

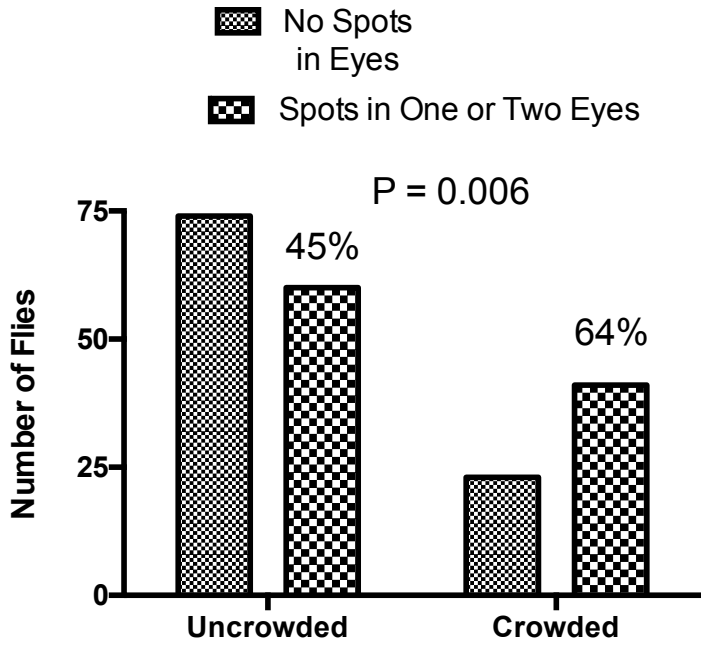

Figure 1. Significant (P = 0.006) increase in mosaic eyes in w^{pch} mutations of *D. simulans* due to movement of the *mariner* DNA element when crowded with *D. melanogaster*.

Since the results of this study confirm that stresses can cause an increase in the rate of movement of the *mariner* DNA element in *D. simulans*, we next intend to test other stressors for their ability to increase the rate of excision of *mariner* elements from the w^{pch} mutation. For example, we will test the ability of copper sulfate to alter the rate of movement of *mariner* in w^{pch} *D. simulans*. Copper sulfate has previously been observed to alter the viability of *D. melanogaster* (Balinski and Woodruff, 2017).

The results of tests of additional stressors on the excision rate of *mariner* will tell us if the mariner/w^{pch} system can be used to identify the presence of stressors in the environment. This is especially important since humans also contain *mariner* DNA elements (Smit and Riggs, 1996; Hartl *et al*., 1997; Hartl, 2001).

A class discussion of the results of this study could include: asking students to go to the literature or internet and find the total number of transposable DNA elements (or the percent of the genome that is transposable elements) in humans, how many of the elements are active and can move, and whether the movement of these elements causes mutations and cancer in humans. For example, students could go to Hancks and Kazazian (2016) and Bourque *et al*. (2018).

References: Arault, C., and I. Dufournel 1994, Genetica 93: 149-160; Balinski, M.A., and R.C. Woodruff 2017, Genetica 145: 131-137; Belyayev, A., 2014, J. Evol. Biol. 27: 2573-2584; Borowski, *et al*., 2019, Dros. Inf. Serv. 102: 83-85; Bourque, G., *et al*., 2018, Genome Biology 19: 199, doi.org/10.1186/s13059-018-1577-z; Capy, P., *et al.,* 1990, Proc. R. Soc. Lond. B 242: 57-60; Capy, P., *et al.,* 2000, Heredity 85: 101-106; Capy, P., and P. Gibert 2004, Genetica 120:5-16; Chakrani, F., P. Capy and J.R. David 1993, Genet. Sel. Evol. 25:121-132; Eeken, J.C.J., and F.H. Sobels 1986, Mutation Research 175: 61-65; Fitzgerald, D.M. *et al*., 2017, Annu. Rev. Cancer Biol. 1: 119-140; Georgiev, P.G. *et al*., 1990, Mol. Gen. Genet. 220: 229-233; Giraud, T., and P. Capy 1996, Proc. R. Soc. Lond. B 263: 1481-1486; Hancks, D.C., and H.H. Kazazian 2016, Mobile DNA 7: 1-28, DOI 10.1186/s13100-016-0065-9; Hartl, D.L., 1987, Annu. Rev. Genet. 31: 337-358; Hartl, D.L., 1989, Transposable element *mariner* in *Drosophila* species. In: *Mobile DNA* (Berg, D.E., and M.M. Howe, eds.). pp. 531-536. American Society for Microbiology, Washington, D.C.; Hartl, D.L., 2001, Genetics 157: 471-476; Hoffman A.A., and P.A. Parsons 1991, *Evolutionary Genetics and Environmental Stress*. Oxford University Press, New York; Imasheva, A.G., and O.A. Bubliy 2003, Hereditas 138: 193-199; Klepsatel, P. *et al*., 2018, Experimental Gerontology 110: 298-

308; Loreto, E.L.S., and C.M. Pereira 2017, Mobile Genetic Elements 7: 1-9 e1314236; Miller, D.M., M.A. Balinski, and R.C. Woodruff 2019, Dros. Inf. Serv. 102: 81-82; Nikitin, A.G., and R.C. Woodruff 1995, Mutation Research 338: 43-49; Pereira *et al*., 2018, Gene 679: 65-72; Piacentini, L. *et al.,* 2014, Chromosoma 123: 345-354; Robertson, H.M., 1995, J. Insect Physiol. 41: 99-105; Russell, A.L., and R.C. Woodruff 1999, Genetica 105: 149-164; Smit, A.F.A., and A.D. Riggs 1996, Proc. Natl. Acad. Sci. USA 93: 1443-1448; Woodruff, R.C., and J.N. Thompson, jr., 2001, Dros. Inf. Serv. 84: 2134-215; Vasilyena, L.A. *et al.*, 1999, Genet. Res., Camb. 74: 111-119.

An undergraduate cell biology laboratory exercise of Nile Red staining to mark lipid droplets in fly eye model of neurodegeneration.

Deshpande, Prajakta[1], Anuradha Chimata Venkatakrishnan[1], and Amit Singh[1,2,3,4,5,6].
[1]Department of Biology, University of Dayton, Dayton, OH 45469, USA; [2]Premedical Program, University of Dayton, Dayton, OH 45469, USA; [3]Center for Tissue Regeneration and Engineering at Dayton (TREND), University of Dayton, Dayton, OH 45469, USA; [4]The Integrative Science and Engineering Center, University of Dayton, Dayton; OH 45469, USA; [5]Center for Genomic Advocacy (TCGA), Indiana State University, Terre Haute, IN, USA; [6]Corresponding Author: Email: asingh1@udayton.edu; Tel: 937-229-2894, Fax: 937-229-2021.

Abstract

The lab exercises for the undergraduate cell biology course have evolved dramatically due to latest developments in the field. In order to provide challenging experiential learning opportunities there is a need to introduce new labs. We have designed a cell biology experiential learning teaching lab to provide a hands-on experience in staining and microscopy with an emphasis on neurodegeneration. In this lab, the undergraduate students learn to visualize the membranes and lipid droplets using easily available dyes and epifluorescence or confocal microscopy. Lipids are an integral part of cells as well as membrane structures. They are present as free lipids in the cytoplasm and sometimes are stored as lipid droplets (LDs) in vesicles. Stressful conditions like diseases or environmental factors can result in the release of lipids that are stored in LDs. These LDs accumulate in the cells, which is toxic to cells. Many Neurodegenerative diseases like Alzheimer's disease, Parkinson's disease etc. exhibit LD accumulation. The Nile Red staining marks the intracellular lipid droplets in *Drosophila melanogaster* retina. Here, we discuss a lab protocol for visualizing LDs in the adult eyes of wild type *Canton-S* control and Alzheimer's disease model of *Drosophila melanogaster*. We have developed this lab to study differences in LDs accumulation and distribution with Nile Red staining and confocal microscopy. **Key words:** *Drosophila melanogaster*, Eye, Nile Red staining, Cell Biology, Confocal Microscopy, lipid droplets.

Introduction

Modern day undergraduate education has incorporated hands-on experience along with teaching key concepts in biology. The experiential learning, which involves the hands-on component, has gained immense importance and emphasis (Puli and Singh, 2011; Tare *et al.*, 2009; Tare and Singh, 2008; Uman and Singh, 2011; Wood, 2009). It is a widely accepted notion that research helps in understanding the concepts in biology, and it provides the application-based understanding (Puli and Singh, 2011; Tare *et al.*, 2009; Tare and Singh, 2008; Uman and Singh, 2011). Thus, research has become an important part of an undergraduate curriculum. Presently, efforts are being directed towards incorporation of biomedical applications in cell biology curriculum including disease models and their cellular and molecular mechanisms. We have developed an undergraduate laboratory to employ Nile Red (also known as Nile blue oxazone) staining to identify accumulation of lipid droplets (LDs), which can serve as one of the biomarkers in the

neurodegenerative tissue. Nile Red is a lipophilic stain, which strongly fluoresces in hydrophobic (lipid-rich) environments and stains intracellular LDs.

The rationale is to introduce the biomedical application of fluorescent staining and epifluorescence or confocal microscopy in the lab curriculum. Generally, immunostaining takes two days followed by imaging. In this lab, adult eyes from Canton-S (wild-type) and flies expressing high levels of amyloid beta 42 (Aβ42) in the differentiating retinal neurons are stained for the lipid droplet (LDs) accumulation using Nile Red staining. It has been reported that accumulation of Aβ42 plaques trigger neurodegeneration (Tare *et al.*, 2011; Yeates *et al.*, 2019). Accumulation of LDs can serve as a biomarker for neurodegeneration (Fam *et al.*, 2018; Liu *et al.*, 2015; Rumin *et al.*, 2015). In this lab, we are using easily accessible adult fly eye retina to demonstrate neurodegeneration by comparing accumulation of LDs by a simple Nile Red staining.

Neurodegeneration can be broadly understood as progressive loss of neuronal structure and function as seen in diseases such as Alzheimer's, Amylotropic Lateral Sclerosis (ALS), Parkinson's, and others. Their onset and progression can be due to various factors ranging from gene mutations to environmental factors. During neurodegeneration, the deterioration of structure and function accompanies the loss of anti-oxidative capacity and increase in ROS production. LDs are recently emerging as a well-studied marker for neurodegeneration (Fam *et al.*, 2018). They are triacylglycerols and cholesterol containing organelles, which are ubiquitously formed from the endoplasmic reticulum membranes. LDs are functionally storage organelles and are required for the maintenance of cellular and energy homeostasis (Olzmann and Carvalho, 2019). In the nervous system, glial cells usually contain LDs and any neuronal dysfunction or neurodegeneration leads to LD accumulation in the glia (Liu *et al.*, 2017; Liu *et al.*, 2015). Therefore, it can be useful to study LD localization and accumulation patterns. Usually, LDs can be detected by fluorometric and calorimetric assays, but to see the localization, various fluorescent dyes and probes have been used, for example, BODIPY 493/503, diazo dyes, Nile Red, Perilipin 2, and so forth (Fam *et al.*, 2018; Listenberger *et al.*, 2016). In this undergraduate cell biology lab, we discuss a protocol for visualizing LDs in *Drosophila melanogaster* adult eyes. This protocol will allow detection of LDs accumulation and distribution with Nile Red staining followed by confocal microscopy. Since LDs are composed of neutral lipids, Nile red is used (Greenspan *et al.*, 1985). Many studies also show that the pathogenesis of Alzheimer's could influence lipid metabolism and lead to LDs accumulation (Farmer *et al.*, 2019; Gomez-Ramos and Asuncion Moran, 2007; Hamilton *et al.*, 2015; Liu *et al.*, 2017). With the increasing focus on studying the interactions between neuronal and glial populations in neurodegeneration, the techniques like Nile Red staining that marks LDs accumulation in the glial cells (Liu *et al.*, 2017), has become a commonly used approach to compare pathological tissues *versus* the healthy tissue.

The protocol for Nile Red staining, which can help visualize the LDs in the adult eye of *Drosophila melanogaster,* has been developed as a laboratory exercise for undergraduate cell biology laboratory. We have used wild-type Canton-S and GMR>Aβ42 flies in this protocol. GMR>Aβ42 is a transgenic neurodegeneration model of Alzheimer's disease where human Aβ42 is misexpressed in the *Drosophila* eye to show a reduced and glazed eye phenotype (Sarkar *et al.*, 2018; Tare *et al.*, 2011; Yeates *et al.*, 2019).

Protocol

The entire protocol can be divided into three major steps, which can be completed in a day: (1) Adult eye dissection, (2) Nile Red staining, (3) Mounting, and Imaging (Figure 1). There is a need to maintain the synchronous cultures of the two fly stocks which are (i) Canton-S and (ii) GMR>Aβ42. The three-day-old adult flies are to be used for the dissection and Nile Red staining. If needed, the older flies can also be used.

Adult eye dissection

We have used *Drosophila melanogaster* (*a.k.a* fruit flies) adult eyes as the tissue source for the Nile Red staining. The fruit flies are easy to rear. A large number of flies can be generated in a smaller time window as life cycle of *Drosophila* is just 12 days long at room temperature (Singh *et al.*, 2012; Tare *et al.*, 2013). We collected 12-15 flies for each genotype. The flies used in our protocol were three days post eclosion flies. The flies were anesthetized on a CO_2 fly pad and stored in cold 1× PBS in a nine well glass plate for 5 minutes. Fly heads were dissected in a drop of cold 1× PBS on a Sylgard plate using dissection forceps. The adult fly retina is present inside the head of the adult fly (Figure 2).

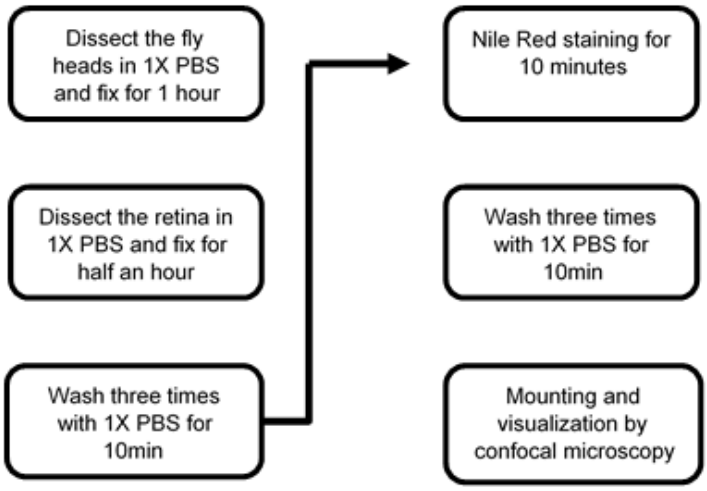

Figure 1. Schematic presentation of time line for Nile Red staining. We have developed a one-day long Nile Red staining protocol for undergraduate laboratory course. This strategy will allow demonstration of this modern-day technique to the undergraduate students.

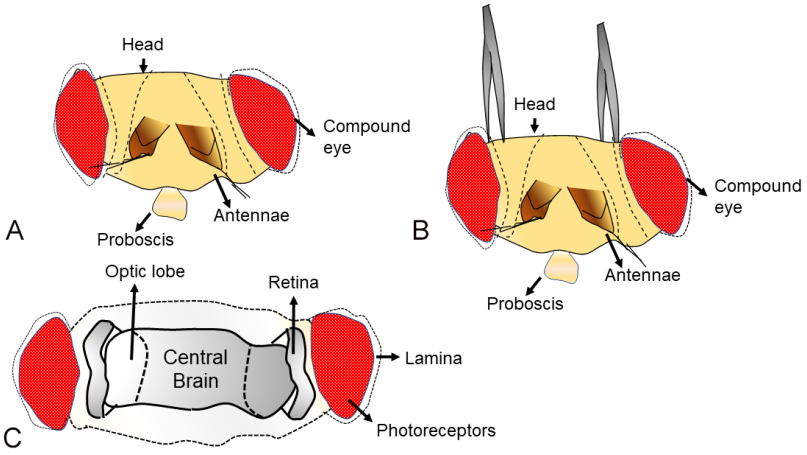

Figure 2. A cartoon showing the dissection of *Drosophila melanogaster* retina from three-day-old adult fly. Cartoon showing (A) Adult fly head, (B) Dissection strategy: places where forceps are employed to remove head cuticle from the fly. (C) The cartoon showing the structure of the adult brain, retina and the optical lobe.

The center of the posterior head capsule was grabbed with forceps and mouthparts (proboscis); fat tissue and tracheae were removed (Figure 2). The fly retina was dissected out along with the brain and then fixed in 4% paraformaldehyde for an hour. The dorsal head cuticle was grabbed with one forceps and the other forceps was used to separate eyes from brain tissue by gently pulling sideways. It is easier to remove the lamina after fixation. The cuticle at the eye margin was removed. The dissected retinae were stored in 1× PBS on ice and then fixed for half an hour in 4% paraformaldehyde. It is critical to make sure the tissue is submerged in the fixative, as it may otherwise not be fixed properly. If necessary, air bubbles are removed with the forceps. Fixative was replaced with 1× PBS. The retinae were then washed three times by 1× PBS

for 10 minutes each (on rotator, at room temperature) to remove any traces of the fixative. The lamina was removed by grabbing it at one side with forceps and gently pulling sideways with the other forceps without injuring the retina. The remaining cuticle was removed as it could fold onto the retina during mounting. These two steps are critical for visualizing photoreceptors, which would otherwise be covered by the lamina and remnants of cuticle during the imaging process.

Nile Red Staining

After fixation, the *Drosophila* retinae were washed with 1× PBS. After washing, the freshly prepared Nile red (1:2000 in 1× PBS) working solution (Table 1) was added to the glass well holding *Drosophila* retinae. The rationale is to replace 1× PBS with Nile Red staining solution. The staining is done in nine well glass plate, which was placed on rotator for 10 minutes. The staining set-up is protected from light by covering with aluminum foil. After 10 min. incubation in Nile Red staining solution, the retinae were washed three times with cold 1× PBS. Precautions are to be taken while washing the retinae to prevent the samples from getting lost.

Table 1. List of reagents and slides used for Nile Red staining laboratory exercise.

Reagents	Composition	Storage
Nile Red (Sigma, Catalogue No: N3013)	1mg Nile Red dissolved in 1ml of DMSO	4°C in dark
1X PBS	1ml of 10X PBS dissolved in 9ml of autoclaved water	Freshly prepared. 4°C
4% Paraformaldehyde	100µl of 16% Paraformaldehyde dissolved in 300 µl of 1X PBS	Freshly prepared.
Vectashield H-1000 (Vector Labs)	commercial preparation, ready to use	4°C in dark
Slides		
Microscope Slides (Fisher Scientific Catalogue No:12-5442)		
Cover Glass (Fisher Scientific Catalogue No:12-548-C)		

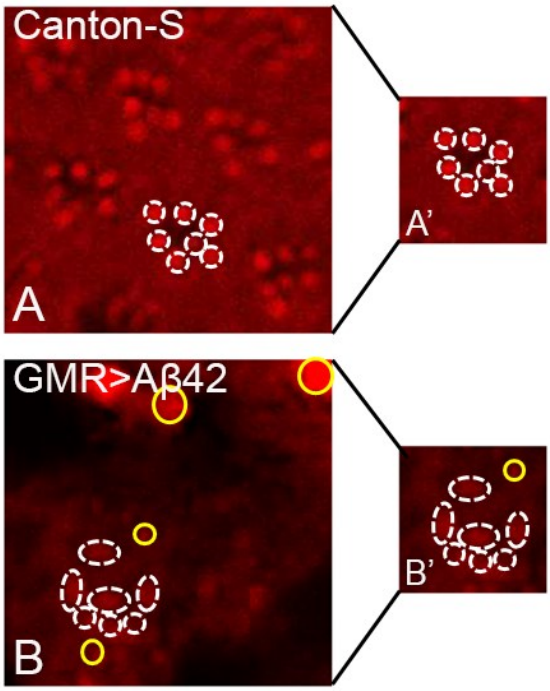

Figure 3. Comparison of Nile Red staining in *Drosophila* adult retina three days post eclosion. (A) Canton-S fly retina serves as the control, (B) and GMR>Aβ42 retina showing neurodegenerative phenotype. Note that no LDs accumulation was seen in control whereas massive amount of LDs accumulation (circled in yellow) is observed in GMR>Aβ42 retina. (A', B') These images are optically zoomed to compare the LD accumulation. LD is accumulated in GMR>Aβ42 as opposed to Canton-S. (A, A') Rhabdomere, which are circled in white, are uniformly arranged whereas (B, B') the rhabdomere are irregularly arranged in GMR>Aβ42 retina.

Mounting and Imaging

On the same day, the stained samples were mounted on a microscopic slide. The retinae were placed on the glass slide (Table 1). The retinae were aligned in order to facilitate imaging. The PBS was removed and Vectashield was added to the sample without drying the samples. The bridge was prepared by keeping the coverslip on both sides of the specimen and then the other coverslip is placed on the top of the bridge. The edges were sealed with transparent nail polish. Images were obtained by Fluoview 3000 confocal microscope. It is advised to take the images soon after mounting of sample on the glass slides as signal is stronger at the time. If the teaching assistant/instructor time schedule does not allow imaging, the slides can be stored at 4°C in a microscope slide box in the dark.

The Nile Red staining (red channel) shows that there is massive accumulation of LDs (circled in yellow) in diseased condition (GMR>Aβ42) as compared to the wild type (Canton-S) (Figure 3). The rhabdomeres (circled in white) serve as a reference point for each ommatidium, are also stained. The rhabdomeres of Canton-S are uniformly arranged as compared to GMR>Aβ42 fly rhabdomeres (Figure 3). This experiment lab will expose students to the cell biology techniques like staining and microscopy as well as the application in disease model by using this simple technique of Nile Red staining.

Advantages

1. Majority of institutions are not willing to implement extensive teaching labs due to financial and time constraints. It is, therefore, important to use cost- and time- effective exercises, which will allow easy implementation of these new labs in the undergraduate lab curriculum. The reagents and glassware (Table 1) used for the Nile Red staining are commercially available and are inexpensive.

2. It is known that experiential learning mode has better retention rates among undergraduate students in comparison to the conventional lecture mode. This teaching note will help provide experiential learning opportunities of the undergraduate students to modern day cell biological technique.

3. Nile Red is a sensitive dye, which can detect the lipid droplets (LDs).

4. This staining protocol is a one-day long and less time consuming for students to complete.

5. Nile Red can be used as a biomarker for studying the lipid accumulation in neurodegenerative diseases.

6. Nile Red staining has also been used for studying LDs and ROS in glial cells.

Conclusion

The use of predesigned kits reduces the basic experiential learning opportunities as well as the exposure of students to the basis behind the technique used. Our laboratory exercises (Puli and Singh, 2011; Tare *et al.*, 2009; Tare and Singh, 2008), including this one, address this problem and are designed to expose students to basic lab skill sets (a) dissections, (b) staining, (c) confocal microscopy. This will improve the skill set of undergraduate students and will help to develop a core of trained individuals suitable for academics or industrial work place settings.

Acknowledgments: This laboratory exercise was designed in the Department of Biology, at the University of Dayton. PD, ACV are supported by graduate program of the University of Dayton. AS is supported by NIH1R15GM124654-01 and Schuellein Endowed Chair in Biology.

References: Fam, T. K., Klymchenko, A. S. and Collot, M. (2018). Materials (Basel) 11; Farmer, B. C., Kluemper, J. and Johnson, L. A. (2019). Cells 8; Gomez-Ramos, P. and Asuncion Moran, M. (2007). J. Alzheimers Dis. 11, 53-59; Greenspan, P., Mayer, E. P. and Fowler, S. D. (1985). J. Cell Biol. 100, 965-973; Hamilton, L. K., Dufresne, M., Joppé, S. E., Petryszyn, S., Aumont, A., Calon, F., Barnabé-Heider, F., Furtos, A., Parent, M., Chaurand, P., *et al.* (2015). Cell Stem Cell 17, 397-411; Listenberger, L. L., Studer, A. M., Brown, D. A. and Wolins, N. E. (2016). Curr Protoc Cell Biol 71, 4 31 31-34 31 14; Liu, L., MacKenzie, K.

R., Putluri, N., Maletić-Savatić, M. and Bellen, H. J. (2017). Cell Metab 26, 719-737.e716; Liu, L., Zhang, K., Sandoval, H., Yamamoto, S., Jaiswal, M., Sanz, E., Li, Z., Hui, J., Graham, B. H., Quintana, A., *et al.* (2015). Cell 160, 177-190; Olzmann, J. A. and Carvalho, P. (2019). Nat Rev Mol Cell Biol 20, 137-155; Puli, O. R. and Singh, A. (2011). Dros. Inf. Serv. 94; Rumin, J., Bonnefond, H., Saint-Jean, B., Rouxel, C., Sciandra, A., Bernard, O., Cadoret, J. P. and Bougaran, G. (2015). Biotechnol Biofuels 8, 42; Sarkar, A., Gogia, N., Glenn, N., Singh, A., Jones, G., Powers, N., Srivastava, A., Kango-Singh, M. and Singh, A. (2018). Sci Rep 8, 13545; Singh, A., Tare, M., Puli, O. R. and Kango-Singh, M. (2012). Dev Dyn 241, 69-84; Tare, M., Modi, R. M., Nainaparampil, J. J., Puli, O. R., Bedi, S., Fernandez-Funez, P., Kango-Singh, M. and Singh, A. (2011). PLoS One 6, e24361; Tare, M., Puli, O. R., and and Singh, A. (2013). In Molecular Genetics of Axial Patterning, Growth and Disease in the Drosophila Eye (ed. A. Singh, and & M. Kango-Singh), pp. 37-75. Springer NewYork Heidelberg Dordrecht London: Springer; Tare, M., Puli, O. R., Oros, S. M. and Singh, A. (2009). . Dros. Inf. Serv. 92, 174-180; Tare, M. and Singh, A. (2008). Dros. Inf. Serv. 91, 160-164; Uman, M. and Singh, A. (2011). Journal of STEM Education: Innovations and Research 12, 58-66; Wood, W. B. (2009). Annu Rev Cell Dev Biol 25, 93-112; Yeates, C. J., Sarkar, A., Kango-Singh, M. and Singh, A. (2019). In Insights into Human Neurodegeneration: Lessons Learnt from Drosophila (ed. M. M. & M. A.), pp. 251-277. Singapore: Springer.

DIS Printed Copies

Printed copies of this and other recent issues of Drosophila Information Service can be ordered directly from an independent publisher

www.lulu.com

On that site, go to “Shop” and enter “Drosophila Information Service” in the search bar. Several issues should be shown. The cost of the printed volume is now lower than previously; they will add shipping costs based on delivery location.

The North American *Drosophila* Board

The Board's duties include: overseeing community resource centers and addressing other research and resource issues that affect the entire *Drosophila* research community. The Board also administers the finances for the annual North America *Drosophila* Research Conference and its associated awards, and it chooses the organizers and the site of the annual meeting. The Board consists of nine regional representatives and four international representatives, who serve 3-year terms. The three elected officers are President, President-Elect, and Treasurer. The three most recent Presidents continue participation on the Board as Past-President. In addition, the Board has *ex officio* members who represent *Drosophila* community resources or centers. For more information about the Board and the summaries of the annual Board meetings, see the FlyBase web site.

Drosophila Board

President: Mark Peifer

President-Elect: Mariana Wolfner

Past-President: Bruce Edgar
Past-President: Deborah Andrew
Past-President: Laura Johnston

Treasurer: Michelle Arbeitman

Regional Representatives:

New England: Kim McCall
Heartland: Erika Geisbrecht
Midwest: Tina Tootle
Mid-Atlantic: Erika Bach
Southeast: Laura Reed
California: Leanne Jones
Great Lakes: Michael Welte
Mountain: Celeste Berg
Canada: Julie Brill

International Representatives:

Asia: Tatsushi Igaki
Australia/Oceania: Coral Warr
Europe: Nic Tapon
Latin America: Helena Araujo

Primarily Undergraduate Institution Representative: Amanda Norvell

***Ex Officio* – Representing *Drosophila* Resources:**

Norbert Perrimon (FlyBase; Harvard Medical School)
Susan Russo Gelbart (FlyBase; Harvard University)

Brian Calvi (FlyBase; Indiana University)
Susan Celniker (BDGP; Lawrence Berkeley National Laboratory, Berkeley)
Kevin Cook (Bloomington Stock Center & Nomenclature Committee; Indiana University)
Patrick O'Grady (Drosophila Species Stock Center; Cornell University)
Jim Thompson (Drosophila Information Service; University of Oklahoma)
Hugo Bellen (Bloomington Stock Center Advisory Committee & P Element Project; Baylor College of Medicine)
Allan Spradling (P-Element Project; HHMI/Carnegie Institute)
Stephanie Mohr (Director, DRSC/TRiP; Harvard University)
Jonathan Zirin (Assistant Director, DRSC/TRiP; Harvard University)
Scott Hawley (Nomenclature Committee; Stowers Institute for Medical Research)
Lisa Meadows (VDRC; Vienna, Austria)
Masanobu Itoh (DGRC, Kyoto; Kyoto, Japan)
Toshiyuki Takano-Shimizu (DGRC, Kyoto; Kyoto, Japan)
Chuck Langley (At-large; University of California, Davis)
Brian Oliver (FlyBase Advisory Board; NIH)

Genetics Society of America:

Lynn Cooley, GSA Board of Directors
Suzy Brown, Senior Director (sbrown@genetics-gsa.org)
Tracy DePellegrin, Executive Director